AD-A068 488 BELL AEROSPACE TEXTRON BUFFALO N Y F/G 21/9.1
CHEMICAL AND METALLURGICAL ANALYSIS OF PROPELLANT STORAGE VESSE--ETC(U)
FEB 79 E J KING, H G KAMMERER F04611-78-C-0012
UNCLASSIFIED 8795-927002 AFRPL-TR-79-6 . NL

1 OF 2
AD
A068488

AFRPL-TR-79-6

LEVEL II

CHEMICAL AND METALLURGICAL ANALYSIS OF PROPELLANT STORAGE VESSELS

FINAL REPORT - MARCH 1978 - OCTOBER 1978

BELL AEROSPACE TEXTRON
DIVISION OF TEXTRON, INC.
P. O. BOX ONE
BUFFALO, NEW YORK 14240

AUTHORS: E. J. KING
H. G. KAMMERER

FEBRUARY 1 9 7 9

Approved for public release;
Distribution unlimited.

Prepared for:
AIR FORCE ROCKET PROPULSION LABORATORY
DIRECTOR OF SCIENCE AND TECHNOLOGY
AIR FORCE SYSTEMS COMMAND
EDWARDS AFB, CALIFORNIA 93523

NOTICES

When U. S. Government drawings, specifications, or other data are used for any purpose other than a definitely related Government procurement operation, the Government thereby incurs no responsibility nor any obligation whatsoever, and the fact that the Government may have formulated, furnished, or in any way supplied the said drawings, specifications, or other data, is not to be regarded by implication or otherwise, or in any manner licensing the holder or any other person or corporation, or conveying any right or permission to manufacture, use, or sell any patented invention that may in any way be related thereto.

FOREWORD

This report was submitted by Bell Aerospace Textron, Division of Textron, Inc., P. O. Box One, Buffalo, New York 14240, under Contract No. F04611-78-C-0012, Job Order No. 305911RM with the Air Force Rocket Propulsion Laboratory, Edwards, CA 93523.

The Project Manager was E. J. King; the Project Metallurgical Engineer was H. G. Kammerer.

This report has been reviewed by the Information Office/XOJ and is releasable to the National Technical Information Service (NTIS). At NTIS it will be available to the general public, including foreign nations.

Herman H Martens
HERMAN MARTENS
Project Manager

John T. Nakamura
J. T. NAKAMURA, Chief
Chemistry Branch

FOR THE COMMANDER

Edward E Stein
EDWARD E. STEIN, Deputy Chief
Liquid Rocket Division

Unclassified

SECURITY CLASSIFICATION OF THIS PAGE (When Data Entered)

(19) REPORT DOCUMENTATION PAGE	READ INSTRUCTIONS BEFORE COMPLETING FORM
(18) 1. REPORT NUMBER: AFRPL-TR-79-6	2. GOVT ACCESSION NO.
	3. RECIPIENT'S CATALOG NUMBER (9)
(6) 4. TITLE (and Subtitle): CHEMICAL AND METALLURGICAL ANALYSIS OF PROPELLANT STORAGE VESSELS.	5. TYPE OF REPORT & PERIOD COVERED: Final Report, Mar[redacted]-Oct[redacted]78,
(14)	6. PERFORMING ORG. REPORT NUMBER: 8795-927002
(10) 7. AUTHOR(s): E. J. King, H. G. Kammerer	(15) 8. CONTRACT OR GRANT NUMBER(s): F04611-78-C-0012 new
9. PERFORMING ORGANIZATION NAME AND ADDRESS: Bell Aerospace Textron, P. O. Box One, Buffalo, New York 14240 (12) (11)	(16) 10. PROGRAM ELEMENT, PROJECT, TASK AREA & WORK UNIT NUMBERS: JON-305911RM (12) 185 P.
11. CONTROLLING OFFICE NAME AND ADDRESS: Air Force Rocket Propulsion Laboratory, LKLR Edwards AFB, California 93523 (11)	12. REPORT DATE: Feb[redacted]979
	13. NUMBER OF PAGES: 173
14. MONITORING AGENCY NAME & ADDRESS (if different from Controlling Office)	15. SECURITY CLASS. (of this report): Unclassified
	15a. DECLASSIFICATION/DOWNGRADING SCHEDULE: N/A

16. DISTRIBUTION STATEMENT (of this Report)

Approved for public release; distribution unlimited.

17. DISTRIBUTION STATEMENT (of the abstract entered in Block 20, if different from Report)

18. SUPPLEMENTARY NOTES

19. KEY WORDS (Continue on reverse side if necessary and identify by block number)

Propellant material compatibility, cryostretched 301 stainless steel, A-286 stainless steel, nitrogen tetroxide (N_2O_4), chlorine pentafluoride (ClF_5), explosive bonding, solid state bonding corrosion products, pitting corrosion, microscopic analysis, long-term storage of propellants

20. ABSTRACT (Continue on reverse side if necessary and identify by block number)

This report covers the examination and metallurgical evaluation of seven tanks after 5 to 8 years storage with N_2O_4 or ClF_5 propellant. The tank materials included cryostretched 301 stainless steel and A-286 stainless steel. The cryostretched 301 stainless steel tanks had positive expulsion devices consisting of ring stiffened diaphragms of 304 stainless steel while the A-286 stainless tanks were unique in utilizing solid state, explosive bonds in place of fusion welds to join the tank components.

DD FORM 1 JAN 73 1473 EDITION OF 1 NOV 65 IS OBSOLETE

Unclassified 408 855

SECURITY CLASSIFICATION OF THIS PAGE (When Data Entered)

79 05 09 059

20. ABSTRACT (cont)
Leakage by pitting corrosion was found in one positive expulsion 304 stainless steel diaphragm. In addition, deep pitting corrosion was found on the exterior shell of the cryostretched 301 tanks. The interior of the A-286 tanks showed a general, but rather shallow attack, probably from the HNO_3/HF etching solution used to remove the heavy steel backup mandrels of the explosive bonding process. This general interior attack was somewhat accelerated in or near some of the bonds by the presence of crevices or local highly strained regions.

Except for these problems, most of which were unusual situations where a cause and corrective action are obvious, these two types of tanks performed quite satisfactorily during the extended storage with N_2O_4 or ClF_5. One proof of the good performance of these tanks was the controlled expulsion of one tank, to an expulsion efficiency of better than 95% with 50 psi pressure differential. This confirmed that, in the absence of a few special problems, the positive expulsion tanks would perform satisfactorily after the completion of extended (up to eight years) storage with oxidizer propellant.

In addition to the metallurgical analysis of various corrosion and storage attributes, mechanical properties of the cryostretched 301 and A-286 stainless steel shells were evaluated and the metallographic structure of the explosive bonds was studied in detail.

TABLE OF CONTENTS

LIST OF TABLES

LIST OF FIGURES

LIST OF FIGURES (cont)

LIST OF FIGURES (cont)

LIST OF FIGURES

LIST OF FIGURES

LIST OF FIGURES (cont)

SECTION I

INTRODUCTION

The long term storability program for liquid rocket propellant systems initiated by the Air Force Rocket Propulsion Laboratory at Edwards Air Force Base has been a continuing effort to supply designers with material environmental response data that may be utilized for the design of liquid propulsion systems in which 5 to 10 year mission life can be obtained with confidence. The subject contract provides insight to the metallurgical response of the precipitation hardenable alloy A-286 and to cryostretched 301 stainless steel. The scope of this contract covers evaluation of representative aerospace tankage in which advanced processing techniques were combined with fabrication and inspection techniques representative of normal aerospace practice. The A-286 tankage, a cylindrical domed end tank, utilized solid state bonds instead of welds, while the spherical 301 cryoformed stainless steel tank contained a brazed ring-stiffened 304 stainless steel internal diaphragm for positive expulsion.

The tanks metallurgically evaluated under this contract had been in long term storage for 5 to 8 years at the Air Force Rocket Propulsion Laboratory, Edwards Air Force Base. These tanks contained nitrogen tetroxide (N_2O_4) and chlorine pentafluoride (ClF_5). The identities and test history are summarized in Table I. This contract is the fourth program conducted by Bell Aerospace Textron for the Air Force Rocket Propulsion Laboratory. Previous programs were reported in References 1 through 3. The program had the objective to ascertain if the integrity of the hardware was affected in a

detrimental manner by corrosion, fabrication techniques or inadequate quality control procedures.

Experience in past programs has shown that leakage of components may be considered as the predominate mode of failure or may be in a stage of advancement that failure may occur. This program, as well as past programs, consisted of the following phases:

Documentation of the propellant tankage in the "as-received" condition. Definition of anomalies and defects that could possibly alter the functional capabilities of the missile tankage and associated components.

Metallurgical analysis of anomalies or defects observed in the storage vessels.

Mechanical performance of the solid state bonds used in the fabrication of A-286 tankage and the performance of the reversing diaphragm for positive expulsion used in the cryogenically stretched 301 stainless steel tankage.

The metallurgical examination of these tanks was carried out in a sequential manner in which both the external and internal surfaces, solid state bonds, welds used in the fabrication of the 301 cryoformed tanks and diaphragms were examined visually and macroscopically in the as-received condition. Photographic documentation, presenting results observed for this condition are presented in Section V.

Prior to sectioning the Arde tankage, each tank was radiographically examined to determine the position of the diaphragm. As part of the examination of these tanks, all diaphragms were leak tested prior to sectioning. Utilizing the radiographic and leak test results, mechanical evaluation of these diaphragms from a functional standpoint was used to further determine diaphragm integrity after storage. Mechanical properties were also obtained on each tank evaluated to substantiate the overall strength of each shell and to demonstrate that corrosion, to a degree that would degrade tank performance, had not occurred.

The in-depth analysis of areas where corrosion was found to exist was performed using standard metallographic techniques. Observations made on both types of tanks are documented in detail with photomicrographs in Section V. In several instances the amount of corrosion observed was to an extent that some question exists on the degree of component integrity remaining, although no leakage or failures were observed during the 5 to 8 year storage period.

BAT assigned numbers to the tanks evaluated in this program. In Table I, the original Martin serial numbers are tabulated along with the BAT tank numbers.

SECTION II

PROGRAM STRUCTURE

A decade ago the Air Force Propulsion Laboratory at Edwards Air Force Base, realizing that future needs of operational liquid propulsion systems would require long-term storage data on materials to be used in tankage and systems, initiated a storability program. This report and the data presented herein form a portion of this program. The initial objective which still remains the primary objective of this storability program has been to bridge the gap between laboratory coupon tests and the basic evaluation of tankage materials, systems and components that have endured long term storability of earth-storable fuels and oxidizers. Tankage materials evaluated after storage have included those of interest to the aerospace industry. This program dealt with the evaluation of two types of tanks that had been in long term storage (5 to 8 years) with N_2O_4 and ClF_5 propellants at the special facilities existing at Edwards Air Force. The tanks are of two types, a cylindrical domed-end tank of A-286, a precipitation hardening stainless steel, utilizing solid state bonds instead of welds and a spherical tank of AISI 301 stainless steel, cryogenically stretched for high strength, containing a ring-stiffened 304 stainless steel diaphragm for positive expulsion. In the course of this program the diaphragm of Tank No. 3 was completely expelled and the displacement efficiency was determined. This effort gave insight to the mechanical evaluation of these diaphragms from a functional standpoint.

Reports by AFRPL illustrating the details and some of the early results of this storability program may be found in References 4 and 5.

The items included in this overall program may be divided into three basic groups: (1) small containers, (2) representative type tankage, and (3) tankage systems with associated expulsion devices and/or feed system components.

The tanks being evaluated after storage in this portion of the program are all from Group II, Representative Tankage. The tanks in this group are of the 10 to 15 gallon size, which makes them typical of the types that would be used in reaction control systems. The tankage in this group was fabricated by current or advanced state-of-the-art methods. Therefore, the range of fabrication and quality control problems encountered in manufacturing these vessels simulate those likely to be encountered during the manufacture of an operational liquid rocket system.

SECTION III

TEST FACILITIES AND PROCEDURES

A. LONG TERM STORAGE FACILITY - AFRPL

The tanks examined in this program were exposed to the oxidizers N_2O_4, and ClF_5. Storage testing at Edwards Air Force Base of tankage loaded with oxidizers is conducted in a metal Quonset hut storage test building equipped to provide a constant controlled environment of 85±5°F and 85±5% relative humidity. The oxidizer building is insulated by a spray-in-place foam. Environmental conditions are maintained by two evaporative coolers and immersion water heaters. Safety provisions in this facility consist of a Firex-type water deluge system, large water drain piping, fire detectors, a continuous vapor detector and closed-circuit television monitoring. Several years ago an automatic conditioner shutdown and scrubbing system, which is operated when an excess of oxidizer vapor is detected by the facility toxic vapor detector was installed.

B. POST-STORAGE TANKAGE ANALYSIS - BAT

The destructive examination of these tanks was conducted in the Bell Aerospace Textron Metallurgical Laboratories. The facilities required to conduct the metallurgical evaluation of these tanks were available and utilized within these laboratories.

After visual examination and photographic documentation of the as-received and as-sectioned vessels, they were examined in detail for corrosion, anomalies or defects using both binocular microscopes at low magnification and higher magnification research microscopes. Photomacrographs of local corrosion and other anomalies were taken on view cameras. Cross sections of leaks, corroded areas, welds, etc. were prepared using automatic rotary and vibratory metallographic polishing equipment. Photomicrographs of these metallographic sections, in the as-polished condition and after etching to reveal the microstructure, were taken on a Leitz research microscope. It was occasionally necessary to use radiographic inspection equipment, especially to examine the suspected leak areas in the diaphragm of Tank No. 2.

Mechanical properties were determined on all tanks evaluated in this effort and the majority of tanks in past efforts to establish the heat treatment conditions or presence of degradation due to corrosion or other long term storage effects. Standard universal testing machines with load ranges from a few hundred pounds to 300,000 lbs. were used for this work.

Other facilities and equipment were used in an auxiliary or routine manner during various portions of this evaluation program. These included hardness testing equipment such as conventional Rockwell or Vickers, Leitz microhardness and a Sonodur for automatic microhardness traverses. Tank sectioning was performed on abrasive cutoff saws, lathes and bandsaws. Photographs of representative equipment used in this work were shown in References 1 and 3.

C. PROCEDURES

The procurement of test hardware and the environmental testing of this hardware with earth-storable propellants have remained essentially unchanged, since initiation of this long term compatibility program, Reference 1. Although these procedures have been previously documented they are also presented here to maintain completeness of the presentation and to provide a convenient reference for the post-test evaluations of exposed hardware being reported on.

Test articles evaluated in this program were procured from aerospace contractors, where primary responsibility for quality control and quality assurance of the test articles was vested. This hardware was fabricated according to specific procedural specifications encompassing detailed inspection and cleaning procedures, as dictated by the alloy being manufactured.

Helium leak testing of all individual tankage in the as-received condition was performed to ensure against the development of leaks and the introduction of contamination during shipment of the test articles from the manufacturer. Upon completion of the leak test, the tanks were loaded with propellant and placed in the appropriate storage facility for storability testing. The fuel tanks were monitored for both leakage and excessive pressure rise, while oxidizer tanks, such as those in this program, were monitored only for visual evidence of leakage.

In the event of excessive pressure rise in a fuel tank, the tank is vented and propellant and ullage gas samples are taken. Tanks which exhibit continued pressure rise are removed from testing and analyzed to determine whether the pressure increase was due to an isolated instance or is indicative of a lack of storability of the material/propellant combination.

Following the above exposure test procedures, in this program and past programs, tanks were selected for destructive examination to ascertain the cause of failure or other observed anomalies. The metallurgical procedures used in the assessment of corrosive damage consisted of an examination of external and internal surfaces of the storage vessels with an in-depth analysis following the procedure outlined below. This procedure was submitted for approval of the project officer prior to initiation of these analyses.

1. APPEARANCE DOCUMENTATION

a. Those anomalies which are in large components will have the anomaly and surrounding material segment removed for ease of handling.

b. Take photomacrographs of anomaly surfaces; remove for analysis any corrosion products or deposits, and take additional photomacrographs if surface changes or new features are involved.

c. If not already visible, section away from defect to reveal inside surface of anomaly area and take photographs of this inside surface.

2. EXAMINATION OF LEAK SURFACES

a. If a leak was suspected but not pinpointed, radiographs and dye penetrant inspection were utilized to verify leak location and extent.

b. The leak area was removed carefully from the surrounding metal.

c. After microscopic examination at 10X to 60X, photomacrographs of exposed corrosion surfaces were taken.

d. A high magnification microscope examination was performed, to determine topography and significant features of corroded surface. In all cases in this report the corrosion observed led to sequential removal of the surface until the depth of corrosion was established.

3. EXAMINATION OF PITTED SURFACES

a. Section through pitted region in a careful manner so that at least two segments of essentially equal pitting were available for study.

b. Perform microscopic examination of one-half of pitted surface to determine topography and significant features of pitted surface.

4. MICROSTRUCTURE AND RELATION TO CORROSION, LEAK OR ANOMALY

a. Mount a cross section through critical area of anomaly.

b. Polish using conventional metallographic techniques.

c. Examine in unetched condition for corrosion penetration of grain boundaries or similar effects and take photomicrographs.

d. Etch with appropriate reagents to bring out microstructure of solid state bond and/or parent metal.

e. Examine and take photomicrographs of microstructure, both as it relates to corrosion effects and also to determine matrix microstructure and material effects.

5. CHEMICAL ANALYSIS OF CORROSION PRODUCTS AND CORRODED MATERIAL

No corrosion products were found in any of the detailed analyses of anomalies studied in this program. Therefore, X-ray diffraction or other analysis techniques were not required.

SECTION IV
FABRICATION HISTORY OF TANKS EXAMINED

In the analysis of corrosion behavior of any component it is instructive, and often necessary, to know the methods of fabrication and the processing details involved, in order to arrive at meaningful conclusions to the cause and significance of observed corrosion effects. Thus, in this program of analysis of test vessels after N_2O_4 or ClF_5 propellant exposure, it has been necessary to collect as much fabrication history as possible to aid in the evaluation. This history is summarized in this section, and is then referred to in detail in the metallurgical analyses discussed in Section V. The reports and references from which this fabrication history were obtained are tabulated in the References (Section VII), with the specific reports from the manufacturers listed, where applicable, in Table II. None of the tanks evaluated were fabricated at Bell Aerospace Textron, therefore, all of this section represents information obtained from reports or observations on the tanks themselves by investigators experienced in many phases of aerospace hardware fabrication.

The tanks in this study had all been procured by the Air Force Rocket Propulsion Laboratory and assigned to this Storability Test program. That program has been described in detail in the previous Section II. The solid state bonded A-286 tanks had all been manufactured by the Denver Division of Martin Marietta Corp. under U.S. Air Force Contract F04611-69-C-0056. The summary of fabrication

characteristics and specific reference to Martin Marietta reports documenting their work are included in Table II. These tanks are of 10 gallon capacity and were fabricated and assembled using advanced techniques of explosive bonding to provide test items that would be representative of production hardware, if this solid state, explosive bonding process were carried forward to a production process. All joints in the tanks were formed by overlapping the mating surfaces, applying strips of explosive, with suitable rigid backup, to form a bond. Unique features of the bonding process, and some of its effects on later corrosive environment service are included in the metallurgical analyses in Section V.

The Arde "cryoformed" tanks represent a somewhat more widely used, but still unique fabrication process. They were produced by Arde Co., Mahwah, NJ, under U.S. Air Force Contract F04700-68-C-0505. The tanks are essentially identical to ones used in a strontium perchlorate injector system in a portion of the Minuteman ballistic missile. The unique feature of these tanks is the cryogenic stretching of the specially controlled chemistry 301 stainless steel shell. This imparts extremely high strength while retaining good toughness. Also unique to these tanks is the use of a hemispherical, reversing diaphragm of 0.008" thick 304 stainless steel for positive expulsion of propellant. This diaphragm is stabilized during expulsion by a series of concentric wire rings brazed to the diaphragm. A brief summary of all of these features is presented in Table II, with details, as they related to the metallurgical analyses of the anomalies, included in Section V, Analysis.

SECTION V

DISCUSSION OF RESULTS

A. VISUAL AND MACROSCOPIC EXAMINATION OF EXTERNAL AND PROPELLANT EXPOSED TANK SURFACES

The first stage in any examination of hardware for corrosion effects is a thorough examination and documentation of the surface appearance. This examination must be done by trained and experienced observers who will pay careful attention to preferential attack of welds, crevices and other susceptible regions. The initial examination of these tanks, after exposure to various propellants and storage room environments, was done in this manner, with complete photographic documentation of the external and, after preliminary sectioning, internal surfaces. The primary purpose of this initial examination (Phase I of metallurgical effort) was to identify those failures, anomalies or unusual conditions which would warrant a more detailed examination and analysis in the Phase II portion of the metallurgical effort. Accordingly, this section of the report documents the surface condition of the tanks as received after the various test exposures, and identifies those anomalies, failures or other corrosion and service effects, which will be considered in Section V, under D, Detail Metallurgical Analysis of Anomalies. A brief summary of these visual observations, on both the exterior and interior surfaces, is given in Table I.

The as-received condition of the exterior tank surfaces was found to be relatively clean and free of any gross corrosion, with no sign of any leaks or serious attack. Overall photographs of that as-received condition are shown in Figures 1 through 7. The Arde cryoformed tanks were bare, with no protective coating and did show some staining and pitting of the surfaces, in addition to a dark spot, almost appearing to be an arc-strike on Tank No. 1 (Figure 1). The pitting observed on the Arde tank shell surfaces was considered serious enough to warrant a detail examination of that condition, which is summarized in Section V.D.2.

The Martin, A-286 stainless steel, tanks were painted with a blue protective paint, as part of the fabrication process. This protective paint was intact and apparently unaffected by exposure over almost the entire surface of the tanks and outlet tubes, except in those areas where "green tape" was used to attach shipping labels or plastic bagging and tube end caps. In some of those areas, when the green tape was removed, the paint peeled away with the tape. None of those "peeled" areas showed any evidence that storage with propellant had any effect on the paint, and hence those areas were not considered significant to the post-test evaluation. This experience with the paint being removed when peeling away tape does serve as a reminder that tanks should be handled carefully before storage, for if that peeling away of the paint had occurred before storage, some corrosion effects might have been noted. One minor area of A-286 Tank No. 5 was found to have the paint scraped or wiped away (Figure 5). A

closeup view of that area is shown in Figure 8. Although the outer blue paint layer was completely gone from this approximately 3/8 inch diameter spot, the inner, primer coat, was still present. A brief examination by sectioning and metallographic polishing through this region (also shown in Figure 8) confirmed that there was no corrosive attack in this location, and therefore this spot was not considered significant to the post-test analysis of the tanks.

In examining the exterior of these Martin A-286 tanks, it was found that the identification decals were attacked and barely legible. An example of one of them is shown in Figure 9. The embossed lettering can be read because of shadow effects, but the printing and general appearance of the decal shows that it was being attacked, probably by the acid fumes in the high humidity storage room. For tank components where proper identification and traceability are required after storage in an area such as this storage facility, a more resistant decal material or coating of the decal with protective film or transparent acrylic spray coating, should be used.

During the initial visual examination of the Arde spheres, with their internal ring-stiffened diaphragms, probing of the interior showed some of the diaphragms to be in unexpected positions. Therefore, all of these spheres were X-rayed to determine the exact location and configuration of the diaphragms. Contact prints of the X-ray film of each of these tanks in the as-received condition are presented in Figures 10 through 14. Taking the appearance of

minor stains around the support cutout to be evidence of the orientation of the tanks during storage (see Figure 12 of Reference 5 for a view of these tanks during storage), it has been possible to orient the tanks in the proper vertical arrangement. This examination shows that two of the tanks, Nos. 1 and 4, were fully expelled with the diaphragms completely reversed. Tanks numbered 2 and 3 have diaphragms that were only partially expelled and evidently were drained without complete reversing of the diaphragm. This only partial reversal of two of the diaphragms made it possible to perform an expulsion test on the diaphragm of at least one tank. This test and its results are discussed in a separate Section, V.B., on the functional test of the diaphragm.

After determining the position of the diaphragms in the Arde tanks through radiographic inspection, these tanks were helium leak tested for possible leaks across the diaphragm. Three of the tanks showed no leakage in this helium mass spectrometer test, but Tank No. 2 did show significant leakage across the diaphragm. The diaphragm of Tank No. 2 was subjected to a detail metallurgical analysis to examine this leakage and is reported in Section V.D.1. The helium leak test involved applying 25 psi across the diaphragms of the tanks. In the case of Tanks 2 and 3 which showed partial movement of the diaphragm as-received, this differential pressure returned their diaphragms to their "normal" position, as seen in the radiograph of Tank No. 2 in Figure 14. It was from this "normal" position that the expulsion trial of Tank No. 3 was begun. Details of that expulsion and its results are presented in Section V.B.

The Arde tanks were sectioned after leak tests (and expulsion test in the case of Tank No. 3) by cutting carefully on either side of the diaphragm attachment weld, using a small diameter abrasive wheel so that the diaphragm would not be disturbed. In this way both the liquid and gas sides of the shell and diaphragm surfaces could be examined with the components still essentially intact. Photographs of these surfaces are shown in Figures 15 through 22. The surfaces were, in general, quite clean and bright. The propellant side of Tank No. 1 showed some staining indicative of a residual amount of propellant drying inside the tank after draining, but the stains were superficial in nature. The propellant sides of both the shells and diaphragms of all other Arde tanks were clean and bright with no stains or residues. The gas side of the shells and diaphragms (which is the side with stabilizing rings brazed to the diaphragm) was also clean and bright, with the exception of Tank No. 2, which was found to be leaking through the diaphragm, and Tank No. 3 which leaked by tearing through the diaphragm in attempting to move the diaphragm back to its original position after expulsion.

The gas side of Tank No. 2, Figure 18, showed stains which indicate that a liquid had been present there when the diaphragm was nested against the shell in the "normal" as-stored position. This would indicate that the leaks in diaphragm from No. 2 had occurred during storage, not after draining, at which time some slight pressure had been applied to the gas side to move the diaphragm away from its "normal" position. This is discussed in more detail in Section V.D.1. The stains on the shell did not

represent any measurable amount of corrosion, but were merely superficial deposits from the drying of the propellant that had leaked through the diaphragm.

The gas side of Tank No. 3, Figure 20, also showed stains, but these were readily identified as the residue of the chromic acid inhibited water used in the expulsion test. This water would have leaked through the diaphragm when the diaphragm tore, during the attempt to return the diaphragm to its original position following expulsion. The stains therefore had no significance for the storage and compatibility service of the tank.

The interior, ClF_5 exposed surfaces, of the A-286 tanks were examined by sectioning the tanks lengthwise. This allowed the tank surfaces to be photographed in their entirety and be examined for overall effects such as "waterlines", which would indicate storage in a partially full condition. Photographs of the tank interiors are shown in Figures 23 through 25. As can be seen in these photographs, all tanks did show some minor evidence of a "waterline" at about the "half-full" location. It is not clear from examination of the tanks or from fill/drain records from AFRPL whether these tanks had ever been completely full, or whether the waterline represents a partial draining after a portion of the storage time. There are minor stain and corrosion effects, both above and below these lines, but since many of these stain or corrosion effects could have been caused by fabrication etching or by vapors from the propellant in the gas space above it, the appearance does not aid in identifying

the meaning of these waterlines. In addition to the "waterlines", there are brownish stains and pitting around the outlet fitting in the domes of each tank. The explosive bond overlap of each tank was somewhat discolored, even in locations where it had been sanded or ground after bonding to blend surfaces smooth for further assembly and bonding. There were some stains and deposits adhering to the bond overlap or appearing to have "weeped" from the interior of the bond. This was the first indication that some of the explosive bonds had interior cavities or gaps and other related defects and is covered in detail under Metallurgical Analyses Sections V.D.5 and V.D.6.

The interior surface of Martin Tank No. 7, Figure 25, showed that it had lain on its side with a small residue of liquid, until that liquid dried. That residue was almost certainly propellant, ClF_5, and caused minor staining and discoloration of the surface. However, this staining and discoloration of the shell interior was all superficial and not significant to the storage service.

The interiors of all of the Martin A-286 shells showed frosting or etching, some rather heavy, while other areas were only lightly attacked. This general, but light, surface attack is discussed in Section V.D.3., as it was considered sufficiently significant to warrant a detail metallographic analysis.

B. FUNCTIONAL TEST OF ARDE DIAPHRAGMS FOR LEAKAGE AND EXPULSION

The four Arde tanks with their ring-stiffened diaphragms were all subjected to a functional test consisting of a leakage test followed by an expulsion test of one of the units, Tank No. 3. As previously described the four tanks were received in the following condition, relative to their diaphragm position:

Tank No. 1 - Diaphragm fully expelled.

Tank No. 2 - Diaphragm moved approximately 2 inches toward expelled position, but only in central, dome region.

Tank No. 3 - Same as No. 2.

Tank No. 4 - Diaphragm fully expelled.

These positions were verified by radiographs of tanks shown in Figures 10 through 13. Discussions with RPL personnel indicate that the expulsions were in an essentially uncontrolled manner, during the draining, flushing and purging of the tanks after storage test. It appears that Tanks numbered 2 and 3 were probably drained "naturally" (by gravity), without any forced expulsion, and the minor movement of the diaphragm occurred during later purging. In discussions with Arde personnel after completing the preliminary evaluation of these tanks, it appears that some unusual conditions must have been involved in the purging or other operations which caused the partial expulsion, since the diaphragms are generally expected to "roll" in expulsion starting with the largest diameter region near the girth attachment weld. This occurs because the differential pressure induced stresses are

higher in the larger diameter outer regions. Thus, even though these diaphragms did not have the specially formed "joggle" sometimes used to insure proper starting of diaphragm expulsion movement, they should still have started "rolling" from the outer rings. Close inspection of the radiographs of the as-received condition of Tanks 2 and 3, at the suggestion of Arde personnel, disclosed that there was some bulging of the diaphragm between stiffening rings. Although not readily apparent in the reproductions in Figures 11 and 12, this bulging was visible in the original films. The bulging is most pronounced in the first 2 or 3 rings as an expansion outward from the liquid toward the gas side and indicates the diaphragms were probably overpressurized (more than 25 psi differential pressure between liquid and gas side) at some time during their life. This bulging would produce enough stiffening of the outer diameter region of the diaphragm to force the expulsion movement of the diaphragm to start at the dome.

Functional test of all diaphragms started with a helium leak test. For this test a 25 psi helium pressure was applied to the "open" side of the tank (gas side for Tanks 1 and 4, liquid side for Tanks 2 and 3), and a helium mass spectrometer attached to the opposite port. No leakage was detected in Tanks 1, 3 and 4. Tank No. 2 did show substantial leakage and is the subject of Detail Metallurgical Analysis No. 1, which is covered in a following section.

The diaphragms in both Tank No. 2 and No. 3 moved back to their "normal" position during this differential pressure leak test. This can be seen in Figure 14. With the diaphragm of Tank No. 3 now in its "normal", liquid storage position, it was possible to perform an expulsion test to determine the expulsion characteristics and efficiency of the diaphragm as a function of applied differential pressure. Therefore, Tank No. 3 was loaded with inhibited distilled water (27.12 pounds) and set up in an available expulsion test rig, that could control and monitor applied differential pressure and measure the diaphragm tank and receiver tank weight to monitor the progression of expulsion. The results of this expulsion are shown in Figure 26. It shows that no diaphragm movement occurred below 10 psid. As the pressure was raised to the 14-18 psid range, the diaphragm moved and expelled approximately 85% of the liquid. The expulsion occurred in increments as the diaphragm rolled past one or more stiffening rings in jumps. Even during this jump, the differential pressure stayed within a 2-3 psid band and was under good control.

Once the amount expelled exceeded 85% of the total liquid, the differential pressure had to be increased considerably, first to 30 psid where the last stiffening ring was passed to bring expulsion up to 93%, and finally to 50 psid where the test was stopped with 95.2% of the liquid load expelled. This is considered a good expulsion efficiency performance for a positive expulsion tank. Higher efficiencies can only be achieved with very sophisticated tank and diaphragm design. A radiograph was made of Tank No. 3 in the expelled condition and is shown in Figure 27. The

diaphragm is completely reversed, as expected. Close examination of the film showed some wrinkling of the diaphragm material between rings, particularly the largest diameter rings.

Despite the presence of the wrinkling, it was felt that re-nesting of the diaphragm might be possible, to attempt another expulsion. This would help determine the life and possible reuse of this type of tank. The tank was therefore reinstalled on the expulsion test stand and filling begun. Approximately 16.25 lbs., or 60% of the full liquid load had been loaded into the tank, at a differential pressure of 15 psid when water became visible in the gas side port, indicating a major leak in the diaphragm.

Upon sectioning of the tank, the diaphragm was found to be badly wrinkled and buckled, Figures 19 and 20, with a tear at a sharp buckle located at the No. 5 stiffening ring. There was no evidence of any corrosion or storage service effects in the tear or other buckled regions. The buckling and gross deformation of the diaphragm occurred during the reversing, probably starting at the light wrinkles already present in the as-expelled diaphragm. It is evident that reuse of these diaphragm tanks cannot be expected. Although reversing of the diaphragm may sometimes be possible, particularly if the original expulsion is not carried to maximum output, the reversal cannot be considered a reliable procedure and should not be used in flight hardware.

C. METALLOGRAPHIC AND MECHANICAL PROPERTIES OF TANK SHELLS AND WELDS

1) Fabrication Sequence that Develops Microstructure and Mechanical Properties of Cryoformed 301 Stainless Steel.

The Arde tankage evaluated in this program consisted of 301 Cres (corrosion resisting) stainless steel spheres and 304 stainless steel diaphragms. In order to achieve a reproducible process, Arde specifies a special chemistry which represents a band within the 301 Cres composition. The chemical composition is specified with low carbon content. In the processing of this material, two basic steps are involved. The first requires cryogenic prestraining at -320°F which induces a martensitic type transformation. This transformation results in an increase in mechanical properties and is referred to as unaged material. The tankage evaluated in this contract was in the unaged condition. The above process achieves the final size and shape, as well as the high strength levels simultaneously. The preform must stretch to the final shape. In the fabrication of spheres if a boss or thickened ring is incorporated in the design of the tank, the boss or ring is designed to stretch uniformly with the sphere body at the attachment point, but may be restrained or sized to prevent stretching near a boss or diaphragm. A solution heat treatment is performed after all welds are completed. This heat treatment prevents or minimizes local alloy depletion which occurs when carbides are formed during welding.

In summary, the microstructure of the 301 cryoformed material is one which depends on the following.

a) A restrictive or lean carbon content 301 Cres composition.

b) A martensitic transformation that occurs at liquid nitrogen temperature, -320°F, during a stretching or thickness reduction process.

c) Solution annealing after welding prior to stretching to reduce alloy depletion by removal of complex metal carbides formed in the heat affected zones of welds.

As part of this study the 304 diaphragm was also examined in detail. This stiffened ring diaphragm is utilized in the annealed condition.

2) Fabrication Sequence that Develops Microstructure and Mechanical Properties of A-286.

The alloy A-286 used in the fabrication of the Martin tankage evaluated in this report is an iron base precipitation hardened alloy. A typical chemical composition is cited for reference.

	%
Carbon	0.04
Manganese	1.60
Silicon	0.65
Sulfur	0.010
Phosphorous	0.015
Chromium	15.00
Nickel	25.25
Molybdenum	1.25
Titanium	2.10
Vanadium	0.30
Aluminum	0.20
Boron	0.003
Iron	Balance

A-286 is a precipitation hardening alloy which develops optimum properties by means of a solution heat treatment followed by a precipitation hardening or aging treatment. The microstructure of the alloy is austenitic under all conditions of heat treatment and fabrication. This alloy in the solution heat treated condition is weldable by all of the present aerospace processes. Heavy sections, or components under restraint, can be troublesome due to cracking difficulties. At BAT this alloy has been used extensively on Minuteman tankage and the control of grain size is known to aid in the prevention of grain boundary cracking. In joining A-286 to other materials the use of Hastelloy W is quite common.

Problems associated with aerospace applications for propellant tankage are reduced joint efficiencies due to cast microstructure, microcracking and shrinkage during the cooling period, and sensitivity of the heat affected zone to fatigue. Of equal importance in overall tankage efficiency is the potential leakage of toxic and highly reactive propellants through weld cracks.

Martin selected this alloy to evaluate solid state bonded joints. This bonding process provides 100% joint efficiency and a zero leak potential by eliminating cast microstructure and substituting a metallurgically diffused bond at each joint. Throughout the BAT evaluation of these tanks the above cited advantages of this joining technique were given detail attention, as the microstructural and mechanical property studies presented in this and subsequent sections of this report will bear out.

3) General Microstructure.

a) Arde Tanks.

The general microstructural studies of the Arde tanks are presented by utilizing photomicrographs taken from Tank No. 4. The basic reason for this was that throughout the microstructural analysis of the various tanks no significant differences existed between tanks, as far as basic microstructure.

The Arde tanks all show, as would be expected, austenite, transformed by cryostretching to martensite. This change from one phase, austenite, to a new phase without a change in composition is accomplished with a relatively low percentage of straining in the range of 8 to 10% at -320°F. The phase change, based on etching evaluations, is the same as that which occurs when 301 stainless steel is work hardened at room temperature and austenite is transformed to martensite. The relationship between the two processes exists in the amount of strain introduced into the austenitic matrix to produce a given strength level.

The dome region and the weld joining the dome to the transition ring are shown in Figure 28. All views show that the austenite has been transformed by cryostretching to martensite. A comparison between views (a) and (b) showed no evidence of directionality due to the processing. Since the transformation is achieved during biaxial stretching, the strain induced would be expected to be uniform throughout the matrix of the 301 stainless steel.

The degree of transformation occurring in the heat affected zone and in the weld structure is shown in views (c) and (d) of Figure 28. The martensitic transformation in these areas was extensive.

Figure 29 shows four microstructures of Arde Tank No. 4 taken in the transition ring between the dome and the diaphragm. These photomicrographs are presented to show the amount of martensitic transformation obtained as a function of tank wall thickness. In this transition region of the tank as one progresses from a thickness of 0.024 inch, view (a), the transformation is complete. The degree present is comparable to that found in the dome region of the tank. Progressing from view (a) to view (d), the thickest portion of the transition area of the tank, the transformation is such that it occurs in discreet areas, or along crystallographic planes that are most susceptible to transformation from austenite to martensite at low energy levels.

The shells of the Arde diaphragm tanks are fabricated by cryostretching a sphere fabricated from hydrospun domes, a set of polar inlet/outlet fittings and a central girth band with a thickened wall. After cryostretching the central girth band is cut open to allow the diaphragm and its outer attachment ring to be welded into place. For this reason, the central, "equator", region of the tank contains several welds. Substantial differences in properties exist both within the high strength cryostretched 301 stainless steel due to the variation in wall thickness, and between the cryostretched 301 stainless steel and the annealed or as-welded

segments of the attachment ring. To further verify the variations that occur in the central region a microhardness number traverse was performed on a cross section through the central area of Arde Tank No. 2 and is presented in Table III. The microhardness number data verifies that the high strength drops off rapidly as the thickness increases. This further substantiates the microstructural studies, where the amount of martensitic transformation decreased as the thickness increased.

Microstructural aspects of the Arde 304 diaphragm are presented in Figure 30. In view (a) of Figure 30 an overall view of the central region of the tank shell shows the diaphragm attachment weld. Although this appears to be a two-pass weld it very likely is a three-pass weld, assuming Arde followed the procedure, which they used on a similar diaphragm tank made for Bell. On the Bell tank they used three passes, (1) a sealing pass, (2) a fusion pass and (3) a filler wire pass. Positive internal gas pressure is used to achieve the weld underbead shape seen in Figure 30. The weld as shown in views (b), (c) and (e) of Figure 30 was found to be sound, as was the diaphragm, view (d). There was no evidence of mechanical or corrosive degradation in this diaphragm that was wetted by ClF_5 propellant since July 1969, and expelled prior to delivery to BAT for evaluation.

b) Martin A-286 Tanks.

The Martin solid state bonded tanks were fabricated from A-286 which is an iron base precipitation hardened alloy. The alloy was solution annealed at 1800°F, water quenched, and aged at 1325°F for 16 hours. The microstructure of Tank Nos. 5 and 6 are presented in Figures 31 and 32. Microstructures were taken

in the axial direction for Tank No. 5 in the dome and cylindrical portions of the tank. Tank No. 6, Figure 32, shows three views, one of which covers the axial direction in the dome end of the tank and the other two views the circumferential and axial directions of the cylindrical portion of the tank. As can be seen in all views presented, the microstructures, regardless of the direction which they represent, are equiaxed possessing a fine grain structure. In the heat treated condition this alloy has an austenitic matrix and is strengthened through precipitation of $Ni_3(Al,Ti)$.

4) Mechanical Properties.

As part of the verification of the general quality of these tanks and to give further insight to corrosion degradation or any other unusual long term storage effect having taken place, all critical joints as well as representative base metal samples were evaluated for mechanical properties. Data obtained on tensile coupons removed from the tanks are presented in Tables IV through X. In evaluating the Arde tanks samples were taken from the gas side and the propellant side of these diaphragm tanks. It was not possible to evaluate the girth welds due to the fact that sectioning of these tanks was done in a manner to preserve the diaphragm and its attachment weld for detailed metallographic studies. The value of utilizing this procedure is substantiated by the results obtained on the diaphragm from Tank Number 2.

The Arde forming process achieves high mechanical properties from 301 stainless steel from two basic processing steps. The first is cryogenic restraining at -320°F which induces a martensitic

transformation and this transformation results in an increase in mechanical properties. This material condition is defined as unaged material. Once the material is cryogenic formed/stretched, it then can be aged at 800°F for 20 hours which results in a further increase in mechanical properties.

Room temperature minimum ultimate strength values for spheres in the unaged condition are reported by Arde, Inc., to be 200,000 psi and for aged material to be 270,000 psi. A review of the data obtained from Tank No. 1 and Tank No. 4, irrespective to whether or not the environment was gas or propellant, shows that the material in these tanks was in the unaged condition. The minimum value of 200,000 psi was not achieved by every coupon but certainly was approached. These lower values are probably explainable by the fact that test specimens removed from a spherical bottle have to be straightened and sometimes the desired alignment for obtaining mechanical properties is not consistently achieved, resulting in lower mechanical properties.

The data obtained on the Martin A-286 base metal shows a good response to heat treatment. BAT specification required minimum values are: ultimate strength - 130,000 psi; yield strength at 0.2% offset - 85,000; and elongation in 2 inches - 15%. On standard control bars typical properties obtained by BAT are ultimate strength 150,000 to 160,000 psi, 0.2% offset yield strength 105,000 to 110,000 psi with an elongation in one inch of 22%. These properties are obtained on machined round bars. The elongation would be and is higher in one inch on these bars than one would

obtain on a sheet specimen. Therefore, the shell metal properties obtained on Tank Nos. 5, 6 and 7 are quite representative for this precipitation hardened alloy which develops optimum properties by means of a solution treatment followed by a precipitation hardening or aging treatment.

The same type of response was obtained for the ultimate and 0.2% yield strength values obtained transverse to the solid state bond. The elongation values were lower than expected due to two factors. In the case of specimen 5C-2 the 9.5% value obtained is attributed to the fracture occurring close to the solid state bond and due to the grinding of the surface of this bonded area during fabrication. The thickness of the shell adjacent to the bond was reduced somewhat in this grinding or blending of the surface. The second reason for the low values exists in the fact that some of the fractures took place beyond the bench marks or gage section of the test bar. This condition was encountered particularly with specimens removed from Tank No. 6. No failures were encountered in either tank at the bond, thereby establishing the integrity of this solid state bonding technique developed by Martin Marietta Corporation, Denver, Colorado. If crevice corrosion or general corrosion of the surface had occurred in these areas the strength of the joint would have been adversely affected.

D. DETAIL METALLURGICAL ANALYSES OF ANOMALIES

The specific anomalies selected for detailed analysis were based on the initial visual examinations performed on all tanks and on discussions with the AFRPL Project Officer. Although only one anomaly represents an actual corrosion penetration of the diaphragm, all seven represent unusual conditions warranting further investigation. All of these anomalies have significance in the handling and long term storage of Air Force liquid rocket propulsion systems. The specific anomalies are listed below and are then considered individually in the succeeding sections:

1. Leak in Diaphragm of Arde Tank No. 2.
2. Pitting on Exterior of Arde Tank Shells.
3. Surface Attack on Interior of Martin A-286 Tanks.
4. Split in Outlet Tube of Martin Tank No. 5.
5. Pitting Adjacent to Outlet Fitting Bond in Martin Tanks No. 5 and No. 7.
6. Interior Stains and Deposits Near Bonds in Martin Tanks.
7. Metallographic Evaluation of Explosive Bonds.

1. Leak in Diaphragm of Arde Tank No. 2

a. Test History and Background

Arde Tank No. 2 containing a diaphragm was placed in storage test in July 1969 along with three other tanks from Arde, all having been produced specifically for this program. As has been described in Section IV, these tanks were produced in the same manner and from the same design as tanks being produced by Arde for the Minuteman program. However, discussions with the Arde Co.

have indicated that they did not receive the final passivation and precision cleaning normally expected of hardware about to be placed into propellant service. This is an important point which will be discussed later in this section. The tank in question, Tank No. 2, along with Tank No. 1, was placed in storage with N_2O_4 propellant. This N_2O_4 propellant was of the green, NO- inhibited type. There is no record in the available histories of the storage tests from 1969 through 1977 of any difficulty with this or the other Arde tanks in storage. However, the test surveillance records are not complete enough to be sure whether the leakage to be discussed below might have been observed if it was in fact present during this time. The four tanks were removed from storage in 1977 having accumulated 8 years of storage. The tanks were drained of their propellant at Edwards Air Force Base and were subsequently sent to Bell Aerospace Textron for evaluation. The initial examination of this Tank No. 2 showed that the diaphragm had been partly expelled, presumably during the draining and flushing of the tank after storage service. This was shown in the radiograph, Figure 11. After initial establishment of the position of the diaphragm, the tank was leak tested with helium. A 25 psi pressure differential existed across the diaphragm. A substantial leak was found. No such leakage was found in any of the other three tanks. Because of the substantial readings in the helium mass spectrometer test, it was possible to measure a volumetric rate of leakage for Tank No. 2 by displacement of water with helium. The results of that investigation are presented below.

Differential Pressure (psid of He)	Leak Rate (Ml/sec.)
3	0.0775
5	0.1225
10	0.2092
20	0.4032

b. Observations.

Once leakage through the diaphragm had been established for Tank No. 2, the liquid side shell was carefully removed in a manner which did not touch or disturb the diaphragm so that the liquid side surfaces of the diaphragm could be closely examined. No obvious leak paths could be seen on microscopic examination at 6-20X magnification. Gas pressure was applied from the gas side of the diaphragm and soap film leak checking was employed to identify the areas where leakage was occurring. These areas were generally distributed near the dome of the tank, but most of the leaks were found in areas between the inner stiffening rings. Six well defined leaks were identified by the soap film testing method and some of these are shown circled in view (a) of Figure 33. Even with the locations of the leaks identified by soap film checking it was extremely difficult to see any surface indication of those leaks. The gas side shell of the tank was similarly removed in a careful manner so as not to disturb the diaphragm and the leak areas already identified on the liquid side were no more visible on the gas side than they had been on the liquid side. The leak area showing some indication of a surface disturbance is shown in view (c) of Figure 33. This particular leak area was sectioned and examined metallographically by polishing through the leak area incrementally. Before the polishing surface reached the first location of visible leakage, a substantial internal defect or pore was found (see view (b) of Figure 34). Continuing the polishing at very shallow intervals through this region of leakage

showed dramatic evidence of internal voids occupying more than half the thickness of the 0.010 inch thick diaphragm leaf. These incremental views documenting extensive internal corrosion are shown in view (c) of Figure 34 and the views of Figure 35. Continued polishing through this segment disclosed additional defect or cavity beyond that shown in the previous views. These are shown in the views of Figure 36. In only one of these sections, view (c), penetration to the gas side of the diaphragm is visible. This very slight penetration to the gas side, compared to the gross pitting of the liquid side verifies that this corrosion started from the liquid side of the diaphragm. View (c) of Figure 36, showing the small but definite presence of a leak path to the gas side, provided metallographic verification of the leak observed in the helium leak test. Polishing further through this defect, the cavities became much smaller and as seen in Figure 37 again became internal cavities with no surface connection but connected to the central portion of the cavity. The total volume in the diaphragm in which this extensive cavity was found extended over a distance 0.050"x 0.050". The cavity visible in all of these views showed definite indication of being a corrosion produced cavity, presumably starting as a pit on one surface and extending into the interior of the diaphragm. There is minor branching and extensive internal expansion of the corrosion process. At no point does it become the highly branched intergranular or transgranular cracking associated with stress corrosion. Instead, it is a pitting or gross removal of metal from the interior areas. This rather large corrosion induced cavity within the diaphragm indicated that these leaks previously thought to be very minor might have substantial significance.

When the gas side shell was removed from this tank, stains were visible on the shell surface (see Figure 18). These stains

showed evidence that a liquid had been in the gas side at a time when the diaphragm was fully nested against the gas side shell. Since this is the gas side of the tank in normal practice, there should not have been any liquid on the gas side and it must be assumed that the stains visible came from a liquid which had leaked through the leaks in the diaphragm. The evidence of close contact of the stiffening rings of the diaphragm with the shell over the entire surface of the diaphragm would indicate that the leakage necessary to produce these stains did not occur after the tank had been drained and purged. This is because the tank was received at Bell Aerospace Textron with the inner rings and diaphragm partly expelled, from the draining process and none of the ring surfaces would have been in contact with the shell at this time. This seems to provide definite evidence that the leakage in this diaphragm occurred during service or perhaps at a very early stage even before the storage service began.

Once the extent of the corrosion volume under an apparently insignificant pit was realized, other areas of this leaking diaphragm Tank No. 2 were radiographed and the films examined at magnification to determine whether other such areas could be identified. Several areas were found, one of which is shown in Figure 38. As with the previous leak location, only a very small pit was seen on the inner, propellant side of the diaphragm, while the gas side shows absolutely no anomalies or visible defects in the known leak area, view (b) of Figure 38. A magnified reproduction of the X-ray, view (a) of Figure 38, shows dramatically the same type of multiple cavity corrosion defect, seen in the previous sectioned

leak. Three major cavities and three minor ones are seen, covering a total area of 0.013 by 0.020 inch, in a diaphragm of only 0.009 to 0.010 inch thickness, and with only one surface indication or pit visible, a line 0.010 inch long by less than 0.001 inch wide. The preferential attack of internal surfaces, being the only surfaces where there was an oxygen depletion in the corrodent, is obvious.

The diaphragm from Tank No. 2 was also closely examined with fluorescent dye penetrant by applying to the propellant side, allowing the dye to sit overnight and using developer on the gas side. This procedure identified at least two additional leak sites. As with the sites identified by radiographs, the propellant side showed a minor pit while the gas side showed no visible evidence of any defect, even though the areas could be well located by the faint dye indication. This area is shown, from both sides, in Figure 39.

The occurrence of significant corrosion in this Tank No. 2 diaphragm made it necessary to further investigate the diaphragms of the other tanks in this series. Although no leaks were found in those other tank diaphragms by helium mass spectrometer, it was possible that corrosion may have started in a manner similar to that in Tank No. 2 and in fact might provide significant information for the analysis of the corrosion process occurring in this tank. The other diaphragms were dye penetrant inspected allowing the penetrant to sit on the diaphragm surface in some cases for 24 hours. No significant indications were found on the surfaces of Tank Nos. 1 and 3. A few very slight but perhaps significant

indications were found on Tank No. 4. Close microscopic examination of the surface did not disclose any pitting. An example is shown in view (a) of Figure 40. When that area was lightly polished, the appearance in view (b) was found. This gave rise to the possibility that some pitting or corrosion may have occurred in this tank. However, when the area was sectioned as shown in view (c) of Figure 40, the region was found to contain nothing but minor mechanical disturbance of the surface, probably due to handling or scratching having occurred at sometime during its manufacture or service. It seems evident that there were no similar corrosion cavities or other anomalies in the diaphragms of any of the other three diaphragm tanks and that the corrosion leakage occurring in Tank No. 2 was an isolated but dramatic occurrence.

c. Metallurgical Analysis

As has been shown in the previously discussed Observations, the diaphragm of Tank No. 2 contained extensive internal corrosion in several locations, at least six of which that could be identified. There was practically no surface evidence of this internal corrosion nor any concurrent surface corrosion. Instead, there was only very slight evidence of a pit or other disturbance of the surface. The internal shape of these corrosion cavities indicated that the stainless steel matrix was being extensively corroded in a manner which allowed substantial internal volumes of the stainless steel to be dissolved. This type of extensive internal corrosion can occur in stainless steel because of the need for stainless steel to have an abundance of oxygen to maintain its passivity and

normally good corrosion resistance. In a region in which there is lack of oxygen such as would occur at the root of a small pit in stainless steel, the oxygen depletion prevents the formation of the chrome oxides which generally provide the good corrosion resistance of this material. Once this pitting became internal and started to expand into the large cavities seen in the views of this section, this condition would have accelerated. The corrosion within these cavities would be due to electrochemical attack where the bulk of the diaphragm with its normal passive film acted as a cathode and the small internal areas where no passive film could be formed became anodic areas allowing a high rate of attack due to the concentration of the current density effects in the electrochemical attack. Once this condition began the extensive corrosion seen in these views could have occurred in a relatively short span of time. The condition is very difficult to arrest since it is almost impossible to obtain the necessary supply of oxygen to form the desired passive film within these internal cavities.

This occurrence of internal corrosion due to oxygen depletion, therefore, is quite understandable and what becomes more important for the significance of this and related aerospace hardware is the mechanism by which this internal corrosion started. It would be generally assumed that some small pit, cavity or crevice would be required before this internal corrosion could proceed. It seems most likely that some form of pitting attack of this stainless steel diaphragm surface occurred to start this internal cor-

rosion. Discussions with the Arde personnel about these tanks and a search of their manufacturing records indicated that although these tanks were being produced in an identical manner and to the design of similar hardware being used in the Minuteman program, the final passivating and cleaning steps normally utilized just before a tank of this type is loaded with propellant were not applied to these tanks at the Arde Company. They were procured by Edwards Air Force Base-Rocket Propulsion Laboratory on an as-fabricated basis with the understanding that they would be cleaned for the specific propellant which was to be later stored in them by the Rocket Propulsion Laboratory. At the time of their manufacture the specific propellant which was to be used was not identified. It appears likely that these tanks were placed in service without the passivating and precision cleaning normally necessary for stainless steel hardware. Any imbedded bits of iron or other tooling or other minor local contaminants may have remained on or slightly imbedded in the surface of the diaphragm when they were loaded with propellant. These minor contaminants could then have produced the start of pitting in a few selected locations of the diaphragm and that pitting would then have grown into the catastrophic leakage that was visible in the preceding figures. As will be discussed in the Conclusions and Recommendations sections which follow, the occurrence of this corrosion in this diaphragm lends further support to the need for rigorous cleaning operations of all liquid rocket tankage hardware which is destined for long term storage or flight usage. The corrosion observed, although dramatic in the

extensive internal cavities formed, produced only very slight leakage and practically no surface evidence of that corrosion and hence would have been very difficult to observe in any in-service inspection or other inspection before a tank might possibly be reused. As is emphasized in these later sections, it is necessary to apply rigorous control and careful handling on all hardware of this type during its fabrication and placement into service since it is so difficult to detect defects or anomalies such as this by any cursory examination.

2. Pitting on Exterior of Arde Tanks

a. Test History and Background

The four Arde tanks examined in this program had all been stored with N_2O_4 or ClF_5 propellant from July 1969 through 1977 in the oxidizer storage facility at Edwards Air Force Base. This facility, a separate Quonset hut, both insulated and with temperature and humidity controlled to provide a constant environment of 85°F and 85% relative humidity contains many tanks, storage systems and associated piping, hardware and manifolds. It has been observed by both Rocket Propulsion Laboratory personnel in their surveillance of this program and by Bell Aerospace Textron personnel in their examination of tanks in previous programs performed in this study that this storage room often contains rather high concentrations of propellant fumes when a tank, manifold, valve or similar hardware fails or leaks. When these propellant fumes, particularly of N_2O_4 or the ClF_5 type propellants become exposed to high humidity conditions, they hydrolize to form nitric, hydrofluoric and similar

acids. These acids form mists, droplets or films on most hardware in the immediate environment of any leakage, whether that leakage happened to have been associated with that particular tank or a neighboring one. Therefore, it must be assumed that the four tanks currently being examined had, during numerous times in their eight year storage history, been exposed to these very corrosive acid fume environments. When the tanks were received for initial visual examination in this program, Arde Tank No. 1 was found to have a dark spot, giving the cursory appearance of being an arc strike on the shell. This had previously been mentioned in Section V under the visual examination. Closer examination of the spot and its surrounding shell surface disclosed that there were numerous small spots or pits on the surface of the shell and a similar examination of the other three Arde tanks showed that they too contained occasional spots or pits. Therefore, this occurrence of pitting anomalies on the shells of the Arde tanks was designated for detailed metallurgical analysis.

b. Observations

The dark spot on the shell of Arde Tank No. 1 which had been identified in the initial visual examination is shown in view (a) of Figure 41. Visible around this dark spot are numerous, very small dots which turned out to be pits. When this region was examined at higher magnification, View (b) of Figure 41, it was seen that this pitting was quite extensive, some of the pits being rather shallow, others appearing to be quite deep. The pitting on Tank No. 1 occurred over much of its exterior

surface, not localized in any particular spot, but occurring in a random nature over a large part of the surface. The other tanks from the Arde series were also examined and found to have similar characteristics, that is, there was a general occurrence of very small pits, some of which appear to be quite deep, others quite shallow, occurring on a random basis over much of the circumference of the tank. There did not appear to be a preferential location for these pits. The welds joining the segments of the shells of these tanks also contained occasional pits, an example of which is shown in view (a) of Figure 42. The pitting on the welds was again of a random nature with no preferential pitting at what would normally be suspect areas such as the edge of weld or heat affected zone. During the eight year storage tests these four tanks all sat in a vertical position resting in circular holders. The location of these circular support frames is clearly visible as a light, superficial stain on the surface of the shells. It is interesting to note that the occurrence of pitting is neither preferentially larger nor absent in and around these stains representing the support frame in which the tank sat. There are some occurrences of pits along the line representing contact with the frame and yet there are many areas along this frame which obviously collected some liquids and fumes during the storage time which contained no pitting. This is a significant observation with respect to the starting of this pitting and will be discussed further in the Analysis Section.

When selected pit areas from two of these tanks were sectioned and examined for depth and configuration of the pits, the results in view (b) of Figures 42 through 44 were found. In general, the pits were of a hemispherical or spherical nature, extending as deeply into the shell thickness as they did around the surface. Some areas, however, contain very deep pits, an example of which is shown in Figure 43. This particular pit in Tank No. 1 extended approximately three-quarters of the thickness of the shell and undercut the surrounding surface beyond the pit area quite extensively. When the sectioning was continued farther from the visible surface pit, it was found that the internal pit had become a large internal cavity. This internal cavity encompassed over 80% of the thickness of the shell at this point and extended over an even greater width than that. There was some evidence that the internal cavity was extending along internal inclusion bands since there is some etching out of an inclusion band in the lefthand portion of the cavity as seen in view (c) of Figure 43. Other than this extension along the inclusion stringer, there was no preferential metallographic attack in these pits. They appear to consist simply of dissolution of the stainless steel matrix in an ever increasing volume. There was no intergranular cracking or transgranular cracking as might be expected from stress corrosion. There was also no crack extension or grain boundary penetration ahead of the major cavity in any of these areas. When sectioning through a pit in a shell weld, view (b) of Figure 42, even in this instance where a rather coarse microstructure could promote intergranular cracking or inter-

granular corrosion penetration, the pit formed was rather smoothly hemispherical. The corrosion cavities formed in this pitting are quite similar to those observed in the leaks in the diaphragm of Tank No. 2 which had been discussed in the above detailed analysis. The same characteristics are observed, that there is a slight surface pit which can in some instances enlarge into a very significant internal cavity.

These internal cavities extend well beyond the surface appearance of pitting to form very significant internal defects. However, in none of the pitting examined in these four tanks was there any evidence that the pits had extended completely through the shell thickness to form a leakage path. Nor was there any evidence from the visual examination of the exterior or interior of these shells that any leakage had occurred during service. Therefore, although these pit induced corrosion cavities were in some instances very deep, occupying more than 80% of the wall thickness of the shell, they did not actually cause any failure of the tanks in question.

c. Metallurgical Analysis

The occurrence of surface pits and deep subsurface cavities on the shells of these Arde tanks represents a similar occurrence from a corrosion standpoint to the leakage inducing cavities found in the diaphragm of Arde Tank No. 2. It can be well justified that a similar corrosion process occurred. That is, small pits are formed on the surface of the shell and at least some of these pits contained at their roots, oxygen starved or oxygen depleted liquid

environments which allowed internal corrosion to proceed. As described in the preceding metallurgical analysis, stainless steels derive their excellent corrosion resistance from the formation of passive oxide layers, primarily chromium oxides. In order for these protective oxide layers to form, oxygen must be present from the environment surrounding the stainless steel. At the root of a pit or an internal cavity where a corroding liquid exists which cannot have easy interchange with the air atmosphere containing oxygen, that corroding liquid will become quickly oxygen starved and a passive oxide film can no longer form on the stainless steel. In this case, the stainless steel surface without its protective oxide film becomes highly anodic to the passive stainless steel of the shell and corrosion proceeds rapidly.

As with the leak in the diaphragm of Tank No. 2, the important feature to be analyzed is the origin of the initial small pits on the surface since once a pit is formed the internal corrosion proceeds rapidly. The stainless steel making up the shells of these Arde tanks is a special controlled chemistry grade of 301SS designed to produce very high strength properties during the cryo-stretching operation that is applied to these tanks. This stainless steel alloy 301 is of a rather lean chemistry that is low in nickel and chromium in order to provide this high response to the stretching operation. The stainless steel will, in acid environments, form pits with relative ease. The pitting of the stainless steel such as this in any acid environment, particularly one con-

taining halide salts or acids is well known.

As part of the Recommendations Section which follows it will be noted that tanks of this material, if they are to be utilized in an environment known to have extended exposure to acid fumes or acid high humidity environments, should be protected with a protective paint or other barrier layer. The fact that pitting did not occur preferentially along the lines surrounding the area where the tanks were in contact with the support circles makes identification at the exact source of the pitting environment somewhat more difficult. As mentioned above in the Observations, although there was some pitting along this line, it was not preferential and not especially deep in this region. It does remain, therefore, a good possibility that the pitting environment which caused these defects in the shells was not during the long term storage tests but perhaps after storage was completed and the tanks were drained and placed in a holding area until they could be examined.

In previous programs corrosion had been noted that could be firmly established as having occurred only after draining when the tank was lying in an abnormal manner. This was not possible in this program. Past experience would indicate that it is equally as possible that the holding area for tanks after the storage tests but before their final evaluation would contain a similar high humidity acid fume environment which could promote

the pitting and this possibility should not be discounted in the consideration of these tanks. A further result or recommendation from this analysis is that every effort should be made, when considering flight usable hardware, that they not be stored in any room or manner in which fumes coming from other unrelated hardware be allowed to form acid environments which could adversely affect the tanks. Since there is no evidence of any leaks to the exterior of these tanks themselves it seems quite likely that if they had been stored in an isolated manner, unaffected by leakage, drainage or accidental propellant discharge from other systems in the area, that none of the pitting observed on these tanks would have occurred.

3. Surface Attack on Interior of Martin A-286 Tank

a. Test History and Background

The A-286 tanks evaluated in this program were produced by Martin Co.-Denver Division in 1968 through 1970 having a capacity of ten gallons.

The unique feature and one which affects several of the anomalies observed in these tanks is the use of explosive bonding to join the segments of the tanks rather than welding. Through this method sheet metal segments were rolled and then explosively bonded to form cylinders. Other sheet metal segments were explosively formed into domed shaped ends and then joined to the cylinders through explosive bonding. Outlet fittings were explosively bonded to their respective domes. Through all of these operations the explosive bonding process involves placing a plastic explosive

against one side of the overlapping joint, backing up the other side with a rigid frame either externally or internally depending on the configuration, igniting the explosive, thereby forming the bond. Several of the joints required to make these tanks involve the use of internal heavy steel mandrels to support the components while the explosive is applied to the exterior. Since these tanks had no flange ports in them, the removal of all internal mandrels required etching with a nitric-hydrofluoric acid solution. This solution was used both to remove the mild steel mandrels in the interior and also as a final cleaning solution after all work had been completed on the tanks. This background is included because it will be pointed out during several of the analyses that it is strongly suspected that some of the pitting and other anomalies appearing on the interior of these tanks were formed during the various fabrication stages that the tanks were submitted to rather than during propellant storage service itself. The propellant storage service for these three A-286 tanks consisted of loading them with ClF_5 in March 1972 and they remained in storage through 1977 for five years of total storage time. As with the Arde tanks previously discussed there are no detailed records to indicate that there was any difficulty with leakage or other anomalies during the storage of these tanks and in fact, exterior examination of these tanks shows absolutely no evidence of corrosion or propellant leakage. In 1977, at the completion of the five year storage period with chlorine pentafluoride, the tanks were all drained by Edwards Air Force Base and then stored preparatory to being shipped to

Bell Aerospace Textron for metallurgical analysis. Upon receipt, all tanks were leak tested with a helium mass spectrometer instrument and no leakage was found in any of the three Martin tanks. The various anomalies discussed in this and succeeding sections were only found upon sectioning of the tank to observe its internal surfaces.

b. Observations

In all cases the interior surfaces of the A-286 showed a frosting or etching, which varied in degree from area to area within a tank shell. The A-286 tank identified as Tank No. 5 possessed surface staining along the bond overlaps to a somewhat greater degree than the other A-286 tanks in this program. As shown in Figure 45, staining occurred at the edge of the solid state bond, and on the surface of the overlap area of the bond. It can also be observed that the internal surface views (a) and (b), Figure 45, were sanded or ground after the bond was made. The external surface edge showed irregularities along the edge of the joint in the circumferential direction and at the area of crossover. A crossover is formed when a dome is bonded to a barrel that contains one or more longitudinal bonds. The edge irregularities were of concern since they gave the impression that localized corrosion could have taken place in this area, although at first glance one could also form the impression that they were mechanically formed, being characteristic of this type of bond. At the crossover area, view (b) of Figure 45, on the inside surface a weld patch existed which is shown at higher magnification in view (c) of Figure 45. Cross sections of the various areas are shown in Figure 46. These views at a 100X magnification show that along the edge of the bond, in

the base metal, at the bond overlap and at the edge of the weld patch, surface attack of a shallow nature occurred. The degree of attack observed when one takes into consideration the exposure period, Table I, certainly is not of a significant magnitude to cause concern.

Detail examination of Tank No. 5 showed pitting to be present in the propellant side of the outlet fitting. This is shown in Figure 47. View (a) of Figure 47 shows staining along the bond and on the fitting surface. Pits in the surface of the fitting in the stain region are shown in view (d), Figure 47. The fabrication history for these tanks show that this fitting was machined from large diameter 321 stainless steel bar stock in a manner such that the surface exposed to the tank interior is a cross section of the original bar stock. Martin-Denver had encountered some difficulty with extensive inclusion stringers when bonding these tanks. BAT evaluation of this pitted surface of the outlet fitting showed that the pitting occurred in clusters, view (c) of Figure 47 and when studied in cross section, view (d) of Figure 47, showed that the pits followed intermetallic particle stringers.

In the examination of Tank No. 7 a distinct waterline was found to exist across the "midpoint" of the tank. This "waterline" led to further macroscopic investigation of the surface of this tank. In Figure 48, view (a), the waterline is shown and a closeup of the surface is shown at higher magnification in view (b). There was no difference in general surface condition of this tank in this "water marked" area. The closeup view as well as the cross sectional

views (c) and (d) extended the microstructural studies of the internal surfaces of these A-286 tanks. Although the "waterline" had prominence as far as visual appearance, it did not cause or add to the general pitting of the internal surfaces of these tanks.

c. Metallurgical Analysis

The exact cause of the internal surface pitting observed in these tanks is not known with technical certainity, however, from the fabrication history of these tanks, etching during fabrication to remove mandrels used to achieve explosive bonds was the probable cause of the surface roughening and pitting observed in the internal surfaces of these tanks. The mandrels were removed by etching with HNO_3/HF pickling solutions. In this process occasional stringers of carbo-nitride particles inherent in A-286, or inclusions inherent in other stainless steels, would have provided sites for corrosion attack especially of the end-grain type.

The photomacrographs and photomicrographs of surface pitting and roughness, particularly Figure 48, give further credance to the probability that the general pitting of the internal surfaces of the A-286, or 321 stainless steel was the result of pickling with HNO_3/HF to remove mandrels used for solid state bonding and not a result of the long term storage to ClF_5. The amount of attack observed is shallow and in retrospect did not harm or contribute in any manner to further surface corrosion during storage that could have affected the integrity of these A-286 tanks.

4. Split in Outlet Tube of Martin Tank No. 5

a. Test History and Background

During the visual examination of the internal surfaces and related components of Tank No. 5, one of the A-286 stainless steel explosive bonded tanks, abnormal staining and other effects could be seen within the upper inlet/outlet tube of the tank. This tube and tank boss assembly was therefore carefully removed from the tank and cut lengthwise for closer examination. When the inner surfaces of the tube were exposed, considerable staining and a transverse split or crack could be seen around approximately one-quarter of the circumference of the tube, as shown in Figure 49. This anomaly was therefore identified as one to be examined in a Detail Metallurgical Analysis.

There was no evidence of any leakage to the exterior of the outlet tube or boss region and therefore this defect or anomaly may have been present for some time, perhaps from the original bonding time. Since there was no external leakage, it would not have been noticed either in post-fabrication inspection, or during any in-service, or post-service surveillance.

b. Observations

As described above, this anomaly was first observed as unusual staining visible inside the outlet tubing of Tank No. 5. When the outlet tube was cut lengthwise to expose the interior, the appearance seen in Figure 49 was found. The tube interior was quite stained and along the circumferential line where the tube was most expanded, it was split over a portion of the circumference.

The split appeared to be mechanical in origin in that there was considerable evidence of deformation around the split area.

Close examination of the bonded tube near the split view (b) of Figure 49, shows that there are severe strain effects in all of the region around the maximum bulge of the tube. When the defect area of the bonded tube was sectioned (Figure 50), the defect was seen to be definitely mechanical in origin with the split occurring along a 45° shear plane adjacent to the maximum strain region in the bond. There are small secondary splits visible, views (b) and (c) of Figure 50, which are transverse fissures at inclusions. There are considerable strain effects visible at these inclusion stringers probably due to their effects as discontinuities when the explosive shock waves are passing through the material. These small fissures or splits may actually have preceded and initiated the main split. In the Martin-Denver report documenting the development of the bonding process, Reference 7, they report some difficulty with bonding of this tube and fitting because of extensive inclusions. The inclusions are discernible in view (c) of Figure 50. A cross section along the tube to fitting bond, 180° away from the split, is shown in Figure 51. The views of Figure 51 show that there were considerable inclusions in this portion of the tube also. Along the widest part of the expanded tube joint there were 45° shear strain indications in this section 180° from the split. These are shown by the arrow in view (c) of Figure 51.

In the area between the tube and fitting of Tank No. 5 there was a slight gap which was opened to the interior of the propellant tank by this split in the tube. Close examination of this cavity,

Figure 52, in cross sections showed no evidence of significant corrosion. However, it is believed that the minor or superficial corrosion of the exposed surfaces in this crevice was the source of the stains which "weeped" back out of the split to discolor the tube interior around the split, and make it so visible.

The explosive bond between the tube and fitting for Tank No. 5 is shown in Figures 52 and 53. Because of the gap between tube and fitting in the bulged region, there are two portions to the bond, the portion between the bulge and the tank interior and the portion beyond the bulge, toward the exterior. The bond in the portion between the tank ID and start of bulge showed good strain and metallurgical bonding effects with good "wave" effects. This is shown in view (a) of Figures 52 and 53. The bond beyond the bulge, view (b) of Figures 52 and 53, showed a much poorer bond with no wave or strain effects. There was evidence of surface layers and contaminants remaining along the bond interface. However, this bond region had obviously remained leak tight during fabrication and extensive storage service. Therefore, the bond was evidently sufficient for the intended service.

Close examination, including metallographic sectioning, showed that no similar split was present in the other two Martin tanks examined in this program. There were strain and deformation effects in the bulge regions similar to those already described, but no splitting or separation in the tubes.

c. Metallurgical Analysis

The bond between the tube and fitting in these tanks was produced by the explosive bonding process, as were all other joints. The explosive bonding of this component was performed by placing the tube within a machined fitting, and placing the explosive charge inside the tube with ignition starting near the tank ID so that good bonding is achieved as the tube is explosively forced outward against the fitting. Details of the bonding process and its development are found in Reference 7. To aid in that bonding, the fitting is recessed to a depth of 0.075 inch larger than the nominal tube OD, giving a strain of 27.3% when the tube expands to the limit of that recess. The portion of the tube closer to the tank interior must also expand, approximately 0.035 inch per side or 12.7% during the bonding process.

For austenitic stainless steels such as the 321 grade used in this component, deformation or strain of 27% during the bonding process should not be difficult to achieve nor should it cause any degradation of the tube. This is verified by the fact that all of the other tube joints examined in this group of three tanks showed no splitting.

The split in this tube from Tank No. 5 is evidently the result of excessive amounts of unfavorably placed inclusions in the tube, causing the shock effects in explosive bonding to be localized and perhaps intensified in the region of maximum strain. When the explosive shock waves from the bonding process pass through the tube and strike the discontinuities represented by the inclusion

stringers, they can be expected to cause enlargement and separation of these discontinuities. A combination of these enlarged discontinuities, occurring in the bulge region where substantial strain must occur as part of the bonding process, is quite likely to cause significant stress concentrating effect. This would make the tube likely to split, even though the apparent strain of 27% should have been within the capability of the material.

This defect, although not causing any actual leakage of the tank, is an indication of the need to have close control and surveillance over the bonding process and its resultant products. Minor variations in incoming material quality or in the bonding process itself may cause defects or degradation of components that were not expected from any process development program. In this aspect, explosive bonding is no different than fusion welding. The most complete nondestructive test procedures feasible should be planned to thoroughly examine bonded hardware, just as is needed to examine critical welds in fusion welded hardware.

5. Pitting at Bond in Outlet Fitting of Martin Tanks

a. Test History and Background

During the visual examination of the interior of the Martin A-286 tanks, Tank Nos. 5 and 7, a bump or protrusion with pitting in the center of the protrusion, was seen near the dome to outlet fitting. Since the pitting in that bump gave the impression of being quite deep, compared to the typical shallow attack seen over the entire surface, this anomaly was designated for detailed

metallurgical analysis. The protrusion or bump was obviously related to the bonding process, but as with the other cases of pitting or interior surface etching of these A-286 tanks, it is difficult to say whether the 5 years of propellant, ClF_5, exposure played any role in the observed pitting.

b. Observations

The bump or protrusion was seen on both Tanks No. 5 and No. 7 at the same location, on the dome about 1/8-inch from the outlet edge of the machined outlet fitting. A view of one of these bumps is seen in view (a) of Figure 54. On the exterior of the dome, there was a radial line at the same location of this interior bump. This bump or protrusion occurred at the outer edge of a flat spot in the dome, apparently where the dome had been in contact with a backup mandrel used to support the assembly during fitting to dome explosive bonding.

As can be seen in view (a) of Figure 54, there was a definite pit or hole in the center of the protrusion, much deeper and more pronounced than the general pitting of the surrounding area.

When sectioned, the pit in the protruding bump was found to be quite deep, approximately 50% of the dome thickness, as shown in view (b) of Figure 54. However, instead of the generally hemispherical or spherical pits found in other areas of the Martin or Arde stainless steel tanks, the pit in this region was quite irregular and preferentially followed elongated paths. When the region was further examined by polishing 0.020 inch farther into the sample (away from the bond), the attack was found to continue,

even though there was no further surface evidence. This is shown in view (a) of Figure 55. The attack had the same general features as at the original section, with a central cavity, and the suggestion of "arms" extending into the interior of the dome wall at approximately 45° to the surface. When the corroded zones were examined at higher magnification, view (c) of Figure 54 and view (b) of Figure 55, the attack was seen to be rather selective. Areas around the intermetallic particles in the A-286 matrix were attacked and these areas were joined by rather tight cracks or fissures. This combination of selective attack of the A-286 microstructure components and the indication in several of the views of Figures 54 and 55 that the zones of attack were sometimes not connected to each other, gave rise to the possibility that the attack was not of a common corrosion variety.

When other areas around the periphery of the fitting to dome bond were examined, by sections in the radial direction, where the relation to the bond could be preserved, extensive strain evidence or even small cavities and separations could be seen, Figure 56, in essentially the same location 0.1 to 0.2 inches away from the edge of the outlet fitting. These strain effects are also quite visible in the sections taken through an identical protrusion and pit in Tank No. 7. Various views of this pit and its cross section are shown in Figure 57. Its surface appearance, views (a) and (b), was essentially identical to that of Tank No. 5. A cross section was made in the radial direction through the central region of the pit, views (c) and (d) of Figure 57. These views are

90° from the cross section shown in Figures 54 and 55 for the pit from Tank No. 5. This explains why the cavity in Tank No. 7 looks somewhat different in overall shape from that in Tank No. 5.

Although the apparent overall shape may be slightly different, the pitted cavity has the same characteristics. It does not represent a volume of metal completely dissolved by a corroding medium. Instead, it is a region in which susceptible portions of the matrix were attacked by a corroding medium which entered the material along pre-existing cracks or fissures, or by attacking selective regions. By careful polishing and light etching, view (e) of Figure 57 was obtained. This view shows intense strain effects ahead of the corroded region, in the direction toward the bond. These strain effects are irregular or "swirled" but generally formed layers within the dome material. It is evident that the pitting has followed these strain patterns or perhaps minor separations or fissures within these strain bands. The total extent of the pitting within this region of Tank No. 7 is approximately two-thirds of the dome wall thickness, indicating that this was a quite serious occurrence. Although no failure or leakage resulted from this deep pitting, it is likely that if this had been a highly pressurized storage service, the tanks might well have failed.

c. Metallurgical Analysis

The appearance and shape of the dome to fitting bond and surrounding areas made it quite evident that the location of the bump and pitting was at the end of the explosive firing travel.

With the explosive firing wave travelling around both sides of this annular joint, the finish point will have extreme shock or strain effects where the two explosive waves meet. This has caused the slight protrusion or bump on both the interior and exterior of this joint.

Review of the Martin-Denver fabrication report, Reference 7, for these tanks showed that this dome to fitting joint was particularly troublesome to achieve consistent high quality. The same joint, when applied to titanium alloy components was particularly difficult. Figure 54 of Reference 7 shows a crack in the titanium dome component at precisely the location of the high strain and pitting in these A-286 components. The reason for the particularly severe strain 1/8-inch away from the bond is seen in the joint configuration, Figure 22 of Reference 7. At this location the dome component is bent or flared to achieve the desired collision angle between the dome and fitting components. Recognizing the limited ductility of titanium, particularly compared to A-286 stainless steel, it is evident that very high strain and shock effects are imparted into the dome at this location during dome to fitting bonding. In the case of titanium tanks, this high strain was sufficient to cause immediate, mechanical failure. In the case of the A-286 stainless steel, its excellent ductility prevented immediate mechanical failure in this location but did leave the matrix highly strained and quite susceptible to rapid corrosion. On a microscopic scale, the strain and shock effects would be magnified even more around inclusions or intermetallic

particles, because of the local interface effects. This probably explains why the attack appeared preferentially along or around these particles in the matrix. This corrosive attack would be much more severe than normally expected for the stainless steel, particularly at the end of bonding location where the shock and strain effects interact and overlap.

As with the other instances of pitting in these A-286 stainless steel tank interiors, it is not possible to specify whether the corrosive attack occurred during fabrication, storage service with ClF_5 or perhaps during the post-storage hold time before evaluation. As with the other Analyses, it seems most likely that this attack occurred during fabrication when nitric/hydrofluoric acid was used to etch away the steel mandrels used to support the shell during dome to cylinder girth bonding, and also to clean the tank after fabrication was complete. The HNO_3/HF solutions are known to lightly pit A-286 surfaces and must generally be used with extreme care and only for short times in cleaning of A-286 components. A location such as this highly strained "bump" region, could be expected to pit rapidly and deeply when exposed to the nitric/hydrofluoric acid solution.

6. Interior Stains and Pitting at Bonds

a. Test History or Background

In examing the interior surfaces of the A-286 tanks, one of the first observations made was that along the solid state bond line there existed prominent stains and deposits. Metallographic examination of these areas, which from color and extent of the deposits became suspect areas for corrosion, were carried out on Tank Nos. 5 and 6.

Work was initiated on stains and pitting in close proximity to bond lines on Tank No. 5 and then expanded in scope to cover Tank Nos. 6 and 7. Although different bond line areas in each tank were studied the observations made showed that the general corrosive attack was quite similar from tank to tank.

Determining the initial cause of the corrosion presented in this section was not possible from metallurgical attributes. The degree of attack observed after sectioning was not extensive and could easily have come from a pickling operation such as that used, Reference 7, as part of the cleaning process, prior to storage.

b. Observations

The internal surface of Tank No. 5 was studied initially since an etched groove was observed along the longitudinal solid state bond Figure 58, view (a). The configuration of the overlap plus the crevice is shown in view (b), with higher magnification photomicrographs of the type of intergranular attack shown in views (c) and (d). In the fabrication of this bond an explosive charge is placed on the inside of the tank. The shallow intergranular attack observed seems to indicate that there may have been a direct connection between the surface reaction observed, which could be attributed to the surface being disturbed by the explosive charge, thereby becoming more susceptible to the HNO_3/HF pickling solution. The degree of attack found in this Tank, No. 5, should be considered minor, being highly localized and not

in any manner attributed to a surface reaction occurring during propellant storage.

Staining was observed in the bond overlap region on the interior surface of Tank No. 6. This staining of the surface occurred in the girth area of the tank where the cylinder is joined to the dome. In making this joint the explosive is on the outside surface, therefore, in contrast to Tank No. 5, the corrosion of this A-286 surface is not the result of a disturbed surface being attacked but is the result of direct attack, which may also be the case for Tank No. 5. Once again, the attack is very shallow in nature and highly localized allowing for the postulation that this type of staining and corrosion is the result of a pickling process performed on the tanks prior to storage. Figure 59 shows surface views of the bond overlap region on the interior surface of Tank No. 6. The degree of attack is presented in the cross sectional views of Figure 60 and is very shallow in depth.

Further studies were conducted on the outlet boss of Tanks No. 5 and No. 6. Figures 61 and 62 show views that are quite similar to each other where pits and corrosion were found and indicate that liquid had leaked out from inside the bond leaving deposits along the bond. No leakage to the outside was observed so microsections through the bond were prepared.

These sections showed that there was an extensive cavity along the bond interface, Figure 63. The only sound bond was a short segment at the exterior side of the bond where the dome overlaps the fitting. All of the rest of the overlap was unbonded and generally separated by a gap 0.001-0.005 inch. Although the

interface toward the tank interior was tighter than the other cavity regions, it was not bonded, hence liquid could be entrapped in that cavity and then work back out. The trapping of etching solutions, propellant or even water in a tight cavity with no exposure to air could easily produce an oxygen starved environment in which stainless steel is no longer protected by a chromium oxide film, and will be corroded. The high magnification views in Figure 63 show a layer of scale formed by such a corrosion process. The gradual leaking of some of this corrosion residue back to the tank interior produced the observed stains and deposits along the bond interface.

Examination of the internal surface of Tank No. 7 showed that after propellant draining a "puddle" of propellant remained for some period of time. This was shown in the overall view, Figure 25. Figure 64, view (a), shows a closeup of the staining observed in this area. In view (b), Figure 64, the surface attack is shown and also the residue of corrosion products found in this area. View (c), Figure 64, shows the degree of attack that occurred. This condition has been observed in other tanks and is the direct result of incomplete draining or drying after the tank is removed from storage.

c. Metallurgical Analysis

Examination of the interior surfaces of the A-286 tanks where stains, deposits and discolored areas existed has shown that the corrosion present was limited to discrete areas and was not extensive. The solid state bond edges, where overlaps exist,

are potential areas for crevice corrosion. Considering the exposure to the oxidizer, these tank surfaces showed no degradation and the overall structural integrity remained sound.

Establishing the initial causes for the corroded areas presented herein is not possible. Postulations made as to the initiation of these stains, deposits and discolored areas as being the result of pickling prior to storage would seem to be the most plausible explanation. Overall the attack on any given tank was shallow and found to be quite limited in depth or penetration of grain boundaries.

7. Metallographic Evaluation of Explosive Bonds

a. Background

The three (3) A-286 stainless steel tanks fabricated by Martin-Denver Co. and evaluated in this program are unique in their use of a solid state explosive bond to join the components into the tank configuration. Some of the unique features of that bond have already been discussed in the previous detail examinations since they affected corrosion or other service associated features. However, the unique nature of this bond and its possible application for further aerospace hardware has made it quite desirable to perform in-depth metallurgical studies of these bonds, whenever possible, so as to increase the available data base for the application and evaluation of this explosive bonding process. A report summarizing the development and evaluation of these bonds plus their specific use in fabricating the containers being examined was issued by the Martin-Denver Division as Reference 7. The

evaluation performed by Bell Aerospace Textron on these three particular tanks has followed much of the same pattern and concept as used in the evaluation by Martin-Denver. It should also be emphasized that in no case has the work in this particular program found any features of the bond which are widely different from those already discussed in the referenced report. It was the intention of this detail metallurgical analysis of the bond obtained in several key portions of the propellant tanks to provide additional background information on this bonding process to be available in the future if the bonding process should be desired for use on flight hardware or other critical items.

The solid state explosive bonding process has several unique features, which were described in the Martin report, Reference 7, among them the ability to join components into a propellant tank without the use of welding. The fusion welding is a generally well understood and controlled process alllowing high quality reliable hardware to be fabricated. It is true that there are some materials, which are extremely difficult to weld and other materials in which the procedures and equipment needed to produce high quality welds result in a very expensive process. It is for this reason that the solid state explosive bonding procedure seems to have definite advantage in some selected areas. It must be admitted that for A-286 tanks specifically being evaluated in this program, there appears no overriding need to utilize explosive bonding as fusion welding can be used quite successfully provided certain precautions are met. However, the objective of the program instituted by the

Air Force Rocket Propulsion Laboratory at Martin-Denver was well founded in providing an opportunity to fabricate some tanks under realistic production processing conditions and then perform long term storage tests with this propellant tankage in order to obtain realistic data on the serviceability of these tanks. Thus, although these particular A-286 stainless steel tanks could probably have been fabricated equally as well and perhaps of slightly higher quality by using more conventional fusion welding techniques, the opportunity to prepare some tankage using this experimental process and then subject it to a propellant exposure service of approximately 5 years represents a unique opportunity to examine this advanced fabrication process. This particular detail examination will cover those aspects of the diffusion of the solid state bonding which provided unique features and yet did not produce any detrimental corrosion effects or other anomalies such as had been discussed in the previous examinations.

b. Observations

The four primary solid state bonds being considered in this examination are the longitudinal cylinder joint, the circumferential dome to cylinder joint, outlet to dome joint and diaphragm stub to dome joint. This last joint was a stainless steel foil diaphragm stub explosively bonded to the dome to simulate the joint that would be used if a positive expulsion diaphragm or bellows device was included in these tanks. These four joints will be considered separately below.

(1) Longitudinal Cylinder Joint. The longitudinal cylinder bond which joins the edges of the rolled sheet to form the central cylinder portion of the tank is the first major bond formed in the processing of the tank. The joint is made by positioning the overlapping edges of the rolled sheet in a massive external mandrel, applying the explosive strip to the interior of the bond surface and then detonating that explosive. Examples of the metallographic appearance of the bond from two different tanks are shown in Figures 65 and 66. A low magnification cross section of this bond is shown in view (a) of Figure 65 and shows the characteristics of this scarf joint in which the edges of the overlapping sheets are ground flush after the bonding so that the joint has a smooth appearance. This was particularly necessary because this joint is made before the circumferential cylinder to dome joints and this bond is required to fit smoothly along the interface of the succeeding cylinder to dome bond. The most obvious characteristic of this bond, as seen in view (a), is the straight bond or actual lack of bonding at the outer and inner edges of the scarf-type of joint. There is a slight separation between the overlapping surfaces at the inner and outer periphery of the bond. As has already been discussed with other bonds in previous detail metallurgical analyses, these unbonded and slightly separated regions provide cavi es which can trap liquids during processing or service and form pockets of slight corrosion. The lack of bonding extends inward approximately 10% of the bond length both from the exterior and interior surfaces. However, this lack of bonding for almost

20% of the bond interface did not degrade the tensile properties across this joint as has previously been discussed in Section V.C. The lack of bonding also did not cause any leakage problems through this joint. The central region of the bond is quite leak-tight and structurally sound and provides sufficient strength to insure that failure does not occur in the bond when a tensile test is performed across these joints. As will be discussed below, however, this lack of bonding, forming a notch at each edge of the bond could be expected to be detrimental to fatigue or other cyclic service performance. The bond interface itself showed several distinctly different regions. The central portion of the bond shown in views (d), (e) and (f) of Figure 65 and (b), (c) and (d) of Figure 66 represent areas where very good bonding was produced by the characteristic jetting and wave formation in the explosive bond. The details of the formation of these waves during the jetting action are covered in the Discussion Section, which follows. The primary observation to be made in this region is that excellent intimate contact and metallurgical bonding has occurred over at least a portion of each wave in this region. One portion of each wave formation also contains a pocket of molten and then refrozen material which formed during the intense plastic deformation of the bonding process. Within some of these melted zones, pores or cavities have formed. Successive polishing stages through these bonds showed that none of the pores or cavities as seen in these views extended for any significant depth along the bond, but rather appeared to be roughly spherical and therefore had

maximum dimensions no greater than the 0.002-0.005" dimensions shown in these views. The excellent bonding and grain growth which occurred in the other portions of each individual wave are quite obvious in examination of these views. Towards each end of the bond in the region approaching the unbonded and slightly separated zones there was a length of interface with no apparent wave action or a very slight ripple to the surface. Along these regions the two components were in intimate contact with no cavities or molten zones created, but without the intense jetting action. The surface oxides, films and other contaminants were not removed and hence a true metallurgical bond was not formed. Examples of these regions are seen in view (c) of Figure 65 and view (a) of Figure 66. These regions are probably sufficiently bonded to aid in providing mechanical strength during constant load service or a tensile test. However, these regions could be expected to be quite susceptible to rapid failure during cyclic service or fatigue stress.

(2) Circumferential Dome to Cylinder Joint. The circumferential dome to cylinder bond is formed, when the dome is joined to the previously bonded cylinder section in a joint wherein the cylinder section is placed within the slightly coned-shaped edge of the dome, using a heavy steel mandrel to back up the interior joint surface. An explosive tape is then applied around the exterior of the bond and ignited. The overlapping bond region of the cylinder segment is tapered slightly in thickness to provide a scarf-joint construction. Examples of this joint from Tanks

No. 5 and No. 7 are presented in Figures 67 and 68. Again, a low magnification view in each figure provides an overall illustration of the joint shape and configuration. It can be noted that the outer surface of the joint after bonding is left in the as-bonded condition with a rather rough and irregular protrusion of the dome component. Even at low magnification the configuration of the joint is quite obvious with a central region having a pronounced wave effect, whereas towards each surface the bond becomes relatively flat with unbonded regions or even slight cavities formed. Metallographic examination of the bond region as seen in Figures 67 and 68 showed this bond to be somewhat different in appearance from that previously described for the longitudinal cylinder joint. In this particular bond there was evidence of intense strain effects in the mating surfaces on each side of the joint producing a pronounced feathery band on either side of the joint. Close inspection along the interface line within this heavily strained band shows occasional regions, that had obviously melted during the bonding process and formed either slight gas pores or other cavities during this bonding process. At no point did the wave action in the bonding appear to produce the crest or overlapping wave effects seen in the previous bond. Instead, the wavy portion of this bond contained a smooth sinusoidal wave shape. It can be noted that the proportion of wavy bond compared to the essentially flat and straight bond portion of the joint is much less in these dome cylinder joints. However, again, there is no evidence of any leak paths from interior to exterior and no loss

in structural integrity as measured by ultimate tensile strength, whe· tests were performed across these bonds. There are substantial leng hs of flat bond region showing a layer of foreign or oxide material along the interface not removed by the jetting action. The presence of the visible intense strain patterns on either side of this joint and their absence from the longitudinal cylinder bond is not well understood, but as will be discussed in the Analysis Section which follows, probably indicate slight differences in the collision velocity and collision angle formed when the two components come together during the explosive bonding process. In view (c) of Figure 68, a set of short cracks are visible in the molten zone within each wave. These cracks in no case extend more than 0.005" in any direction. However, they do illustrate a potentially degrading feature of this bonding process in that molten material is formed during this process and it is no longer a truly solid state bond as generally described. Whenever a molten zone is formed, there is the possibility for "hot-short" cracking or other freezing effects, which can cause defects and anomalies similar to that found in fusion welding. Again, this feature will be discussed below in the Analysis Section.

(3) Outlet Fitting to Dome Joint. This bond is formed when the explosively formed dome is joined to the machined outlet fitting by placing the explosive strip around the outer periphery of the joint with the dome overlapping the outlet fitting on the outside and backing up the interior of the outlet fitting with a massive steel mandrel. The outlet fitting is machined with a

tapered faying surface, whereas, the dome is left with constant thickness but with the shell bent upwards to achieve the desired collision angle. As seen in view (a) of Figure 69, the cross section of this joint achieves the desired scarf interface surface by the machining of the outlet fitting. The dome segment itself remains with a somewhat irregular overlapping configuration. The extensive corrosion seen in the righthand corner of view (a) of Figure 69 has already been discussed as part of Detail Examination No. 5 in this section. The metallographic appearance of this bond interface is shown in views (b) and (c) of Figure 69 for Tank No. 7. As with the dome to cylinder joint there is only a short length of wavy bond with the bulk of the bond interface being essentially flat and often showing slight cavities or unbonded areas.

In metallographic appearance the wavy bond portion of this joint is slightly different from both of the previous joints discussed. Although a definite wave action is noted in view (b) of Figure 69, there is very little obvious strain markings showing as was the case with the cylinder to dome bond, nor is there the intermittent, excellent bonding shown by the longitudinal cylinder bond. Instead there is an almost continuous layer of material between the two components with occasional regions in the overlapping portion of the waves, where there is an obvious molten zone. The other portions of the wave, however, do not show high quality metallurgical bonding between the components. These components, one being machined 321 stainless steel bar stock and

the other explosively formed A-286 stainless steel sheet metal do have slightly different microstructure appearances. However, it is still evident that there was only intimate contact and not the removal of surface oxides and films as had been the case in the previous two bonds. Therefore, even in this wavy bond region the metallurgical quality of the dome to fitting bond must be considered poor. When the flat portions of this bond are examined, view (c) of Figure 69, the bond quality is seen to be even worse. There are occasional pores or cavities along the bond line itself and an almost continuous film of oxide or foreign material that was not removed in the desirable jetting or wave action of the bonding process. The metallographic section shown in this Figure 69 was from Tank No. 7. It should be noted that in the metallographic section from Tank No. 6 which had previously been discussed in "Detail Metallurgical Analysis No. 6", which preceded this section, the bond for this outlet fitting to dome joint was even poorer with a considerable length of the interface completely separated and bonding only over a very short length of the interface. Thus, it is apparent that the bonding parameters used for this joint gave a poor and intermittent bond, one which was capable of sealing and avoiding any leak paths, but not one in which the large proportion of the interface was bonded nor one which would be satisfactory from a structural standpoint.

Another interesting feature of this outlet fitting to dome joint was the occasional tearing loose of the inner edge of that joint. As can be seen in Figure 70, when examined at some

magnification, the inner edge of the bond between the outlet fitting and the dome was slightly separated and gave the appearance of being torn. This is shown in view (b) of Figure 70. When examined in a metallographic cross section through one of the areas, where the tear did not appear to follow the exact joint interface, view (c) of Figure 70, it can be seen that the extreme edge of the joint was bonded but that the thin tapered edge of the outlet fitting separated or tore at some stage either during the bonding process itself or during processing or service. In this way the length of unbonded interior joint interface was open to the interior of the tank. A slight amount of corrosion can be seen, wherever the outlet fitting and dome components came together. This can be seen in view (c) of Figure 70. At the junction between the dome and fitting there is corrosion both in the interior of the tank and within the bond interface where the split in the outlet fitting allowed that bond interface to be exposed to the interior of the tank.

(4) Diaphragm Stub to Dome Joint. This bond was added to the dome portion of each of the tanks to simulate the type of joint that would be necessary to join a positive expulsion device to the interior of a propellant tank such as this. No positive expulsion device was actually used, rather a simple strip of stainless steel foil was used to simulate the diaphragm or bellows that would be used in this device.

The metallographic appearance of the joint produced with this diaphragm stub is shown in Figure 71. The joint interface

covered a distance of approximately 0.3", however, less than one-half of that interface length actually contained a bonded interface. The bond seen in view (c) of Figure 71 did not contain the wavy or highly strained material normally associated with good bonding in A-286 or other stainless steels. However, there did appear to be intimate contact between the AISI 321 stainless steel foil simulating the diaphragm and the A-286 stainless steel tank shell dome. It must be concluded that the very thin stainless steel foil, while being brought into intimate contact with the shell, did not provide the type of collision velocity and collision angle normally needed to produce the characteristic wavy joint. The balance of the joint interface contained material in which there was an obvious gap or foreign material between the two components and hence no significant bonding. Attempts to peel portions of the diaphragm stub away from the shell showed that the diaphragm foil material would tear rather than separating the bond, indicating that the bond did have good structural strength. However, it is somewhat doubtful that this bond would have been leak tight and hence may not have been suitable for the intended purpose of joining a diaphragm or other positive expulsion device to the shell.

c. Metallurgical Analysis

Explosive bonding, although a complex process operating at velocities equal to or approaching the velocity of sound in the material, is a reasonably well understood process. The critical features of the process in producing a sound metallurgical bond

between two materials are the ability of the process to remove or render harmless the naturally occurring oxide films and other contaminants on the surface of any two mating metal surfaces. These metal surfaces, no matter how carefully cleaned and prepared, will inevitably have layers of oxide or other contaminant materials and the explosive bonding process, like any other bonding process, must remove these materials. The mechanism by which these contaminating layers are removed in an explosive bond is by the formation of a collision between the two metals to be bonded at sufficient velocity and proper angle such that a jet is formed which sweeps away the contaminating films from the mating surfaces. This jet formation occurs when the collision velocity between the two materials is sufficiently high, near the velocity of sound in the material, and the collision angle between the two materials is proper such that material at the point of impact is blasted loose and blown clear of the joint as the bond is being produced. The jetting impact between the two components must be sufficient to sweep away those oxide layers and any interfering irregularities between the two materials such that the material behind the jet, when brought into intimate contact, consists of only clean metal surfaces which can then, upon the action of the extreme pressures generated by the explosive, form an intimate metallurgical bond. Since the bond occurs with collision velocities approaching the speed of sound in the material, it should be a slightly unstable situation, alternately causing depressions in one and then the other component of the bond. This alternate impact into one or

the other component is what produces the wave interface commonly associated with explosive bonds. When this wave action is coupled with a proper jetting velocity to sweep away the oxides and surface contaminants, an excellent bond such as that in the longitudinal cylinder joint shown in Figure 67 will be produced. When the collision velocity or collision angle is too low to produce proper jetting effect to remove the surface layers, the relatively flat and poor bond seen at the ends of these joints or seen over much of the length of the outlet fitting to dome bond will be produced. The wave action generated by the instability of the collision at sonic speeds has the desirable advantage of breaking up any tendency from minor porosity or collection of oxides along the joint interface such that even when minor defects or anomalies are remaining in the joint they are isolated and cannot cause major unbonded regions or difficulties in the bond. The presence of pockets of melted and refrozen material along the joint interface, whether wavy or flat, is an indication of the extreme amounts of energy imparted to the joint by the explosive bonding process. The extreme energy generated and released along the collision front is sufficient to melt at least thin layers of the adjoining materials and then during the wave action of the collision process these thin layers of molten material collect in the pockets. This generation of molten zones in an explosive bond leads to certain problems not normally expected in what is described as a solid state bonding process. Because of the presence of these molten zones, it must be realized that this is not truly a solid state

process occurring only between solid materials. Instead, at least small pockets of molten material are generated and these pockets can lead to the difficulties of hot shortness or cracking usually expected only in a fusion weld. As was described in the "Observations Section", these pockets of molten material are isolated from each other and generally surrounded by well bonded material in other segments of the wave action. Therefore, even though minor porosity or cracking may occur in the molten zones they will not generally cause any degradation of the bond. It is for this reason that the presence of molten zones in the explosive bonding process do not cause any serious difficulty even in those materials where brittle intermetallics or other unusual conditions occur when the two materials being bonded are brought together. The explosive bonding process does have several critical variables, particularly embodied in the collision velocity and collision angle. It is believed from the examination of the bonds in these tanks that minor variations in these critical parameters are the cause of some bonds showing little or no apparent strain influences on either side of the bond while other joints, particularly the circumferential dome to cylinder bond, showed extensive layering of feathery strain effects on either side of the bond interface. There is no evidence that these strain effects, although quite prominent in the microstructure, cause any degradation of the metallurgical or structural integrity of the joint. It must be admitted that if this material being bonded had less tolerance for strain and deformation than the A-286 used in these tanks, perhaps the

presence of the considerable amount of strain in the joint could have led to degradation of the joint. The variability of the metallographic appearance of the bonds produced does, however, point out that this bonding process cannot be considered as a simple, routine process capable of low cost joining under a wide variety of production processing conditions. Instead, in order to produce desirable high structural integrity and leak tight joints as would be required in a propellant tank, the bonding process must be closely controlled, both to the geometry and interface angles of the mating components. The type or intensity of explosive charge applied and the degree of structural restraint provided by mandrels are other features that must be closely controlled.

Thus, while this joining process appears to offer significant advantages from cost and convenience standpoint compared to fusion welding, it would still be necessary to apply stringent controls on the bonding process itself in order to insure that consistent high quality and leak tight bonds are produced. Another feature of these bonds not readily considered in this particular program, but perhaps of very great importance in the application of this bonding process to flight hardware, would be the strong possibility, that these types of joints would not be suitable for any structure in which significant fatigue or cyclic load service is required. All of the joints examined in this program contained some degree of unbonded interface near either edge or in some cases actual cavities, where the two surfaces did not come into contact during the bonding process. While these unbonded edges of the bond caused no degradation

of ultimate tensile strength properties across the bond, this does not offer any assurance, that the preexisting notch effects in the unbonded region would not cause difficulty under cyclic stress. In fact, it seems quite likely that notch effects in these bonds would cause a degradation of structural integrity during cyclic loading. It is difficult to establish any general statement as to whether fatigue or cyclic load capability would be required for propellant tankage as all specific systems generally have slightly different operating and service conditions. However, in general it is usually assumed that there are significant cyclic stresses, even in a propellant tank being held at nominally constant operating pressure. These variations in stress occurred due to temperature cycling of the surrounding environment and the variations in applied pressure as caused by regulator operation and pressurizing gas supply. An additional source of cyclic stress service is the several cycles of stress applied to a tank during its fabrication, testing and initial preparation for service. It seems quite likely that tanks such as these with a preexisting notch due to the explosive bond might suffer some degradation in service life just due to the several cycles applied in fabricating tanks, proof testing them and preparing them for service. These effects would have to be studied in detail, through the testing and evaluation of flight type hardware, before the use of a bonding process such as this could be allowed in most critical systems.

It should be emphasized, however, that these particular tanks, although having some deficiencies in the bonds produced,

AD-A068 488 BELL AEROSPACE TEXTRON BUFFALO N Y F/G 21/9.1
CHEMICAL AND METALLURGICAL ANALYSIS OF PROPELLANT STORAGE VESSE--ETC(U)
FEB 79 E J KING, H G KAMMERER F04611-78-C-0012
UNCLASSIFIED 8795-927002 AFRPL-TR-79-6 . NL

2 OF 2
AD A068488

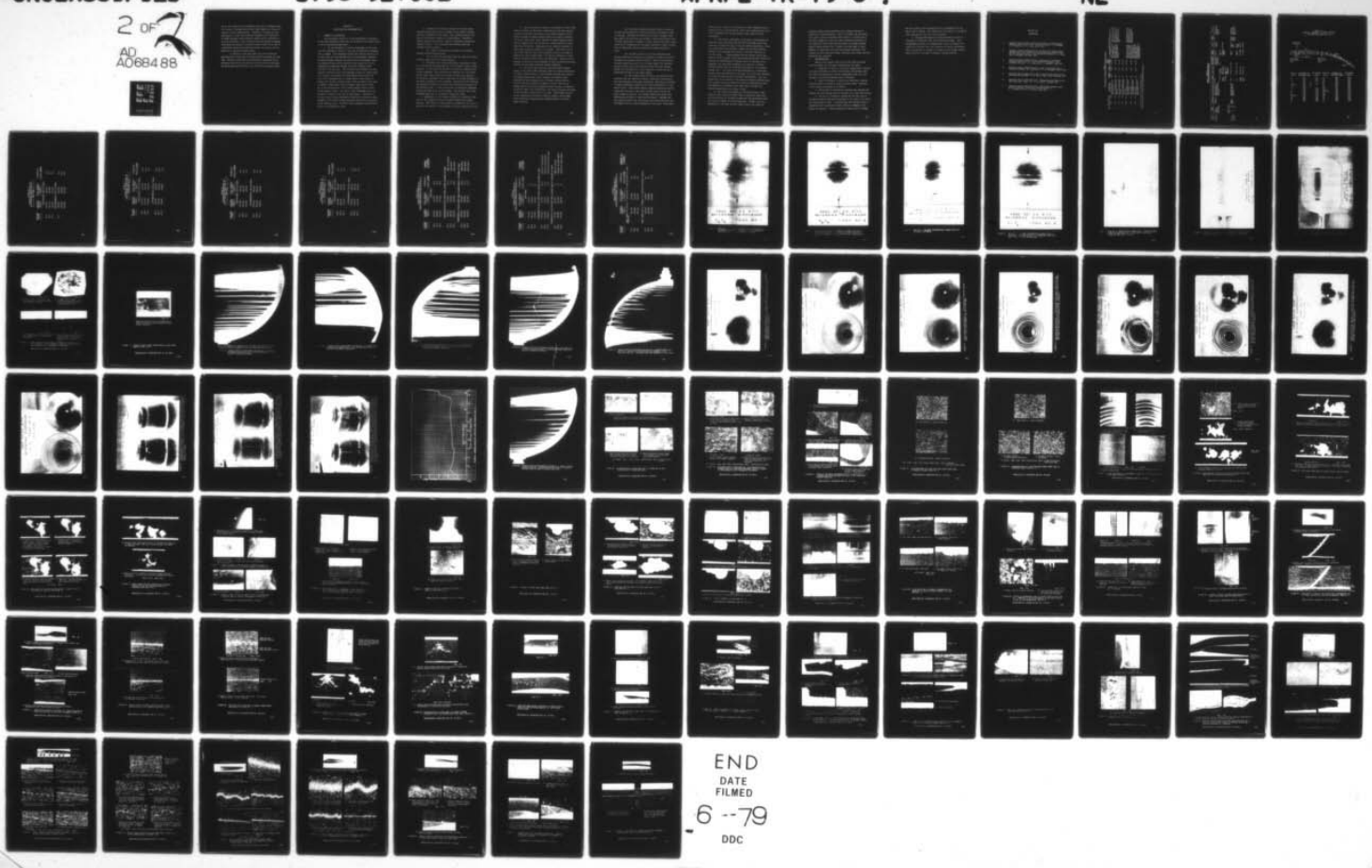

END
DATE FILMED
6 -79
DDC

did in fact operate quite successfully and with no leakage during the 5 years of storage service with a quite aggressive liquid propellant, chlorine pentafluoride. Therefore, it seems that this application of solid state explosive bonding to the fabrication of A-286 stainless steel propellant tanks could be considered to be quite successful. Only a detailed test and evaluation program subjecting such hardware to specific service cycles to be used in a particular system would determine whether the process could be applied to a specific hardware system.

It should be noted that these tanks were fabricated approximately 10 years ago, utilizing advanced processes for that time. The minor deficiencies and potentially degrading factors discussed above should not hide the fact that for the technology and design goals at that time, these were quite acceptable tanks.

SECTION VI

CONCLUSIONS AND RECOMMENDATIONS

A. SUMMARY OF CONCLUSIONS

The conclusions arrived at in the metallurgical evaluation of the Arde and Martin A-286 tanks are presented in a sequence which is one of decreasing significance.

1. In the evaluation of the Arde diaphragms it was found that the diaphragm in Tank No. 2 had lost its functional integrity due to leakage. This diaphragm failure was initially picked up on a helium leak test and substantiated by metallographic analysis. The metallographic analysis has shown that this diaphragm failed by pitting corrosion which initiated on the liquid side of the diaphragm and progressed through the 10 mil stainless steel material to the gas side. Once corrosion was initiated as a pit, internal corrosion of the 304L diaphragm occurred by cavity formation, which is attributed to electrochemical attack where the bulk of the diaphragm with its normal passive film acted as a cathode and the small internal areas, where no passive film could be formed, became anodic areas allowing a high rate of attack due to the concentration of the current density effects in the electrochemical attack. The cause of this diaphragm failure is discussed in detail in the text of this report. Initiation of the pits found in this diaphragm is attributed to particles being embedded in the surface during fabrication which were not removed by the cleaning cycle. The three other diaphragms evaluated were found to be structurally sound.

2. Pitting of the exterior surfaces of the Arde tanks occurred during eight years of storage in the oxidizer storage facility at Edwards Air Force Base. This pitting occurred over much of the exterior surface in a random nature. Variations existed between tank surfaces, however, pitting was present and random in nature. It is concluded that pitting could have resulted from two sources:

(a) from the environment existing in the oxidizer storage facility during storage,

(b) or from the environment that the tanks were stored in after completion of the storage period.

3. Following leak testing radiographic inspection of Tank No. 3 showed that the diaphragm was in its "normal" liquid storage position. It was therefore possible to perform an expulsion test on this diaphragm. This expulsion was completed in a very satisfactory manner with 95.2% of the distilled water load expelled. The expulsion performance after eight years of storage demonstrated structural integrity of this diaphragm. Renesting of the diaphragm was attempted although it was known that wrinkling had occurred on the expulsion cycle. It was not possible to renest the diaphragm, tearing occurring early in the attempt. This verifies that these diaphragm tanks must be considered "single-use" items.

4. Examination of the interior surfaces of the Martin A-286 tanks in all instances showed a disturbed surface with random staining. This feature of these tanks is concluded to be a direct result of the removal of steel mandrels by nitric hydrofluoric acid.

5. The blue protective paint on the outside of these A-286 tanks was intact and apparently unaffected by long term exposure. No areas of corrosion were found on the outside surfaces of the shells although the identification decals were heavily attacked. The use of "green tape" after exposure to attach shipping labels, plastic bagging, tube and end caps, when removed, peeled the paint away from the surface. Examination of the exterior surfaces in these areas showed no evidence of corrosion. This effect of the use of this tape has led to the conclusion that in all stages of handling of these painted tanks, care must be exercised in order, that the protective paint coat is not disturbed. The use of this coating of paint has a real advantage in that its presence, prevents exterior pitting under long term storage conditions.

6. The solid state explosive bonds produced by Martin-Denver in the three A-286 propellant tanks were quite satisfactory for their intended purpose of fabricating a storage tank capable of holding propellants, without leakage, for several years. Although the bonds examined were of variable quality and had several deleterious features, summarized below, there was no leakage and the structural integrity across the bond, as measured by tensile tests, was satisfactory, with tensile failures occurring in the base metal rather than in the bond. These bonds did have several potentially deleterious features, however, which might cause difficulty in applying this bonding process to critical flight hardware.

(a) The bonds characteristically contain a cavity or at least an unbonded zone at both the interior and exterior ends of the bond. Although not affecting the tensile strength (even when 20% of the bond line was unbonded), these notch effects would be quite deleterious to fatigue or cyclic service, and these joints could not be recommended for any tanks subjected to cyclic service, such as temperature cycling causing the internal pressure to cycle.

(b) The same cavities at the bond interface cause another deleterious condition in providing a location for crevice corrosion and corrosion product buildup. Even if the corrosion is merely superficial (as it was in these tanks), the corrosion product buildup could form sufficient salts and other foreign matter to be deleterious to valve operation or plug orifices in downstream portions of any flight system.

(c) The intense strain effects in and near the joint interface from the explosive bonding, caused minor difficulties with this stainless steel tank construction, and would be expected to cause considerable difficulty for tanks constructed of a less ductile alloy. These strain effects promoted selective corrosive attack near the bond of the outlet to dome joint, but did not cause leakage or failure. The intense strain also caused local melting along portions of some bond interfaces. Although this local melting caused some isolated gas pores and cracks they did not degrade the leak tight performance of the tanks. These minor

defects would, however, be deleterious to tanks undergoing cyclic pressure service, and are another reason this bonding process cannot be recommended for flight hardware usage without further development.

7. The overall performance of the Arde, cryostretched 301 stainless steel tanks with ring-stiffened diaphragms during the seven year storage with N_2O_4 or ClF_5 was quite satisfactory. There were discrepancies and problems, notably the corrosion induced leakage of one diaphragm and pitting of the shell exteriors of all four tanks. These problems had well defined sources and could be cured by proper action during fabrication, such as precision cleaning and passivating to eliminate sites for pitting of the diaphragm, and protective painting of the exterior to prevent external pitting from the acid-fume environment of the oxidizer storage room. One proof of the good performance of these tanks was the controlled expulsion of one tank, to an expulsion efficiency of better than 95% with 50 psi pressure differential. This confirmed that, in the absence of the special problems described above, these positive expulsion tanks would perform satisfactorily after the completion of extended (up to eight years) storage with oxidizer propellants such as N_2O_4 or ClF_5.

8. The overall performance of the Martin-Denver, A-286 stainless steel explosive bonded tanks is considered quite good, as they withstood the extended storage with ClF_5 propellant quite well, with no leakage or obvious corrosion. In fact, the only degradation of the tank interior seems to have been caused by

excessive attack during fabrication and cleaning (etching to remove steel bonding mandrels), prior to storage, and the propellant service did not accelerate these effects. As described in the detail summaries, there were some deleterious attributes of the bonds, which would make them unsuitable for flight hardware usage in their present form. However, the basic goal of this program, to demonstrate the long term storage capability of an oxidizer in these explosive bonded, stainless steel tanks, has been satisfactorily completed.

B. RECOMMENDATIONS

Based on the analysis made on the seven tanks evaluated in this program, the following recommendations are made:

1. Suppliers of tanks for long term storage should exercise every means available to insure that internal and external parts are clean from fabrication induced contamination that as a rule initiates a corrosion mechanism such as "pitting".

2. Prior to storage of a particular propellant, internal surfaces should be cleaned to insure a passive state, resistant to the chemical propellant to be stored.

3. Care should be exercised in insuring that fittings and adapters are also cleaned prior to induction of a tank into storage.

4. The use of a protective coating such as that used on the Martin painted tanks may be desirable on all tanks to be stored for long periods of time. It follows that this coating should be compatible with the metallic surface and not be damaged in any manner once applied. Careful handling of tanks prior to storage

and after removal from storage would be a prerequisite for the use of such a coating. The condition of the surface of the Martin tanks demonstrates that this can be achieved.

5. Thorough draining and flushing operations should be performed on propellant tanks after long term storage. This recommendation cannot be overemphasized in that if improper procedures are followed, then the evaluation of overall performance after long periods of storage is clouded by past storage effects, which would not be present in properly cleaned hardware.

SECTION VII

REFERENCES

1. Technical Report AFRPL-TR-74-82 "Analysis of Liquid Rocket Tankage" Final Report, Bell Aerospace Textron, J. Salvaggi, H. G. Kammerer, E. J. King, April 1975.

2. Technical Report AFRPL-TR-75-73, "Analysis of Liquid Rocket Tankage from Model LR58-RM-4 Liquid Propellant Thrust Unit for the Bullpup Missile", Bell Aerospace Textron, E. J. King, and J. Salvaggi, February 1976.

3. Technical Report AFRPL-TR-77-25, "Analysis of Propellant Storage Tanks After Four Years Hydrazine Storage", Bell Aerospace Textron, E. J. King and H. G. Kammerer, May 1977.

4. Technical Report AFRPL-TR-69-82, "Long Term Storability of Propellant Tankage and Components", J. E. Branigan, April 1969.

5. Technical Report AFRPL-TR-72-126, "Long Term Storage Testing of Propellant Tankage", H. M. White, Capt. USAF, December 1972.

6. Technical Report AFRPL-TR-69-49, "Packaged System Storability Test Articles", Arde, Inc., F. D. Mollo, January 1969.

7. Technical Report AFRPL-TR-71-69, "Solid State Bonded Liquid Rocket Propellant Containers", Martin-Denver Co., C. L. Caudill and R. L. Kerlin, July 1971.

TABLE I
TANKS RECEIVED FOR EVALUATION FROM ROCKET PROPULSION LABORATORY

TANK NO.	MANUFACTURER	MFR. S/N	TANK TYPE MATERIAL FEATURES	PROPELLANT STORED	PLACED IN STORAGE	REMOVED FROM PROPELLANT STORAGE	VISUAL EXAMINATION EXTERNAL SURFACE	VISUAL EXAMINATION INTERNAL SURFACE
1	Arde	None	301 SS Cryostretched sphere with ring stiffened 304 SS diaphragm.	N_2O_4 **	7/3/69 *	July 1977	Lightly frosted or etched with occasional small pits. Obvious stain in circle where tank sat in support ring. Tank No. 1 contained small dark discolored spot suggesting arc strike.	Generally clean and bright both on shell and diaphragm. Occasional streaks on propellant side may have been from residual propellant. Some discolored streaks on gas side of Tank No. 2 where diaphragm leaks were found.
2	Arde	None	301 SS Cryostretched sphere with ring stiffened 304 SS diaphragm.	N_2O_4 **	7/3/69	July 1977		
3	Arde	None	301 SS Cryostretched sphere with rings stiffened 304 SS diaphragm.	ClF_5	7/3/69	July 1977		
4	Arde	None	301 SS Cryostretched sphere with rings stiffened 304 SS diaphragm.	ClF_5	7/3/69	July 1977		
5	Martin	001	A-286 Cylinder 10 gal. capacity, with solid state (explosive) bonds in place of welds.	ClF_5	3/1/72	July 1977	Painted with a blue protective paint. Painted surfaces were unaffected by exposure. One small area on Tank No. 5 where paint was washed away down to primer. Even in that area no apparent attack. Decals with tank serial numbers, etc. had been attacked and were barely legible, with stenciling washed away and even embossing partially obscured by pitting.	Lightly etched or frosted over entire surface. Occasional obvious pits, particularly near or in outlet fitting. Stains and deposits near or leading out of bond regions.
6	Martin	002	A-286 Cylinder 10 gal. capacity, with solid state (explosive) bonds in place of welds.	ClF_5	3/1/72	July 1977		
7	Martin	003	A-286 Cylinder 10 gal. capacity, with solid state (explosive) bonds in place of welds.	ClF_5	3/1/72	July 1977		

* Date placed in storage is taken from AFRPL Report, Reference 1.

** N_2O_4 was of the "green", NO inhibited, type per NASA Specification MSC-PPC-2A.

TABLE II
SUMMARY OF SIGNIFICANT FABRICATION
CHARACTERISTICS FOR TANKS EVALUATED

TANK MATERIAL	SERIAL NUMBER		MANUFACTURER	GENERAL TANK DESCRIPTION	COMPONENTS	TYPE OF JOINT	HEAT TREATMENT AFTER JOINING	SOURCE MATERIAL	FORMING	HEAT TREATMENT	REFERENCE
301 SS Ardiform or Cryostretch	1,2,3,4 (Numbers arbitrarily assigned, no S/N on shells)		Arde, Inc. Mahwah, NJ	Spherical tank with wire reinforced positive expulsion diaphragm welded at girth, holding 3.4 gallons.	Dome		Solution Anneal after welding but before cryostretching.	0.025 inch sheet	Hydroform to hemisphere	None	RFL TR-69-49 "Packaged System Storability Test Articles" (Ref. 6)
					Girth ring	TIG Weld-Dome/Ring	None	0.10 inch sheet			
					Outlet fitting	Manual TIG seal weld to dome		bar-standard MS33656-8 fitting	Machining		
					Diaphragm	Copper Brazed Rings TIG Weld-Ring/Diaphragm					
	Program No.	Martin No.									
A-286 Precipitation Hardening Stainless Steel	5	001	Martin-Marietta Denver	10 gallon cylinder with domed ends; small diameter outlet port at each end.	Barrel	Explosive bond	None	.044 inch sheet	Roll form single longit. bond	Solution treat and age after forming	RFL TR-71-69 "Solid State Bonded Liquid Rocket Propellant Containers" (Ref. 7)
	6	002									
	7	003									
					Dome	Explosive bond	None	.044 inch sheet	Explosively formed.	"	
					Outlet fitting	Explosive bond		Bar (321SS)	Machined		
					Outlet tubes	Explosive Bond		Bar (321SS)	Machined		

TABLE III
HARDNESS TRAVERSE IN CENTRAL REGION
OF ARDE TANK SHELL NO. 2

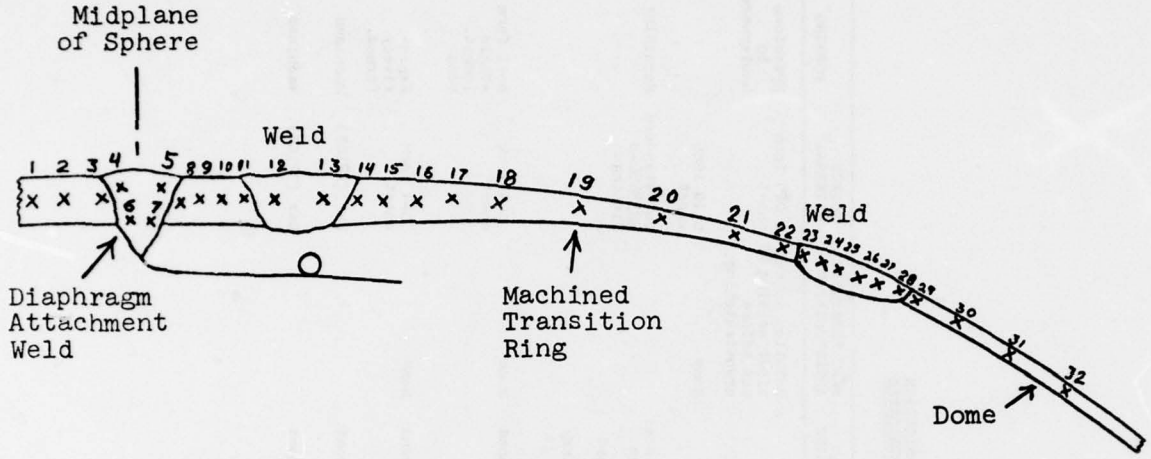

STATION NO.	HARDNESS NO. (VICKERS 10Kg)	THICKNESS (IN.)	STATION NO.	HARDNESS NO. (VICKERS 10Kg)	THICKNESS (IN.)
1	146	.115	17	297	.055
2	157	.115	18	345	.043
3	141	.120	19	413	.030
4)	155		20	473	.020
5) Weld	155	.140	21	455	.020
6)	147		22	464	.020
7)	129		23)	421	.020
8	143	.120	24)	351	.025
9	144	.120	25) Weld	413	.035
10	144	.115	26)	380	.035
11	144	.115	27)	405	.025
12) Weld	182	.116	28)	425	.020
13)	191	.116	29	459	.020
14	233	.094	30	468	.020
15	222	.084	31	468	.020
16	253	.072	32	468	.020

TABLE IV
MECHANICAL PROPERTIES OF
ARDE CRYOFORM SHELL TANK NO. 1
GAS SIDE

SPECIMEN NUMBER	ULTIMATE STRENGTH (psi)	YIELD STRENGTH 0.2% OFFSET (psi)	ELONGATION % IN 2 INCHES
	LONGITUDINAL AXIS OF SHELL		
1A-1	201,000	158,000	9.0
1A-2	190,600	148,800	8.0
1A-3	195,800	147,300	8.0
	CIRCUMFERENTIAL AXIS OF SHELL		
1C-1	199,200	153,500	9.0
	202,500	156,900	10.0
	200,800	152,900	10.0

TABLE V
MECHANICAL PROPERTIES OF
ARDE CRYOFORM SHELL TANK NO. 1
PROPELLANT SIDE

SPECIMEN NUMBER	ULTIMATE STRENGTH (psi)	YIELD STRENGTH 0.2% OFFSET (psi)	ELONGATION % IN 2 INCHES
	LONGITUDINAL AXIS OF SHELL		
1PA-1	204,500	157,500	12.0
1PA-2	201,600	161,400	10.0
1PA-3	202,800	159,200	9.0
	CIRCUMFERENTIAL AXIS OF SHELL		
1PC-1	196,200	149,300	11.0
1PC-2	194,900	148,500	10.0
1PC-3	192,600	148,600	8.0

TABLE VI
MECHANICAL PROPERTIES OF
ARDE CRYOFORM SHELL TANK NO. 4
GAS SIDE

SPECIMEN NUMBER	ULTIMATE STRENGTH (psi)	YIELD STRENGTH 0.2% OFFSET (psi)	ELONGATION % IN 2 INCHES
	LONGITUDINAL AXIS OF SHELL		
4A-1	201,800	163,100	9.0
4A-2	202,400	163,700	9.0
4A-3	199,600	159,400	8.0
	CIRCUMFERENTIAL AXIS OF SHELL		
4C-1	206,300	166,300	8.0
4C-2	205,300	166,400	7.0
4C-3	202,600	159,500	9.0

TABLE VII
MECHANICAL PROPERTIES OF
ARDE CRYOFORM SHELL TANK NO. 4
PROPELLANT SIDE

SPECIMEN NUMBER	ULTIMATE STRENGTH (psi)	YIELD STRENGTH 0.2% OFFSET (psi)	ELONGATION % IN 2 INCHES
	LONGITUDINAL AXIS OF SHELL		
4PA-1	209,900	180,900	4.0
4PA-2	209,600	180,900	6.0
4PA-3	215,300	194,400	4.0
	CIRCUMFERENTIAL AXIS OF SHELL		
4PC-1	206,000	172,000	6.0
4PC-2	213,700	182,700	5.0
4PC-3	211,500	191,600	4.0

TABLE VIII
MECHANICAL PROPERTIES OF
SOLID STATE BONDED A-286 TANK NO. 5

SPECIMEN NUMBER	ULTIMATE STRENGTH (psi)	YIELD STRENGTH 0.2% OFFSET (psi)	ELONGATION % IN 2 INCHES	COMMENTS ON AREA OF RUPTURE
		BASE METAL		
5B-1	166,400	115,300	16.0	
5B-2	164,800	101,900	16.0	
5B-3	165,600	114,300	16.0	
	TRANSVERSE TO SOLID STATE BOND JOINING CYLINDER OF TANK			
5C-1	163,600	110,400	12.0	Edge of overlap.
5C-2	158,500	107,000	9.5	Base metal.
5C-3	166,300	112,200	14.0	Base metal.
	TRANSVERSE TO SOLID STATE BOND JOINING DOME TO CYLINDER OF TANK			
5D-1	165,300	119,500	12.0	Base metal.
5D-2	165,500	120,600	11.0	Base metal.
5D-3	168,000	125,300	11.0	Base metal.

TABLE IX
MECHANICAL PROPERTIES OF
SOLID STATE BONDED A-286 TANK NO. 6

SPECIMEN NUMBER	ULTIMATE STRENGTH (psi)	YIELD STRENGTH 0.2% OFFSET (psi)	ELONGATION % IN 2 INCHES	COMMENTS ON AREA OF RUPTURE
		BASE METAL		
6B-1	167,300	116,400	17	
6B-2	165,100	114,600	17	
6B-3	164,800	113,900	16	
		TRANSVERSE TO SOLID STATE BOND JOINING CYLINDER TO TANK		
6C-1	164,700	117,300	10.5	Failed at bench mark.
6C-2	163,900	117,000	10.0	Failed at bench mark.
6C-3	165,600	118,500	9.5	Failed beyond bench mark.
		TRANSVERSE TO SOLID STATE BOND JOINING DOME TO CYLINDER OF TANK		
6D-1	157,400	117,200	8	Edge of overlap.
6D-2	164,800	121,300	9	Outside of bench marks.
6D-3	165,800	122,200	8	Outside of bench marks.

TABLE X
MECHANICAL PROPERTIES OF
SOLID STATE BONDED A-286 TANK NO. 7

SPECIMEN NUMBER	ULTIMATE STRENGTH (psi)	YIELD STRENGTH 0.2% OFFSET (psi)	ELONGATION % IN 2 INCHES	COMMENTS ON LOCATION OF RUPTURE
	Gage length was across a "waterline" of discoloration at tank midplane.			
7W-1	161,000	110,800	25	
7W-2	163,200	113,800	24.5	
7W-3	161,000	112,300	22	
	Gage length was in "puddle" or discolored deposit region.			
7P-1	160,900	115,400	22	
7P-2	158,000	108,800	22	
7P-3	157,600	107,900	21.5	

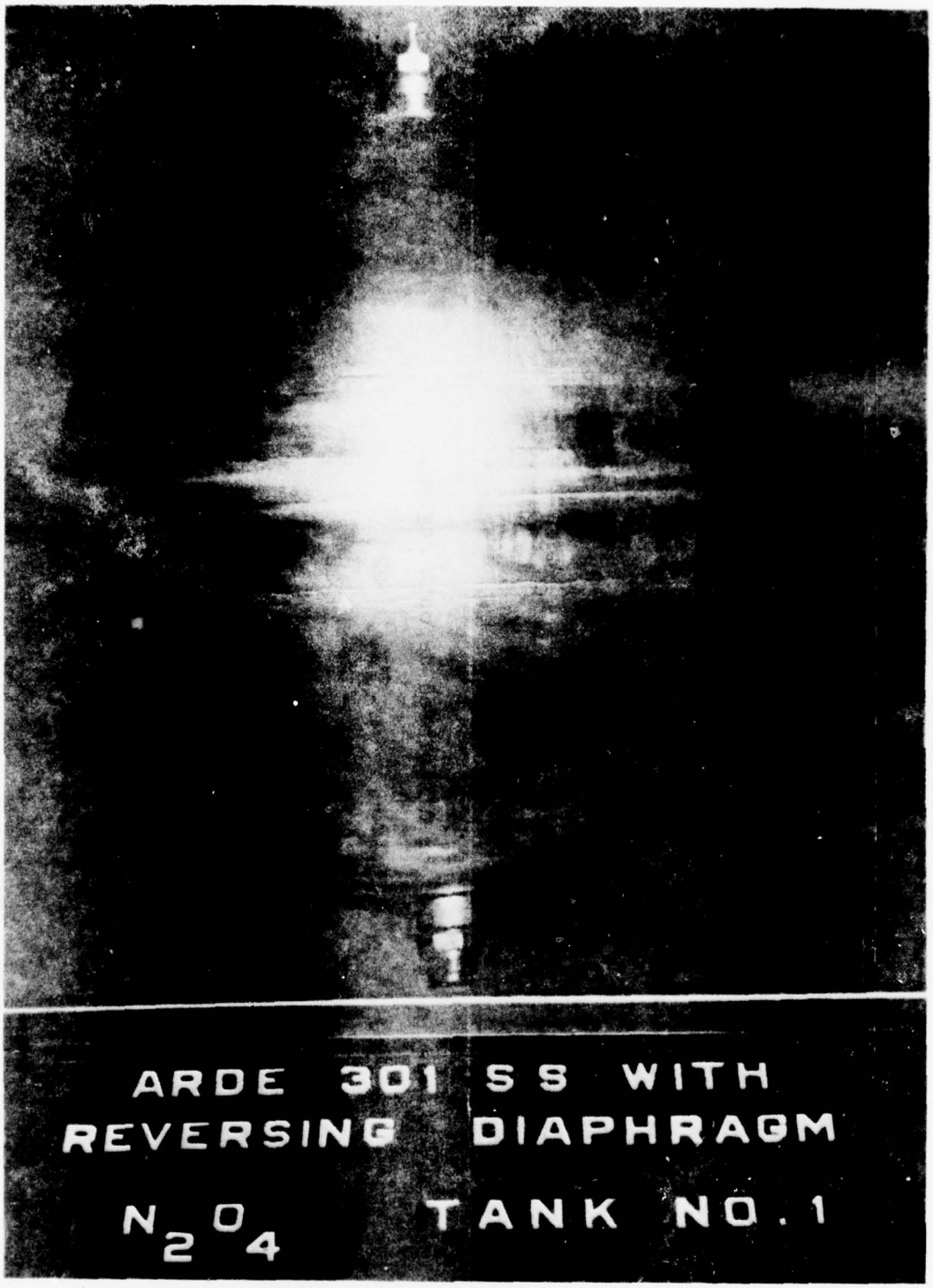

FIGURE 1. TANK NO. 1, AN ARDE CRYOSTRETCHED SPHERE WITH RING STIFFENED DIAPHRAGM. DARK SPOT APPEARS TO BE ARC STRIKE BUT MAY BE LOCAL CORROSION EFFECT.

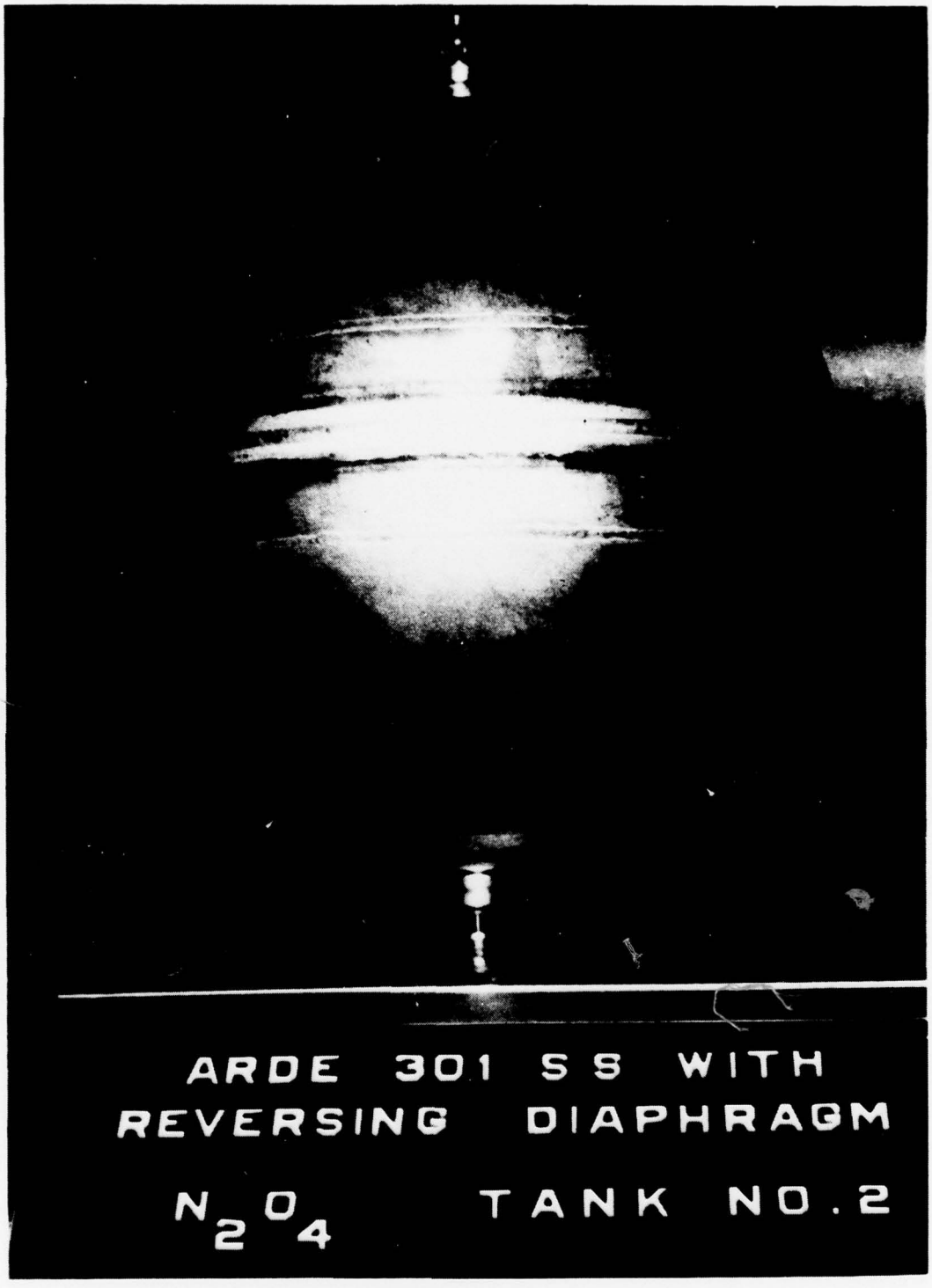

FIGURE 2. TANK NO. 2, AN ARDE CRYOSTRETCHED SPHERE WITH RING STIFFENED DIAPHRAGM. ALL FOUR OF THESE SPHERES SHOW STAINS (AT ARROWS) FROM THE SUPPORT THEY WERE SITTING IN.

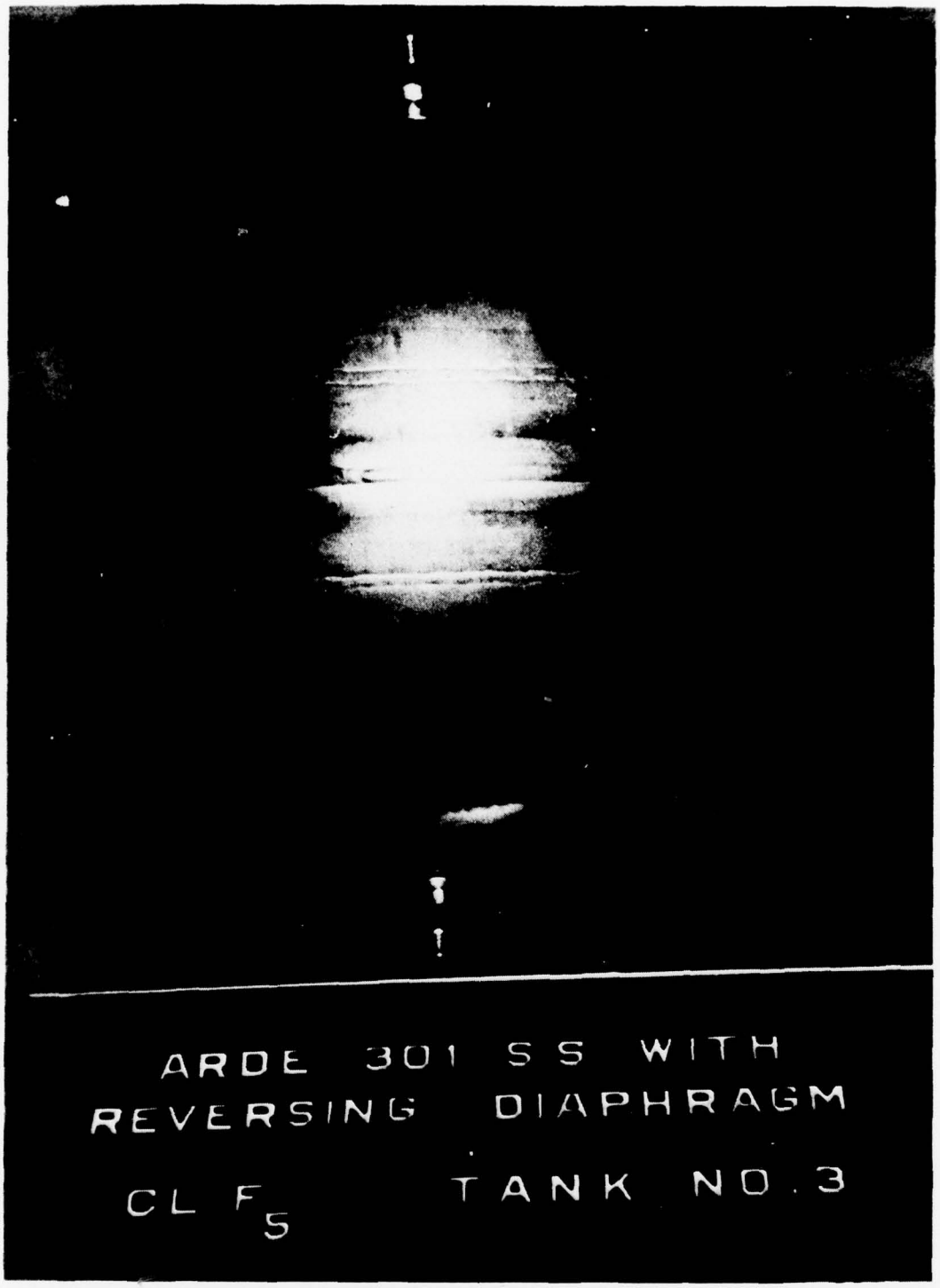

FIGURE 3. TANK NO. 3, AN ARDE CRYOSTRETCHED SPHERE WITH RING STIFFENED DIAPHRAGM.

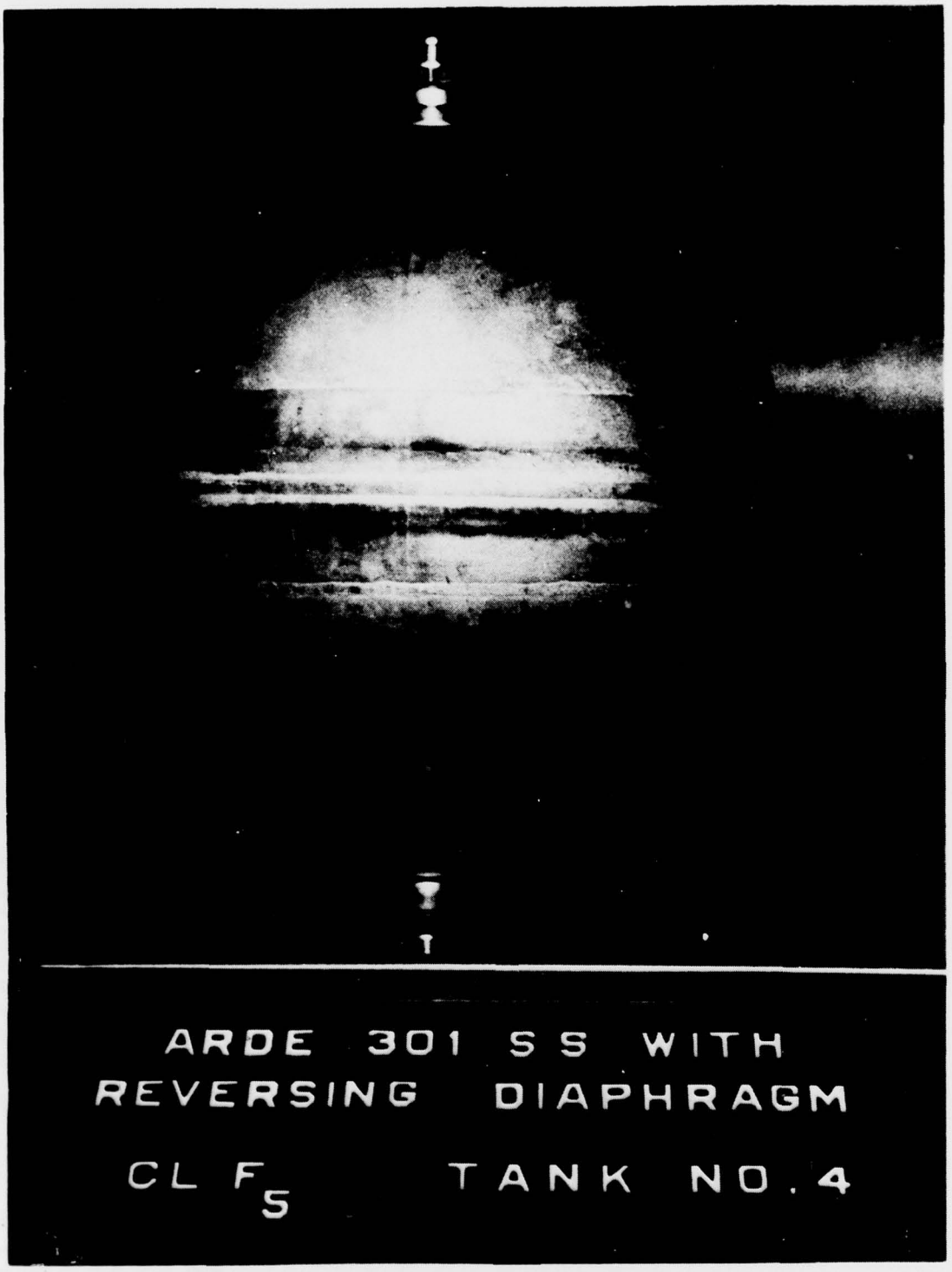

FIGURE 4. TANK NO. 4, AN ARDE CRYOSTRETCHED SPHERE WITH RING STIFFENED DIAPHRAGM SHOWING NO CORROSION OTHER THAN VERY MINOR PITTING AND STAINING.

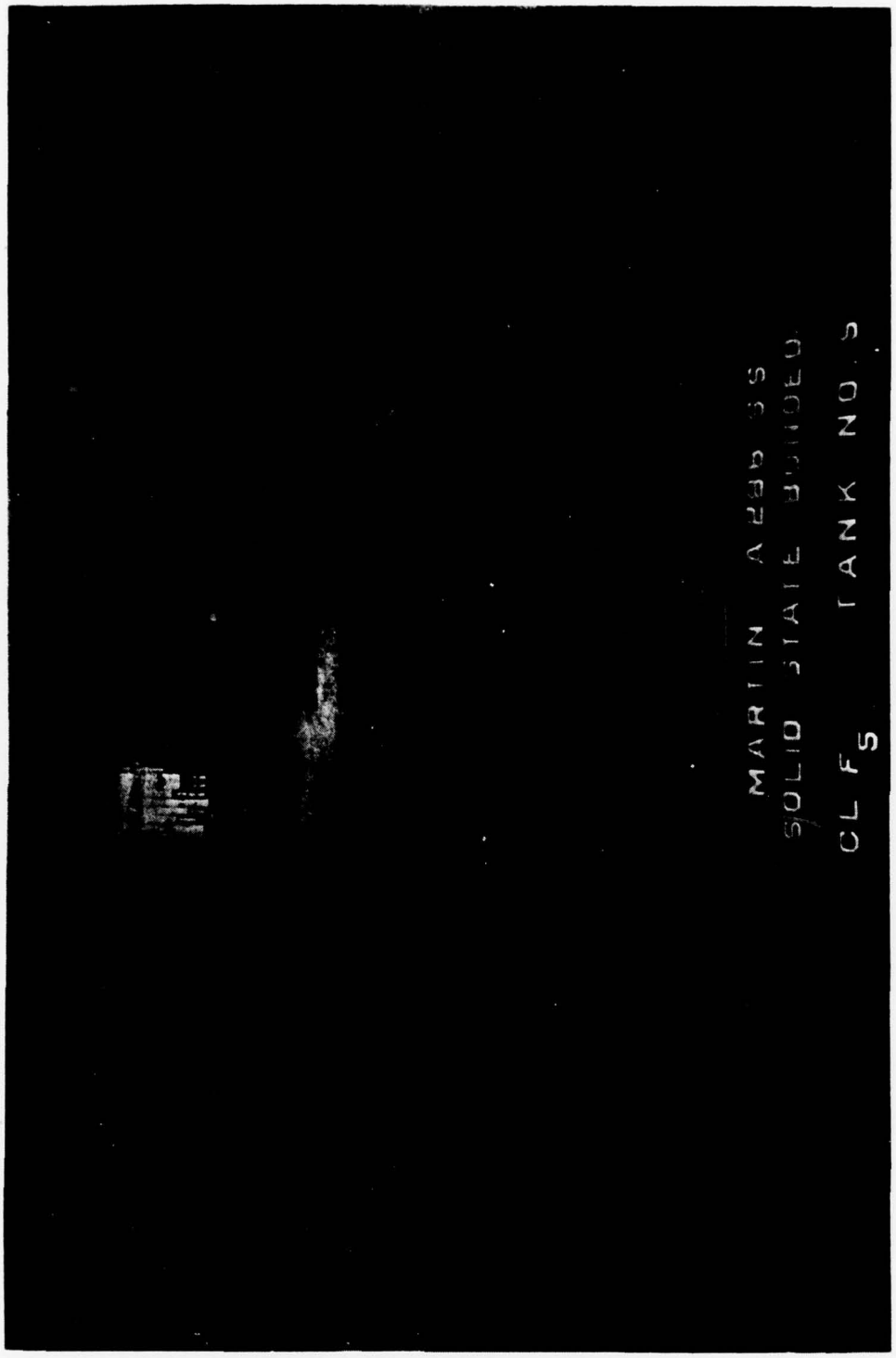

FIGURE 5. TANK NO. 5, SOLID STATE BONDED A-286, SHOWING A SPOT ABOVE THE NAME TAG WHERE PAINT WAS MISSING AND CORROSION MAY HAVE OCCURRED.

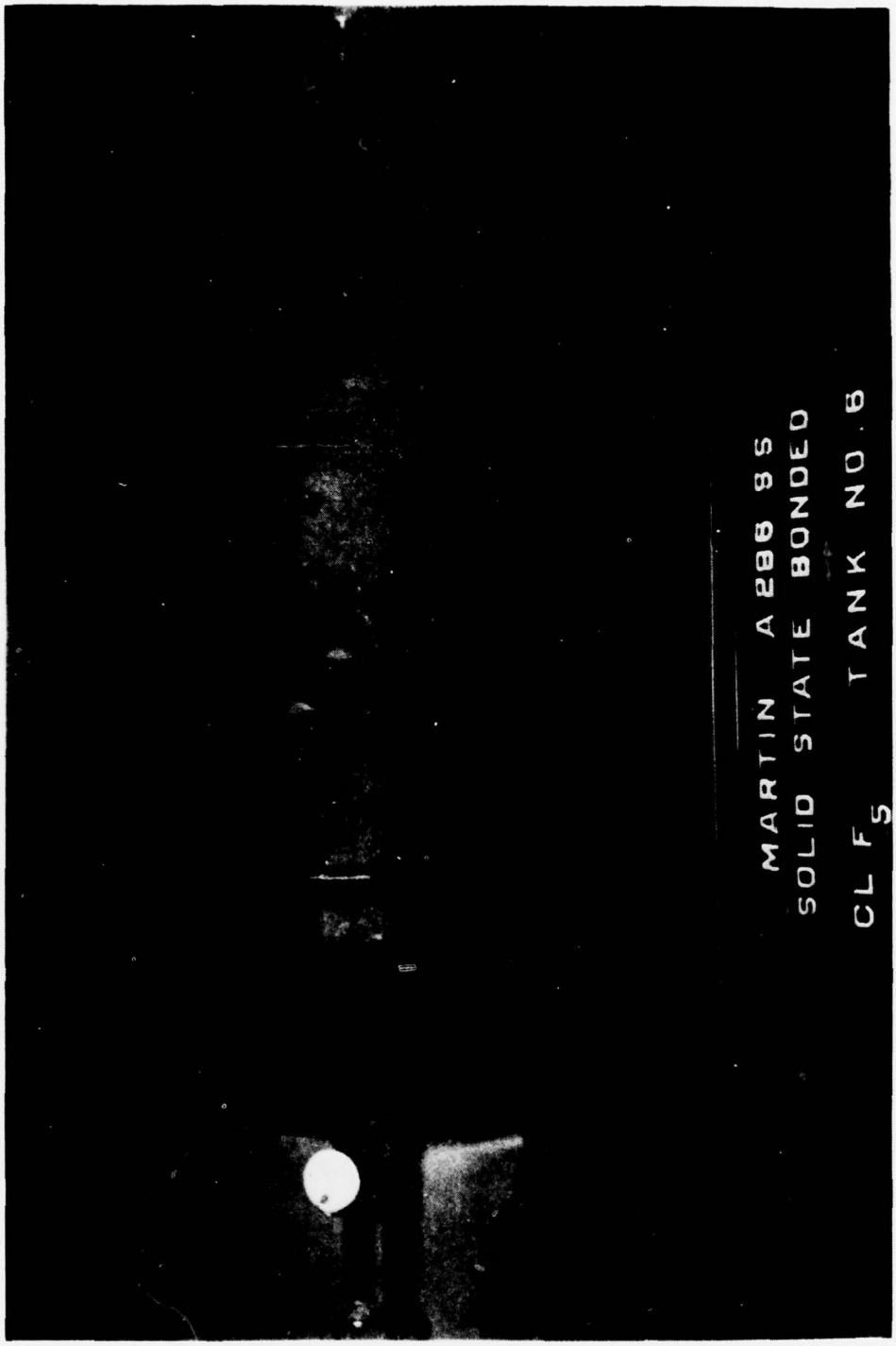

FIGURE 6. TANK NO. 6, SOLID STATE BONDED A-286, SHOWING NO APPARENT CORROSION OR OTHER DAMAGE ON EXTERIOR.

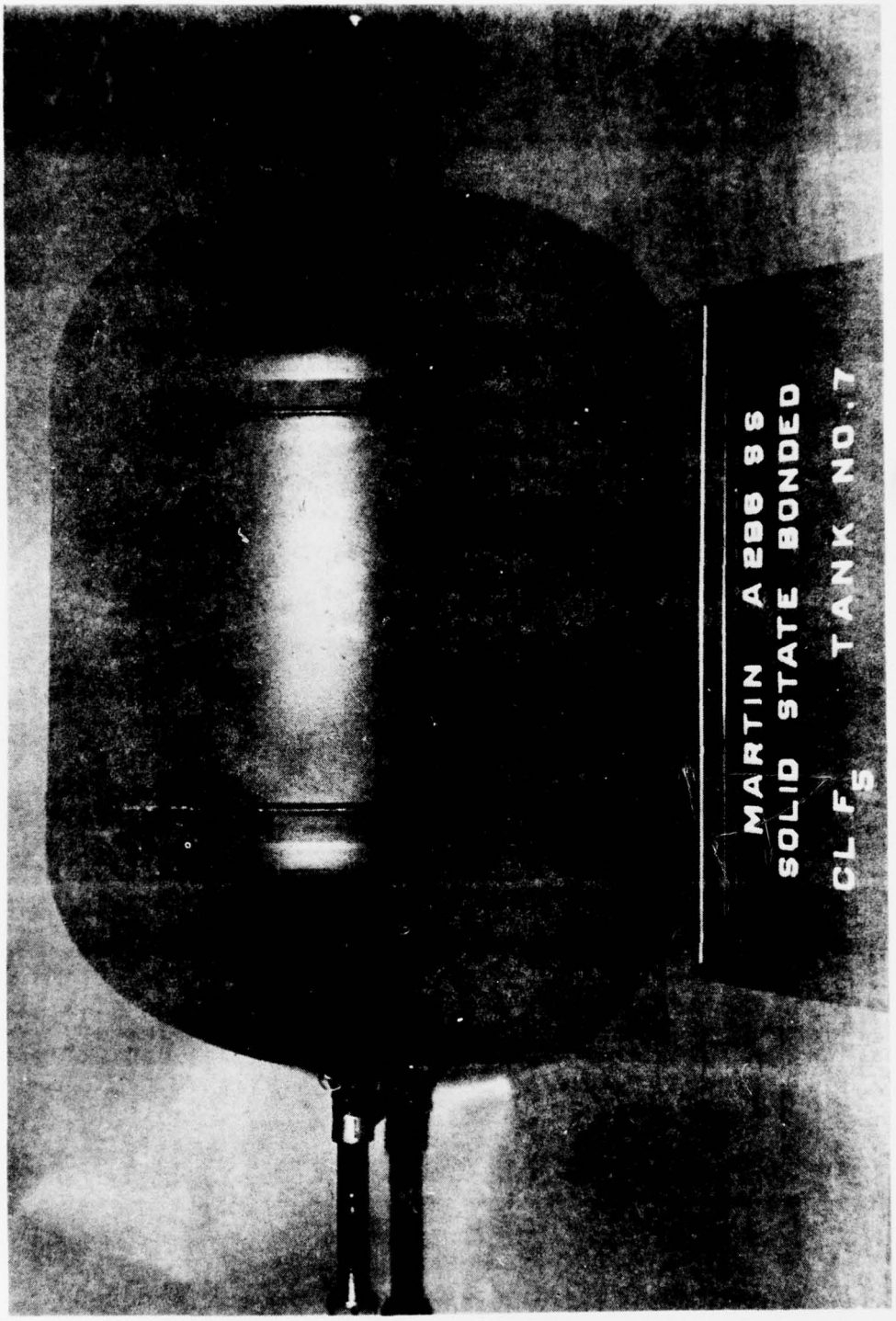

FIGURE 7. TANK NO. 7, SOLID STATE BONDED A-286, SHOWING NO APPARENT CORROSION OR OTHER DAMAGE ON EXTERIOR.

Mag: 1X

a) Overall view of spot which was on cylindrical portion of dome near bond to cylinder.

Mag: 4X

b) Closeup view of spot. Blue protective paint was washed or scraped away revealing the orange primer coat.

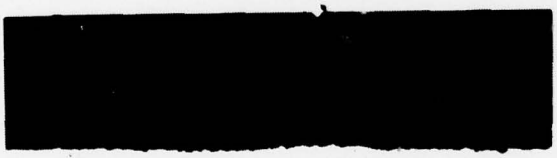

Mag: 100X

c) Cross section at surface of A-286 shell under spot. No corrosion is visible.

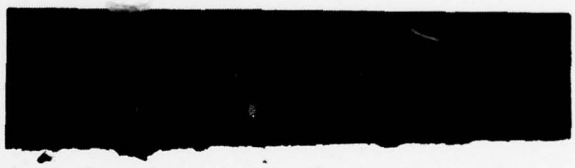

Mag: 100X

d) Cross section at interior surface showing greater amount of attack (due to fabrication etching) than occurred under spot.

FIGURE 8. DETAIL VIEWS OF SPOT NOTED ON EXTERIOR OF MARTIN TANK NO. 5 SHOWING IT TO BE MERELY A REMOVAL OF THE PROTECTIVE PAINT LAYER WITH NO CORROSION OF THE SHELL.

METALLURGICAL LABORATORY MET NO. 78-79011

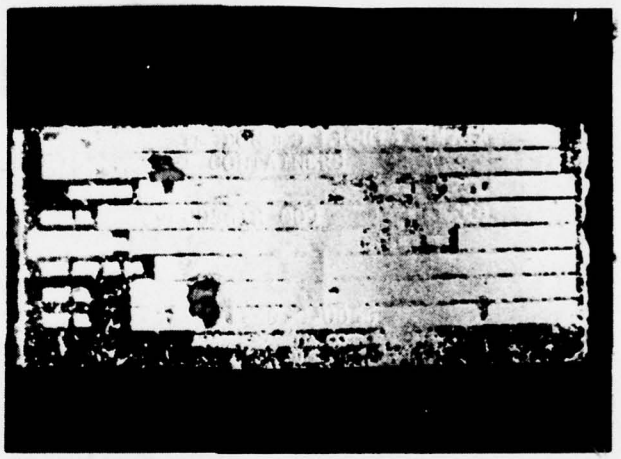

Mag: 1X

Embossed nomenclature and numbering is still visible but decal has been extensively corroded.

FIGURE 9. VIEW OF TYPICAL TANK IDENTIFICATION DECAL FROM MARTIN A-286 TANKS.

Note - In Figures 10 through 14, all tanks are shown in as-stored condition, that is bottom of tank is toward bottom of page.

FIGURE 10. CONTACT PRINT OF RADIOGRAPH OF TANK NO. 1, AN ARDE RING STIFFENED DIAPHRAGM TANK IN THE AS-RECEIVED CONDITION SHOWING COMPLETE EXPULSION.

FIGURE 11. CONTACT PRINT OF RADIOGRAPH OF TANK NO. 2, AN ARDE RING STIFFENED DIAPHRAGM TANK IN THE AS-RECEIVED CONDITION SHOWING ONLY PARTIAL EXPULSION.

FIGURE 12. CONTACT PRINT OF RADIOGRAPH OF TANK NO. 3. AN ARDE RING STIFFENED DIAPHRAGM TANK, IN THE AS-RECEIVED CONDITION SHOWING ONLY PARTIAL EXPULSION.

FIGURE 13. CONTACT PRINT OF RADIOGRAPH OF TANK NO. 4, AN ARDE RING STIFFENED DIAPHRAGM TANK, IN THE AS-RECEIVED CONDITION SHOWING COMPLETE EXPULSION.

FIGURE 14. CONTACT PRINT OF RADIOGRAPH OF TANK NO. 2 AFTER PRESSURIZED LEAK TEST, SHOWING THAT DIAPHRAGM HAD RETURNED TO ITS ORIGINAL POSITION. DIAPHRAGM LEAK WAS DETECTED IN THIS TEST.

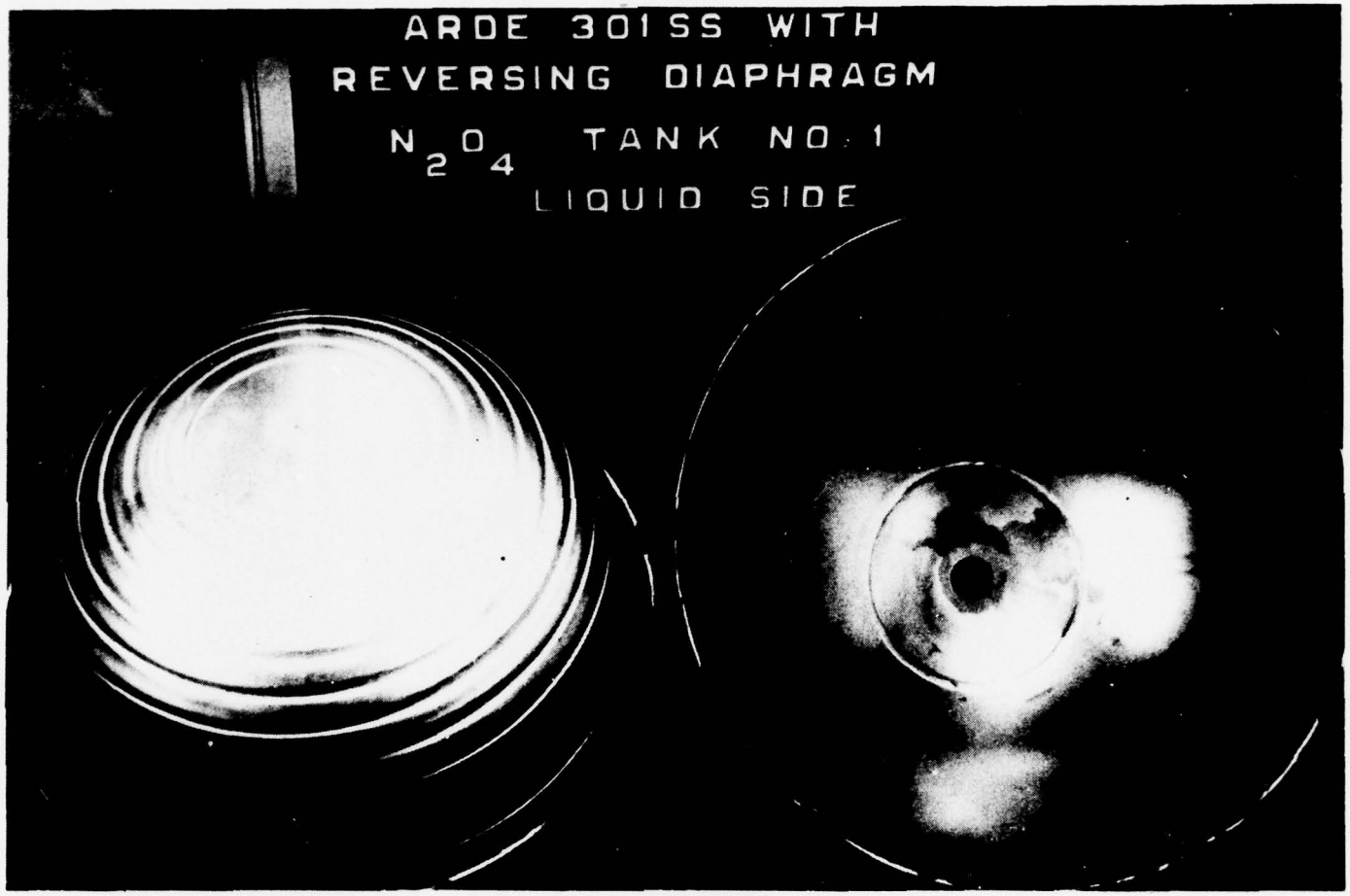

FIGURE 15. LIQUID SIDE OF ARDE TANK NO. 1 SHOWING INTERIOR OF SHELL AND THE DIAPHRAGM AFTER EXPULSION. STAINING IS THE RESULT OF INCOMPLETE DRAINAGE WITH PROPELLANT HAVING EVAPORATED.

FIGURE 16. GAS SIDE OF ARDE TANK NO. 1 SHOWING INTERIOR SURFACE OF SHELL AND THE DIAPHRAGM AFTER EXPULSION.

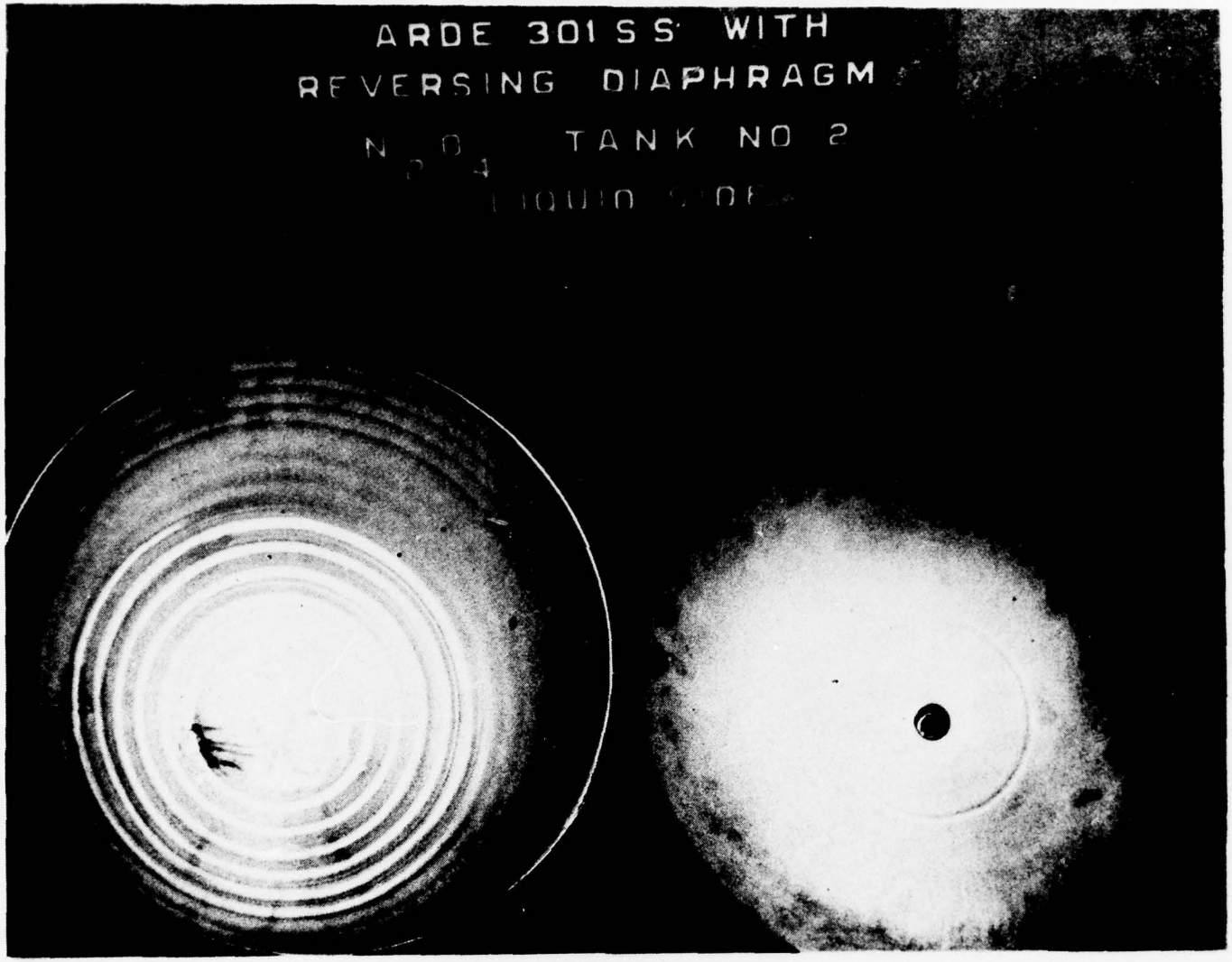

FIGURE 17. LIQUID SIDE OF ARDE TANK NO. 2. THIS DIAPHRAGM CONTAINS PINHOLE LEAKS IN THE UPPER DEFORMED SECTION OF THE DOME.

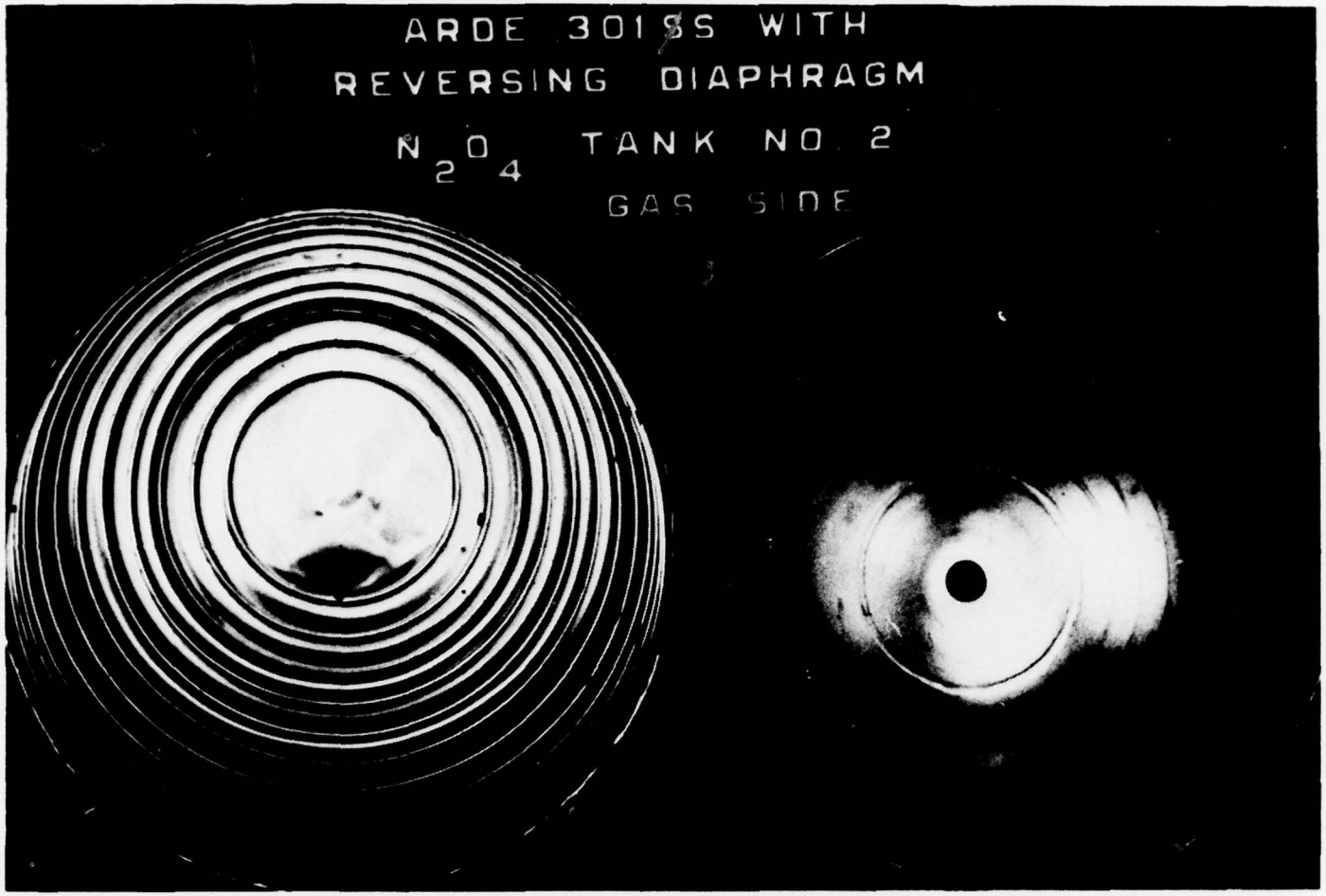

FIGURE 18. GAS SIDE OF ARDE TANK NO. 2. STAINS EXIST ON THE SHELL SURFACE AND THE WRINKLING/BUCKLING OF THE DOME IS VISIBLE. THE PINHOLE LEAKS NOT VISIBLE ARE CLOSE TO THE CENTER TOP SURFACE OF THE DIAPHRAGM.

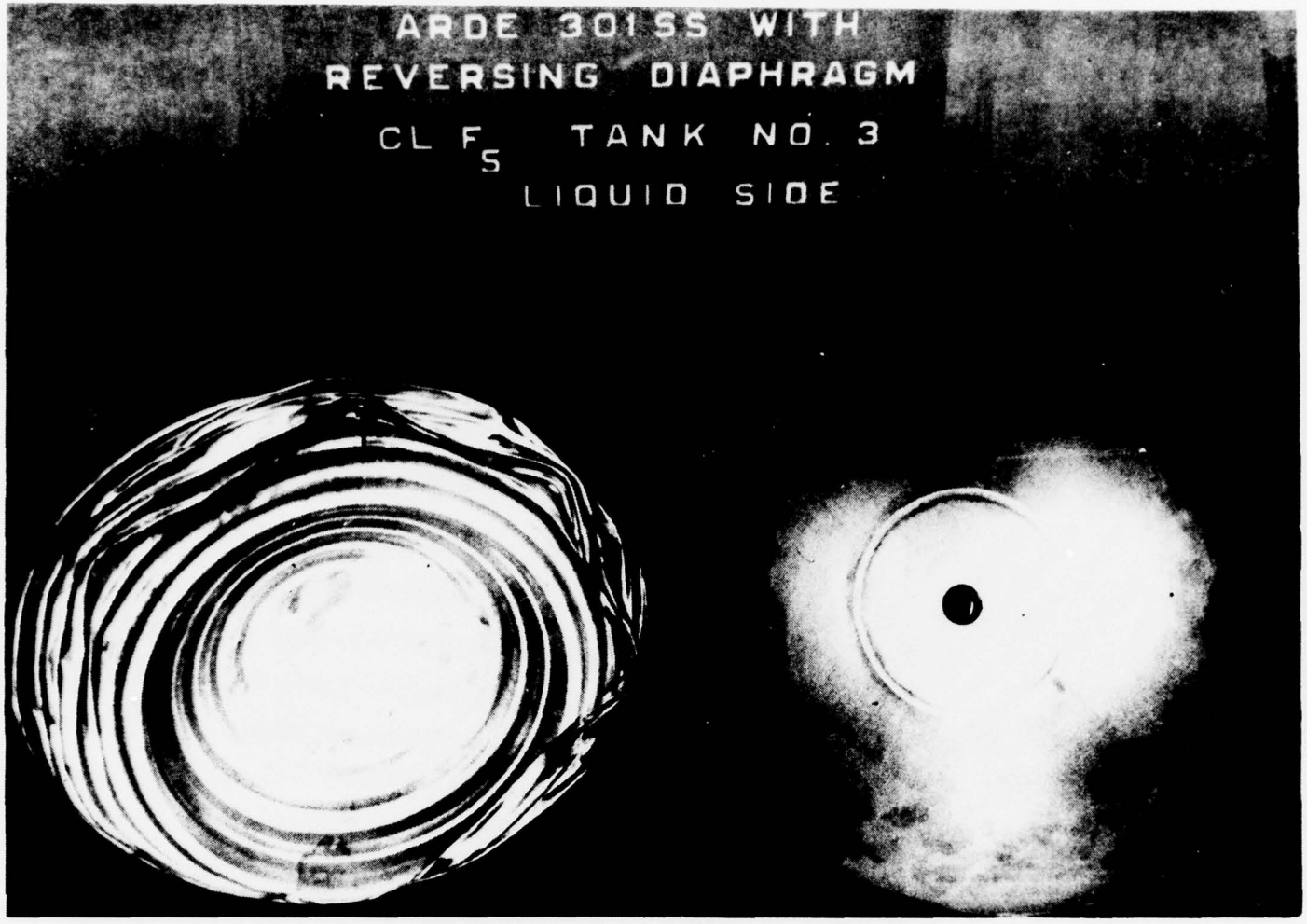

FIGURE 19. LIQUID SIDE OF ARDE TANK NO. 3. THE CONDITION OF THE DIAPHRAGM IS A DIRECT RESULT OF AN ATTEMPT TO REVERSE THE DIAPHRAGM AFTER COMPLETION OF AN EXPULSION TEST. LEAK OCCURRED AT SHARP BUCKLE (ARROW).

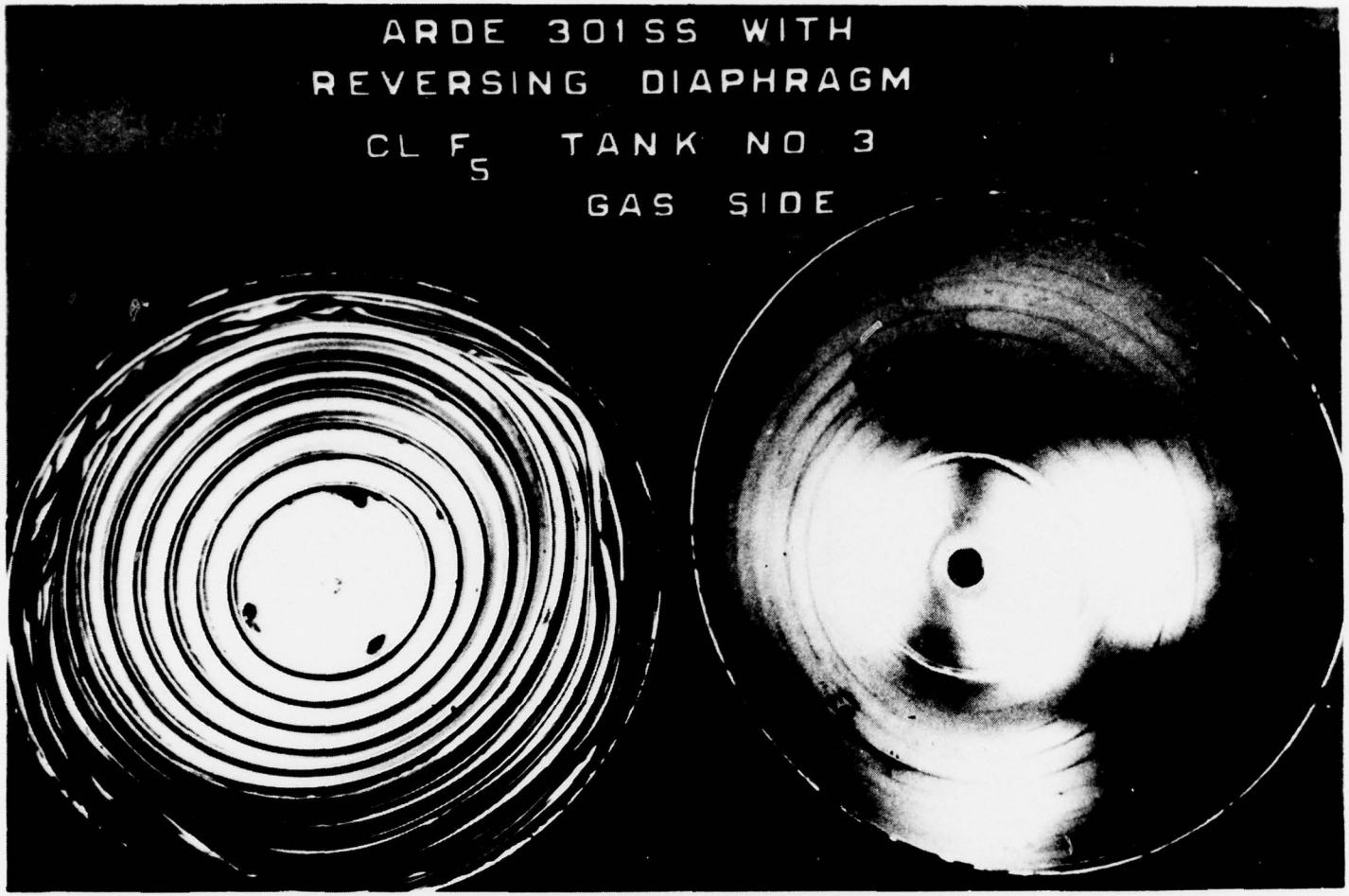

FIGURE 20. GAS SIDE OF ARDE TANK NO. 3. BUCKLING OF THE DIAPHRAGM IS QUITE EVIDENT IN THIS VIEW. THE STAINS IN THE SHELL ARE FROM THE EXPULSION TEST AND ARE NOT ATTRIBUTABLE TO CORROSION.

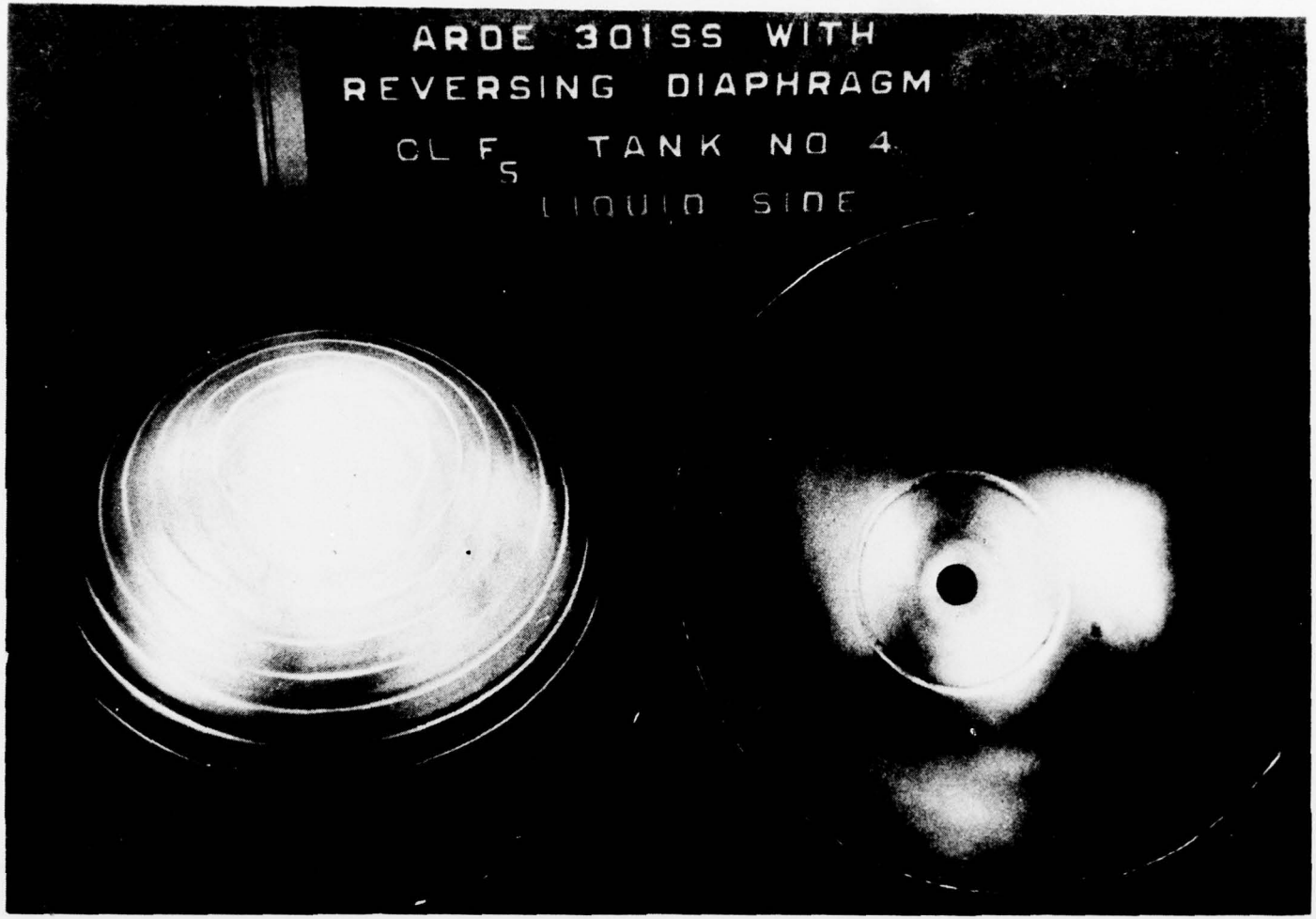

FIGURE 21. LIQUID SIDE OF ARDE TANK NO. 4. THIS TANK WAS RECEIVED IN THE FULLY EXPELLED CONDITION. SURFACES OF SHELL AND DIAPHRAGM WERE FOUND CLEAN AND FREE OF CORROSION FROM STORAGE.

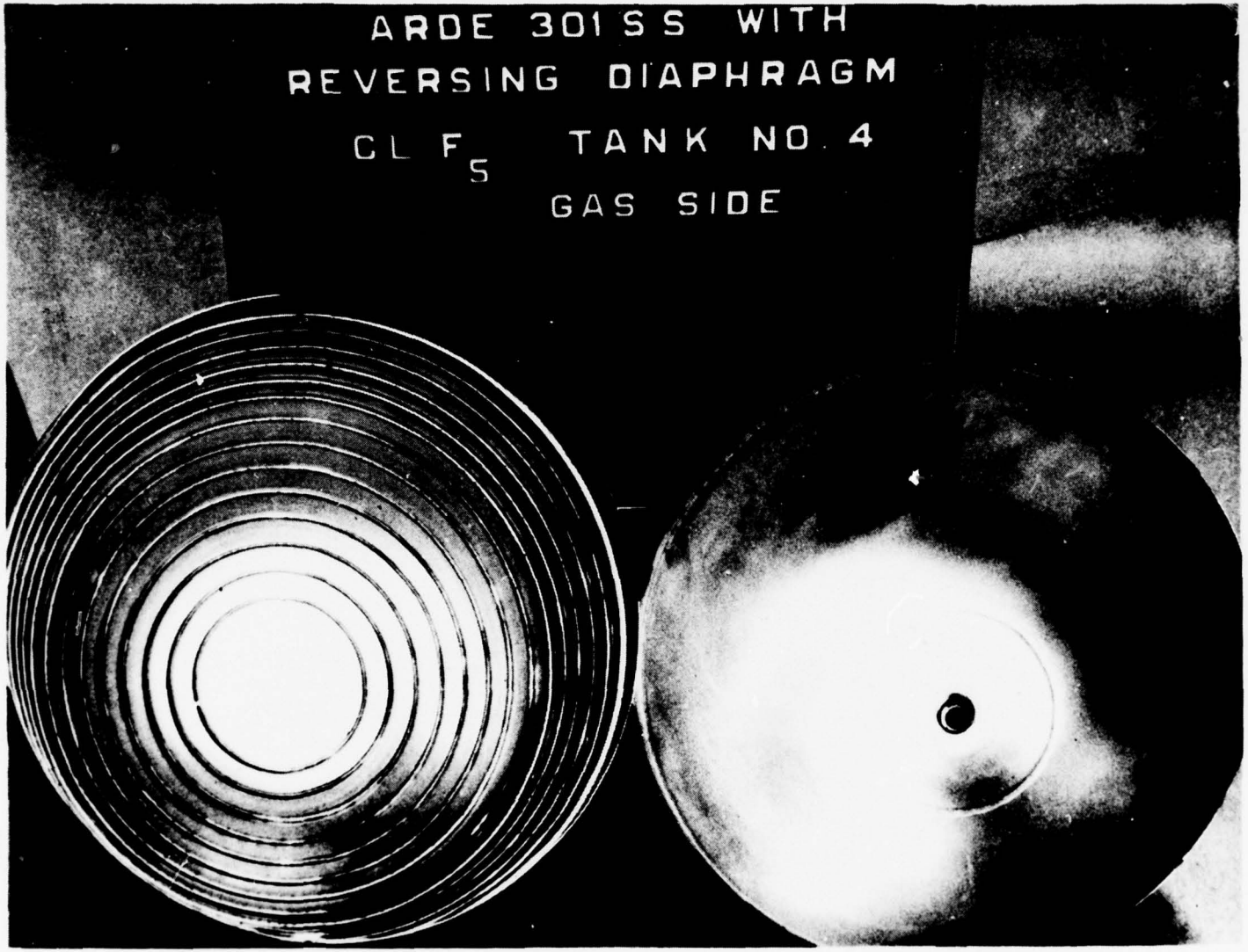

FIGURE 22. GAS SIDE OF ARDE TANK NO. 4. NO EVIDENCE OF CORROSION OR STAINING WAS FOUND.

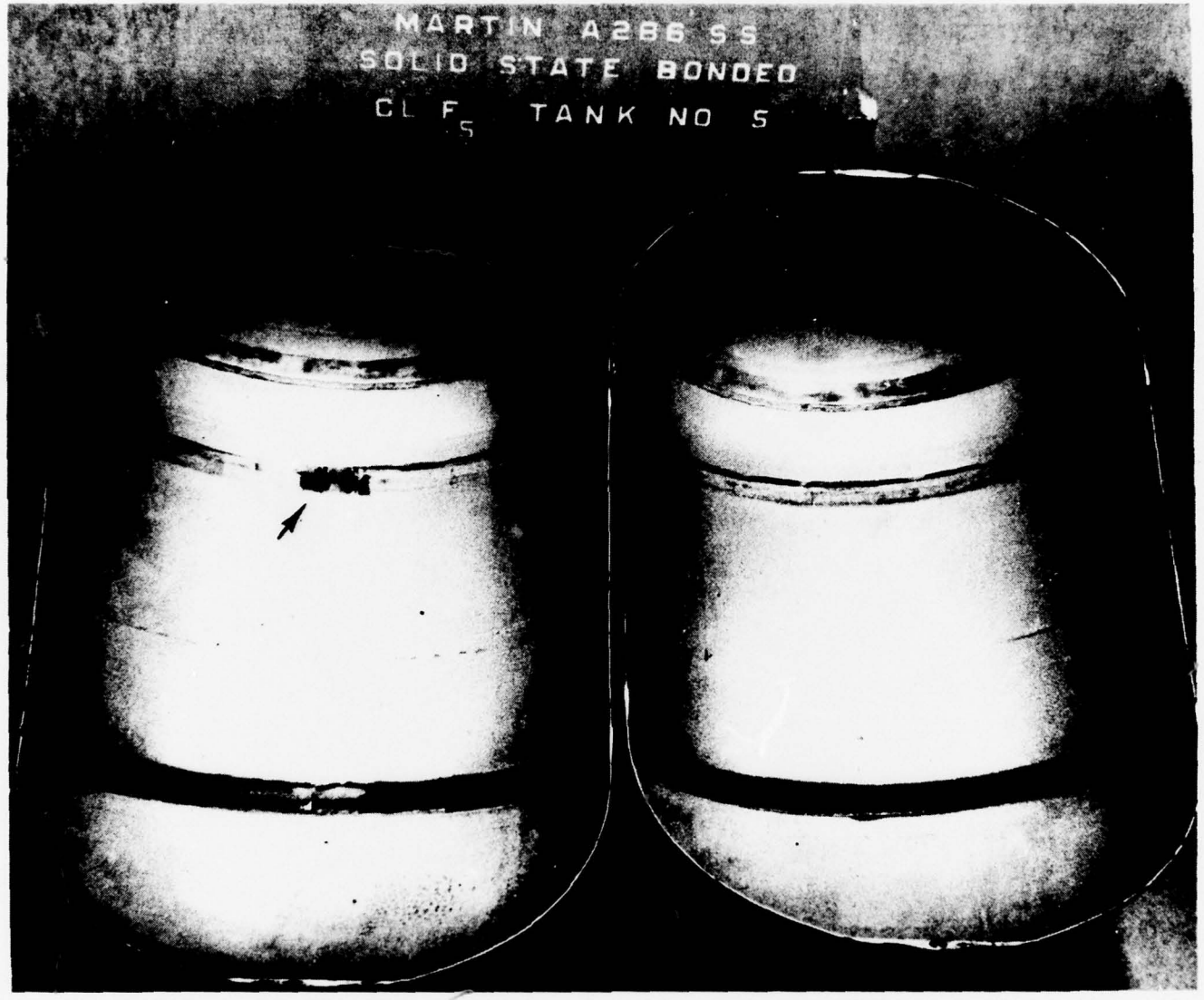

FIGURE 23. . INTERIOR SURFACES OF TANK NO. 5. OVERALL CONDITION OF SURFACE APPEARS TO BE UNAFFECTED BY STORAGE. LOCALIZED AREAS HAVE BEEN MARKED WITH ARROWS WHERE A MORE DETAIL EXAMINATION OF THE SURFACE IS REQUIRED TO ESTABLISH IF CORROSION OCCURRED.

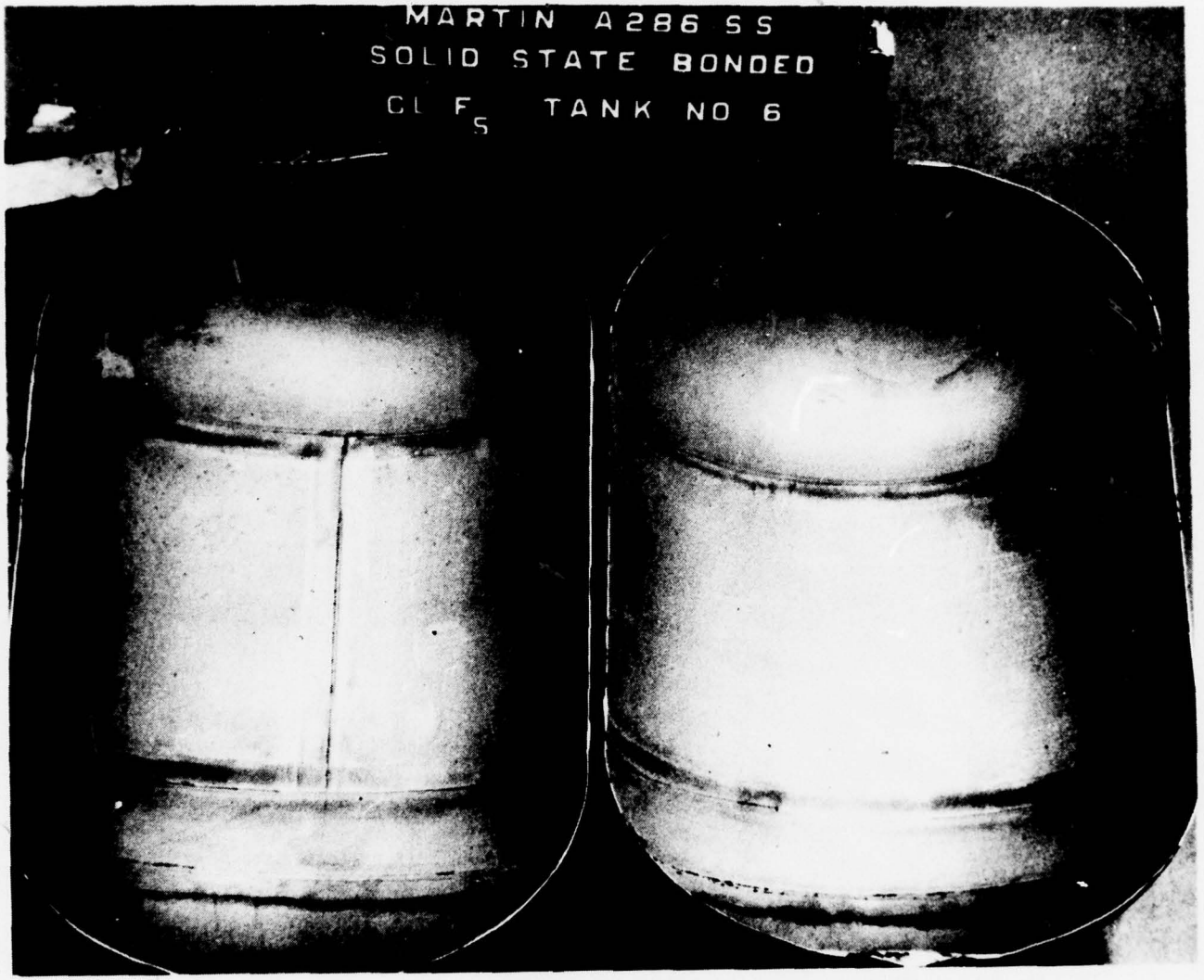

FIGURE 24. INTERIOR SURFACES OF TANK NO. 6. GENERAL SURFACE CONDITION WAS FOUND TO BE FREE OF STAINS, HOWEVER, SOME PITTING IS PRESENT AROUND PERIPHERY OF UPPER BOSS (RIGHTHAND VIEW OF SHELL), AN ARROW HAS BEEN USED TO SHOW THE AREA OF CONCERN. THIS REGION WILL BE INVESTIGATED IN GREATER DEPTH.

FIGURE 25. INTERIOR SURFACES OF TANK NO. 7. STAINING OF THE SURFACE IS ATTRIBUTED TO INCOMPLETE REMOVAL OF ALL PROPELLANT. AFTER UNLOADING TANK LAID ON ITS SIDE AND EVAPORATION OF CL F_5 TOOK PLACE, CAUSING STAINS AND CORROSION OF THE INTERIOR SURFACE. REACTION OF PROPELLANT WITH SURFACE NOT ATTRIBUTABLE TO STORAGE.

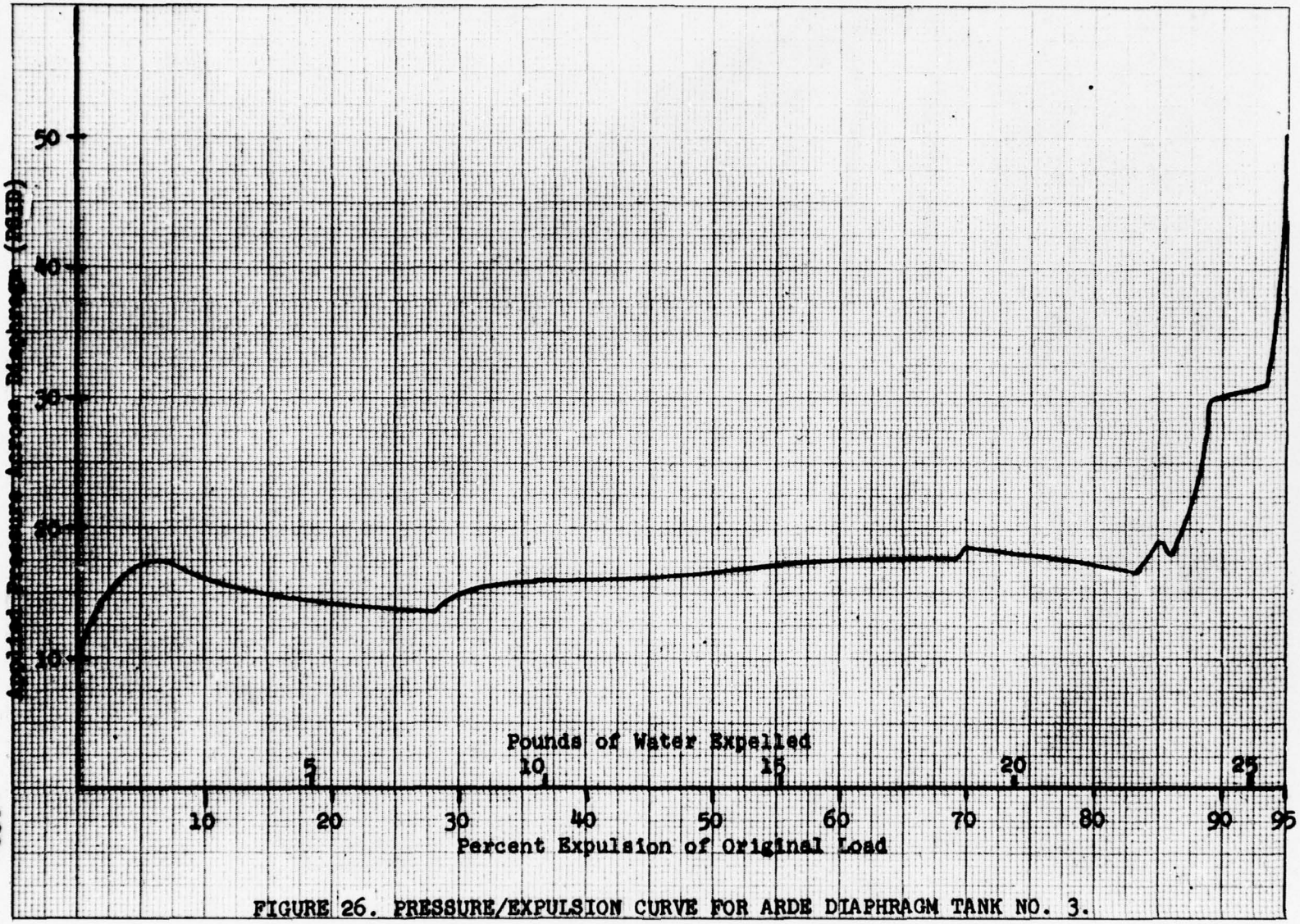

FIGURE 26. PRESSURE/EXPULSION CURVE FOR ARDE DIAPHRAGM TANK NO. 3.

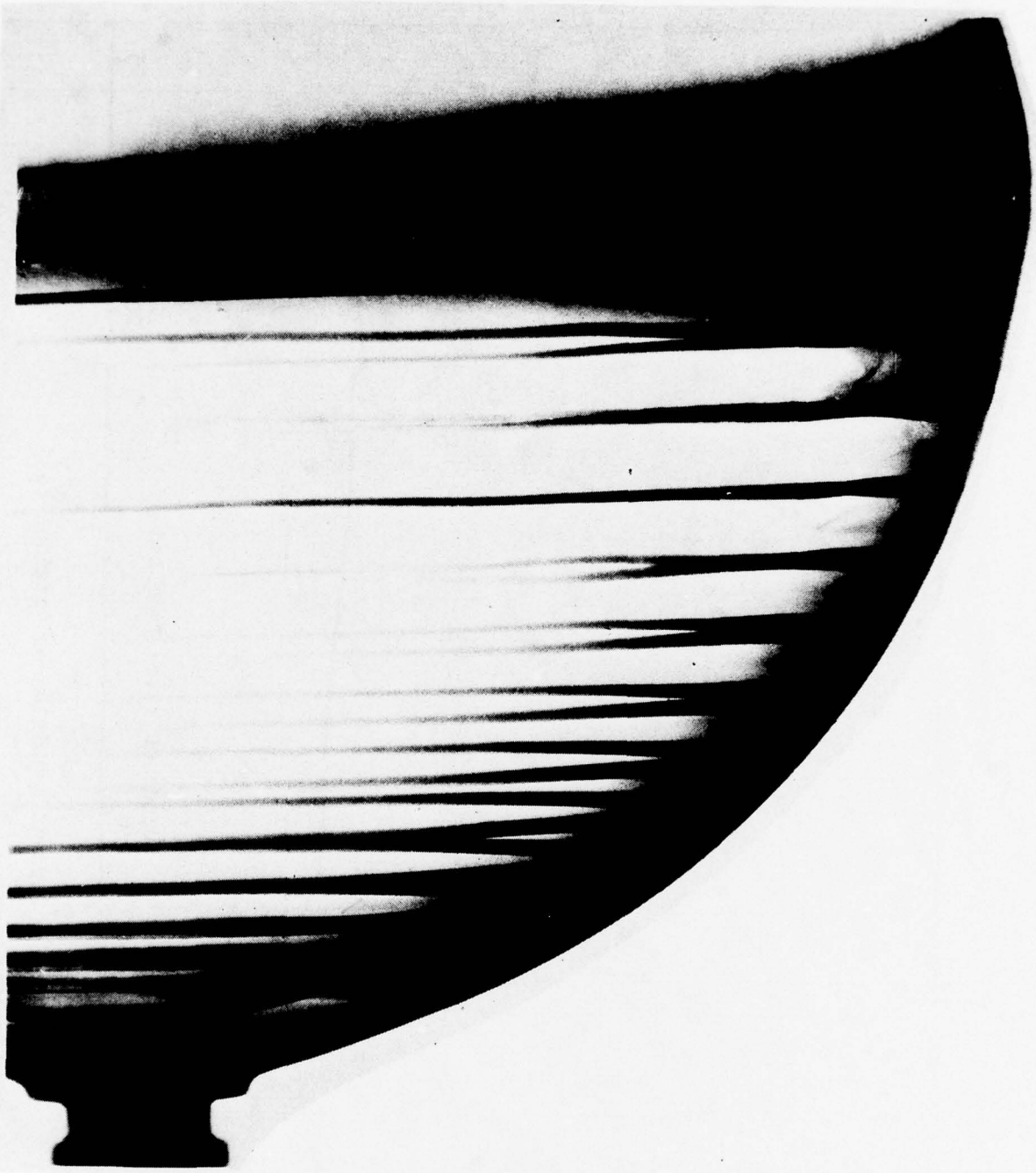

FIGURE 27. CONTACT PRINT OF RADIOGRAPH OF TANK NO. 3 AFTER COMPLETE EXPULSION AT BAT. WRINKLING AND BUCKLING OF DIAPHRAGM BETWEEN RINGS IS SEEN IN UPPER RIGHT SIDE.

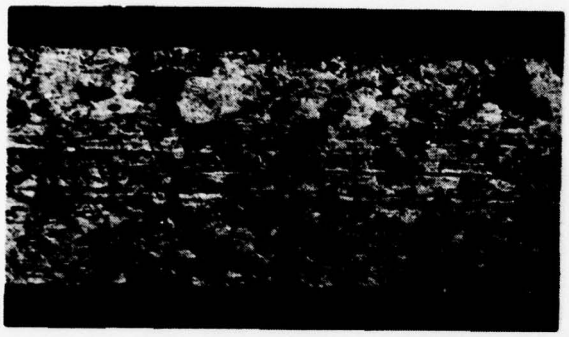

a) Axial direction.

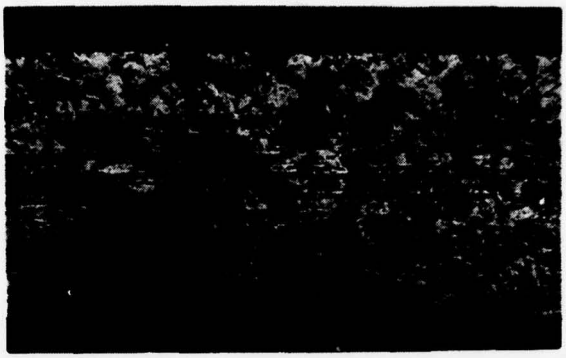

b) Circumferential direction.

Dome microstructure showing transformed nature of stainless steel, structure, and lack of any directionality.

c) Edge of weld and heat affected zone showing extensive transformation through entire region.

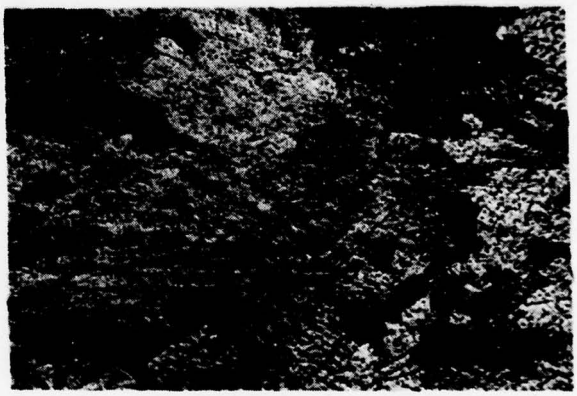

d) Weld structure showing coarse weld grains also transformed by cryostretching.

All Views: Mag. - 100X Etch - Mixed Acids Matl.-Cryostretched 301SS

FIGURE 28. MICROSTRUCTURE OF ARDE TANK NO. 4 IN DOME AND IN WELD JOINING DOME TO TRANSITION RING.

METALLURGICAL LABORATORY MET NO. 78-79011

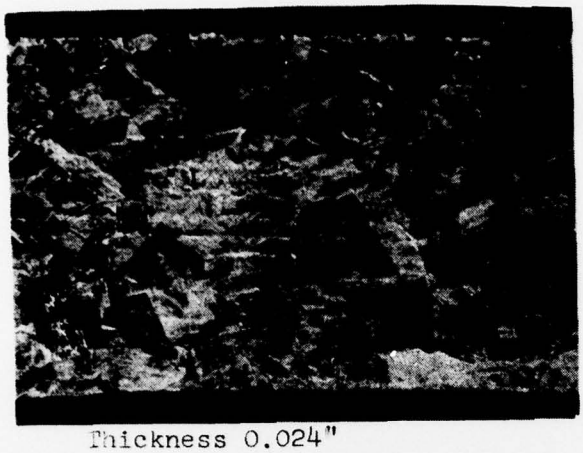

Thickness 0.024"

a) Structure near ring to dome weld where ring approximates dome thickness and shows structure same as dome.

Thickness 0.050"

b) Thicker region where transformation structure is coarser.

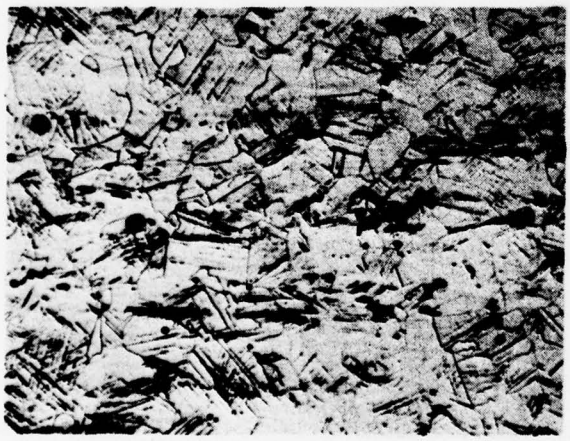

Thickness 0.075"

c) Thicker region where transformation is no longer complete.

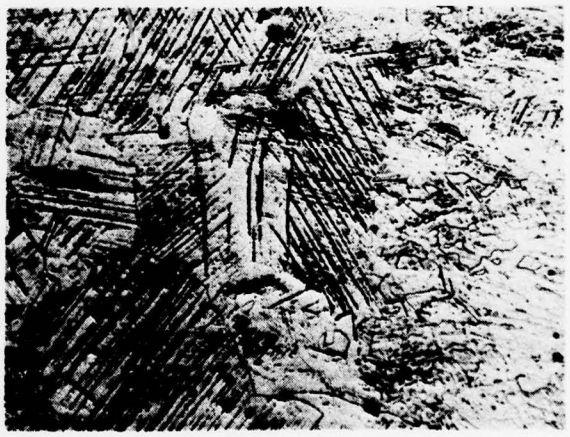

Thickness 0.094"

d) Thickest portion of transition ring (at weld) where only discrete transformation has occurred.

All Views: Mag: 100X Etch: Mixed Acids Matl: Cryostretched 301SS

FIGURE 29. MICROSTRUCTURE OF ARDE TANK NO. 4 IN TRANSITION RING BETWEEN DOME AND DIAPHRAGM ATTACHMENT SHOWING DECREASE IN TRANSFORMATION WITH INCREASING THICKNESS.

METALLURGICAL LABORATORY MET NO. 78-79011

Mag: 3X

a) Overall view of central region showing diaphragm attachment weld.

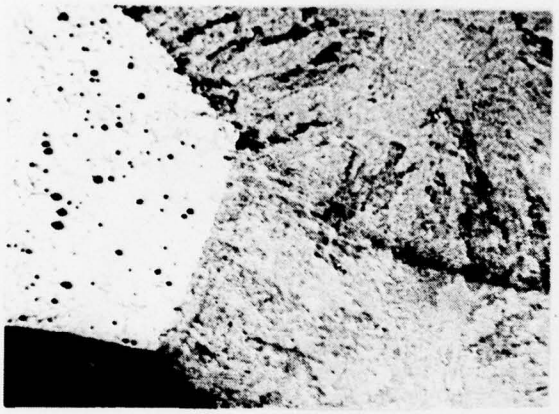

Mag: 25X

b) Weld interface region where second pass of diaphragm attachment weld covers first pass.

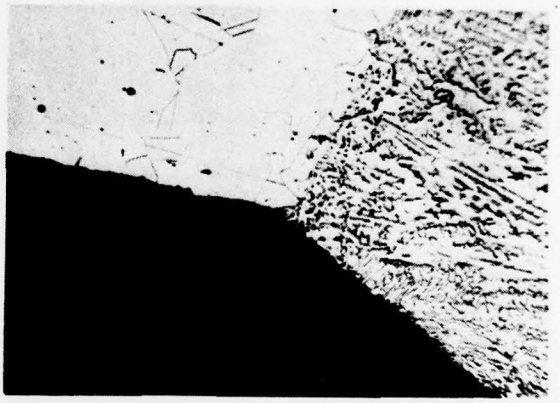

Mag: 100X

c) Closeup view of edge of weld on propellant side showing lack of any corrosion.

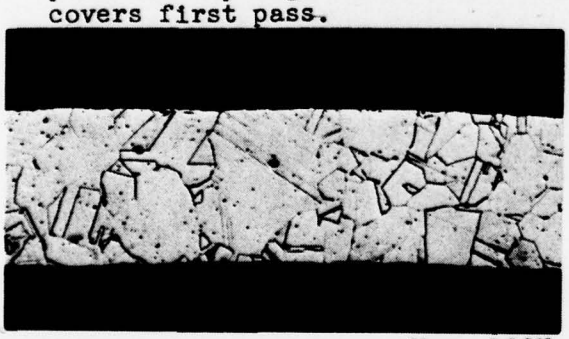

Mag: 100X

d) Cross section and microstructure of diaphragm leaf showing typical stainless steel structure.

Mag: 50X

e) Critical region at diaphragm to weld edge showing no cracks or degradation.

FIGURE 30. VIEWS OF DIAPHRAGM ATTACHMENT REGION IN ARDE TANK NO. 4 ILLUSTRATING THE SOUND WELD AND LACK OF ANY PROPELLANT INDUCED CORROSION.

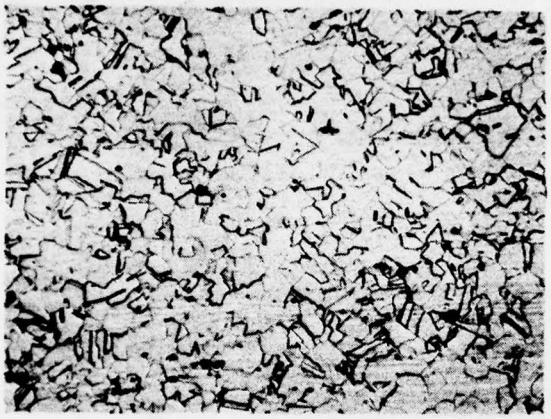

a) Dome Section - Axial Direction.

b) Cylinder Section - Axial Direction

All Views - Mag: 100X Etch: Mixed Acids Matl: A-286 SS
Solution Treat & Age

FIGURE 31. MICROSTRUCTURE OF A-286 STAINLESS STEEL SHEET USED TO FABRICATE MARTIN TANK NO. 5.

METALLURGICAL LABORATORY MET NO. 78-79011

a) Dome section - axial direction.

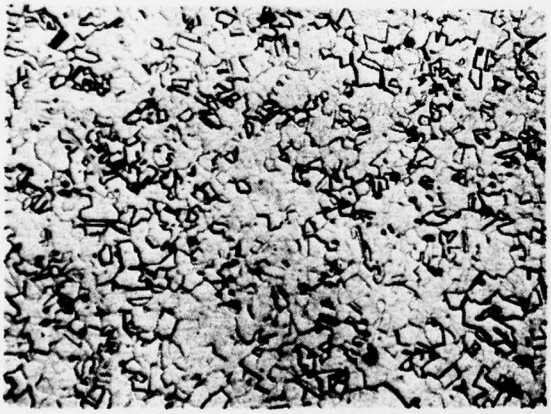

b) Cylinder section - circumferential direction.

c) Cylinder section - axial direction.

All Views - Mag: 100X Etch: Mixed Acids Matl: A-286 SS Solution Treat plus Age

FIGURE 32. MICROSTRUCTURE OF A-286 STAINLESS STEEL SHEET USED TO FABRICATE MARTIN TANK NO. 6.

METALLURGICAL LABORATORY MET NO. 78-79011

Mag: 3/4X

a) Propellant side with several leak sites, detected by soap film bubbling, marked.

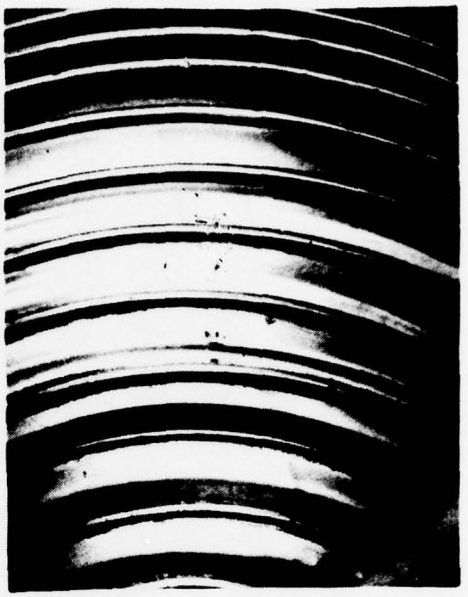

b) Gas side with with leak areas marked.

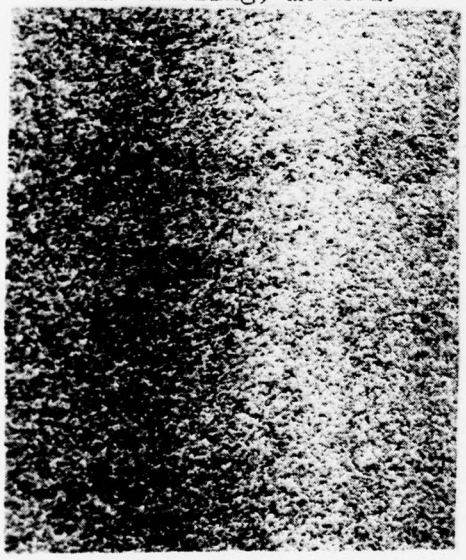

Propellant Side Mag: 15X Gas Side

c) Closeup views of one of the few leak sites where surface indication could be identified.

FIGURE 33. VIEWS OF SURFACE OF DIAPHRAGM OF TANK NO. 2 IN REGION WHERE LEAKS WERE DETECTED.

METALLURGICAL LABORATORY MET NO. 78-79011

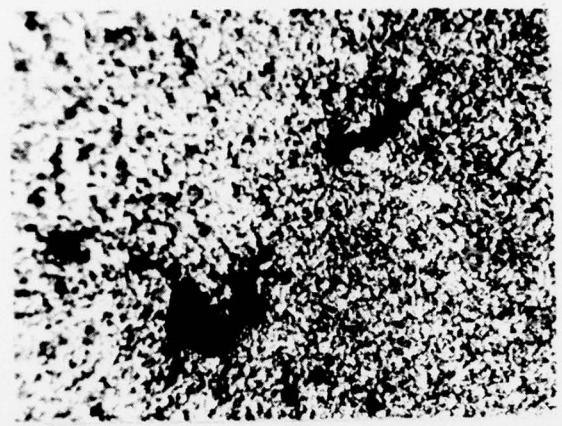

a) Detail view of propellant side surface showing pitted nature of leak area.

Mag: 100X

b) Initial observation of internal defect 0.002 inch before first surface evidence.

Mag: 200X Unetched

Mag: 200X
Unetched

c) Cross section 0.002 inch beyond view (b), where first surface connection is seen.

FIGURE 34. DETAIL SURFACE VIEW AND INITIAL SECTIONS THROUGH ONE LEAK PATH IN DIAPHRAGM FROM TANK NO. 2.

Unetched Mag: 200X

a) Section 0.0035 inch beyond initial site of corrosion. Total width of internal corrosion at this point is 0.021 inch.

Mixed acid etch Mag: 200X

b) Section 0.008 inch beyond initial site. Corrosion has become much less. Etched view shows corrosion is at least started by intergranular penetration.

FIGURE 35. ADDITIONAL CROSS SECTION VIEWS THROUGH LEAKING DEFECT.

a) Section 0.0175 inch beyond initial site. In the 0.009 inch region between last view and this, corrosion cavity became very small. This area is associated with second pit seen in view (a) of Figure 34.

b) Section 0.0185 inch beyond initial site. Corrosion is approaching gas side surface for first time.

c) Section less than 0.001 inch beyond view (b). This is only location where penetration to gas side is seen.

d) Section 0.001 inch beyond view (c). Gas side penetration has disappeared already.

All Views: 200X

FIGURE 36. CROSS SECTIONS THROUGH LEAKING DEFECT IN AREA OF SECOND PIT VISIBLE IN VIEW (A) OF FIGURE 34.

a) Section 0.007 inch beyond start of second pit, view (a) of Figure 36, and 0.025 inch beyond initial corrosion observation.

b) Final view of corrosion, 0.030 inch beyond initial indication. In 0.005 inch further progression, metal was sound.

Both Views: Mag: 200X

FIGURE 37. FINAL CROSS SECTIONS OBTAINED IN POLISHING THROUGH ONE OF THE LEAKING DEFECTS IN DIAPHRAGM FROM TANK NO. 2.

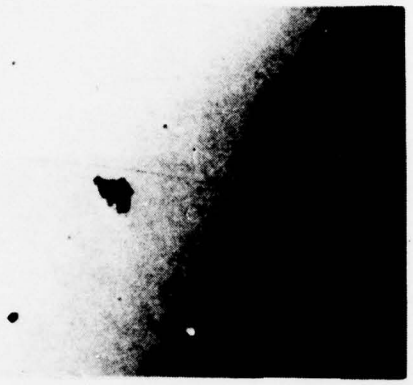

Mag: 15X

a) Reproduction of X-ray film magnified 15 times and direct, positive printed so that corroded, "porous" area appears black.

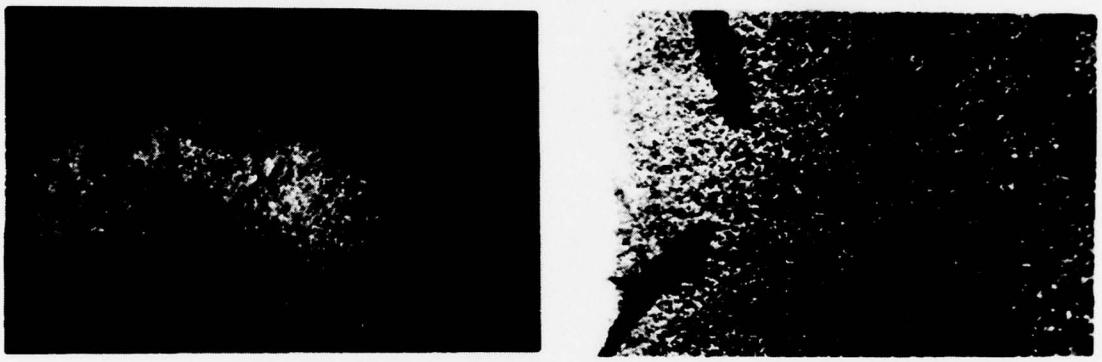

Propellant Side Mag: 15X Gas Side

b) Macroscopic views of surface at leak and radiograph indication site.

FIGURE 38. VIEWS OF DEFECT FOUND BY X-RAY IN REGION CLOSE TO DEFECT SECTIONED IN PREVIOUS FIGURES 34 THROUGH 37.

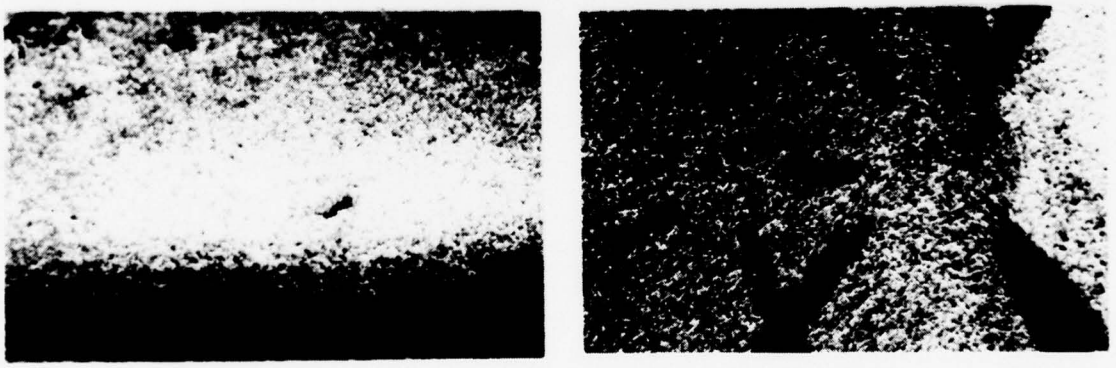

Propellant Side Mag: 15X Gas Side

FIGURE 39. SURFACE VIEWS OF LEAKING DEFECT FOUND BY FLUORESCENT PENETRANT SEEPING THROUGH DIAPHRAGM OF TANK NO. 2.

Mag: 100X

a) Surface view in penetrant indication region showing only pronounced grain boundaries and slight pits.

b) Region after light polishing with 600 grit paper to remove surface layer.

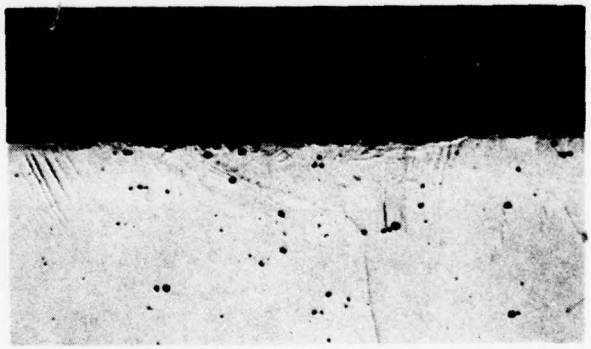

Unetched Mag: 100X

c) Cross section through indication region showing disturbance of subsurface layers but no appreciable depth of attack.

FIGURE 40. AREA NEAR APEX OF DIAPHRAGM IN ARDE TANK NO. 4 WHICH SHOWED A DYE PENETRANT INDICATION WHICH HAD NO SIGNIFICANT DEPTH NOR WAS A TRUE PIT.

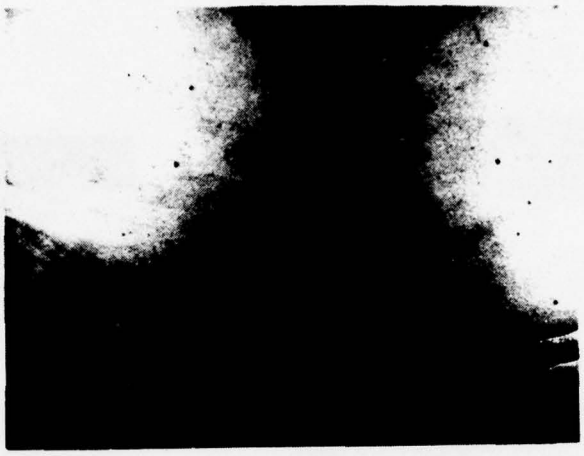

Mag: 1X

a) Overall view in area of dark spot on shell. Pits are barely visible.

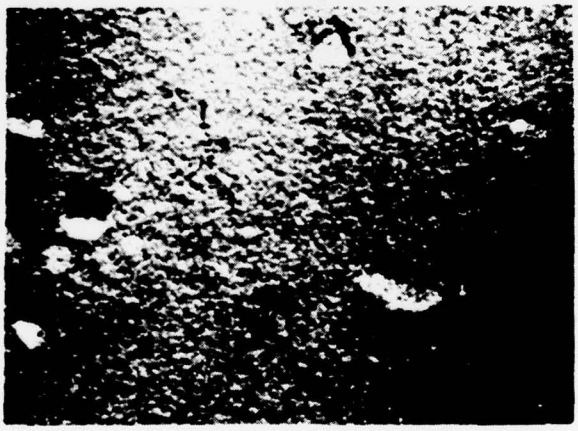

Mag: 15X

b) Detail view showing that pits varied from very deep to shallow.

FIGUR 41. VIEWS OF PITTING ON EXTERIOR SURFACE OF SHELL OF ARDE TANK NO. 1.

Mag: 15X

a) View of weld surface showing pits. All pits seen of weld surfaces appeared relatively shallow.

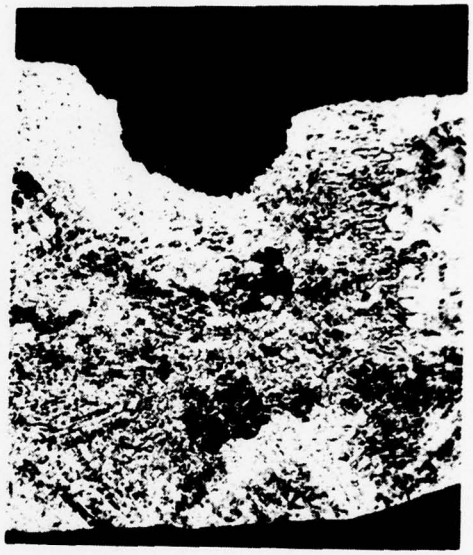

Mag: 100X

b) Cross section through typical pit in weld.

FIGURE 42. PITTING IN SHELL WELD FROM ARDE TANK NO. 1.

METALLURGICAL LABORATORY MET NO. 78-79011

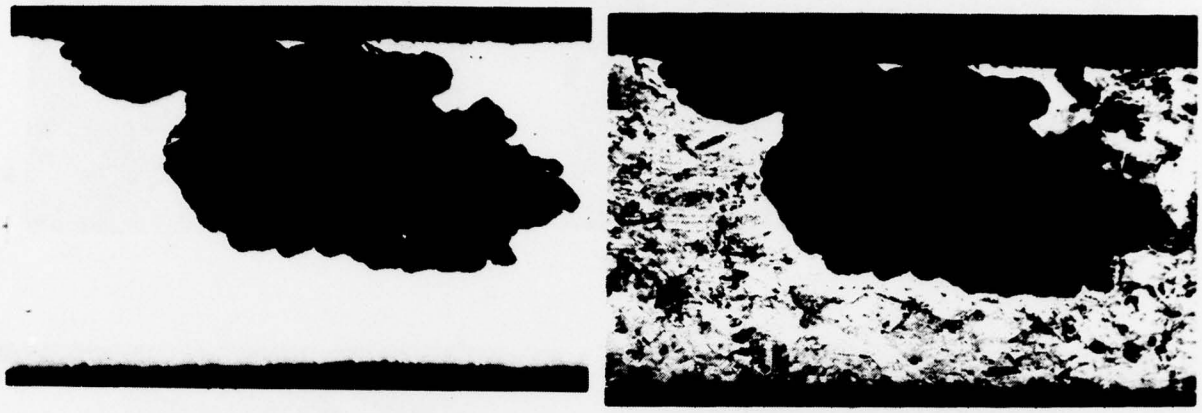

Mag: 100X

a) Unetched view showing absence of intergranular or other penetration ahead of main pit.

b) Etched view showing pit in matrix of cryostretched material.

Mag: 50X

Mag: 100X

c) Views of pit after polishing 0.010" farther from above views. Pits never penetrated through to interior surface to become a leak.

FIGURE 43. SECTIONS THROUGH DEEP PIT FOUND NEAR DARK SPOT OF ARDE TANK NO. 1.

METALLURGICAL LABORATORY MET NO. 78-79011

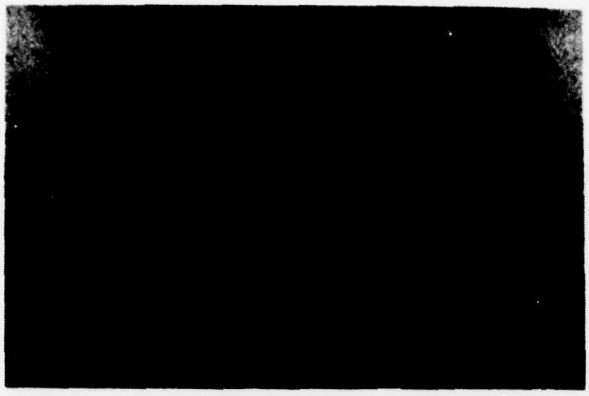

Mag: 2X

a) Overall view of portion of shell.

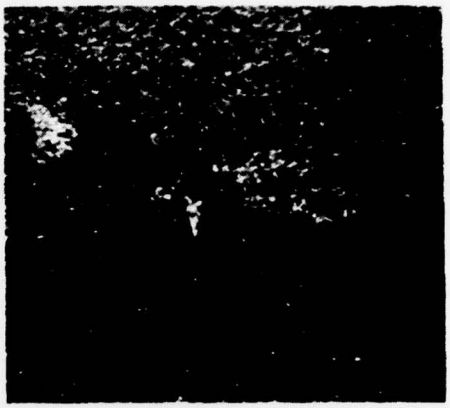

Mag: 15X

b) Closeup view of pit composed of three cavities.

Mag: 100X

c) Section through double pit portion of region.

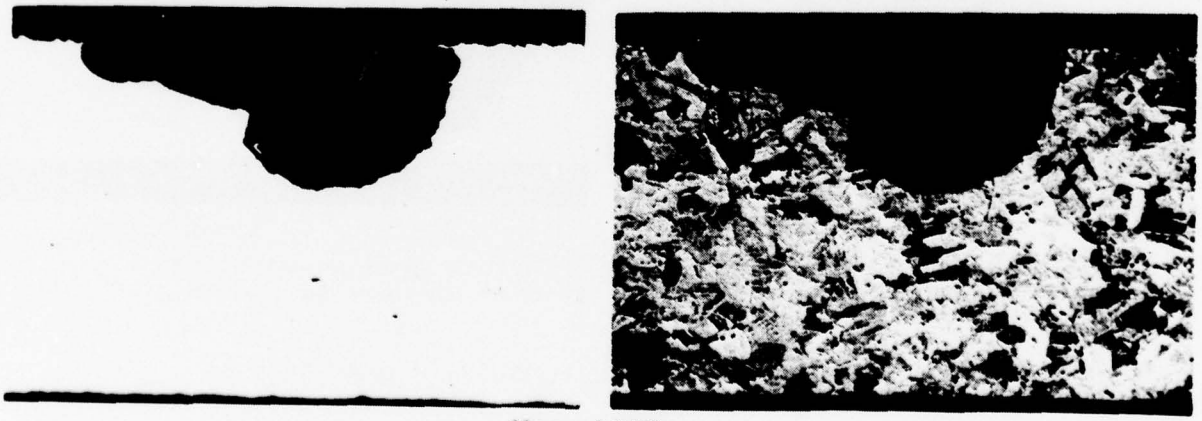

Mag: 100X

d) Section where pits have joined into single cavity.

FIGURE 44. PITS IN SURFACE OF ARDE TANK NO. 3.

METALLURGICAL LABORATORY MET NO. 78-79011

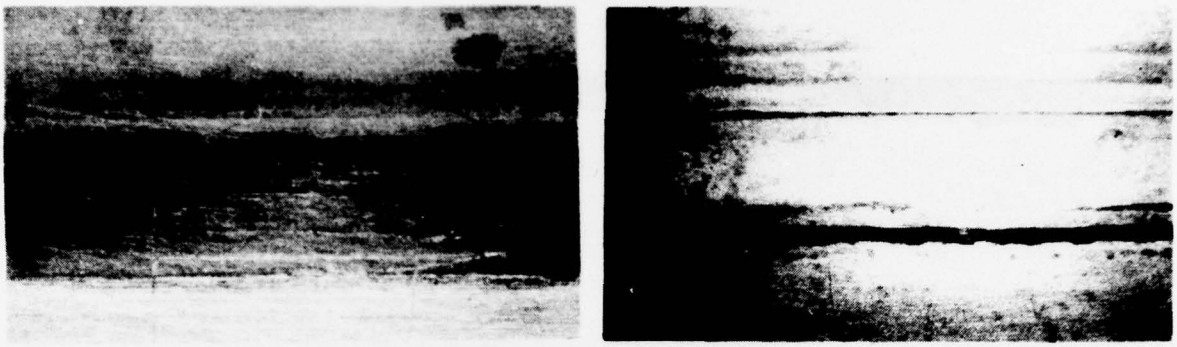

Inside Surface Mag: 1X Outside Surface

a) Upper circumferential bond joint showing discoloration along the interior overlap.

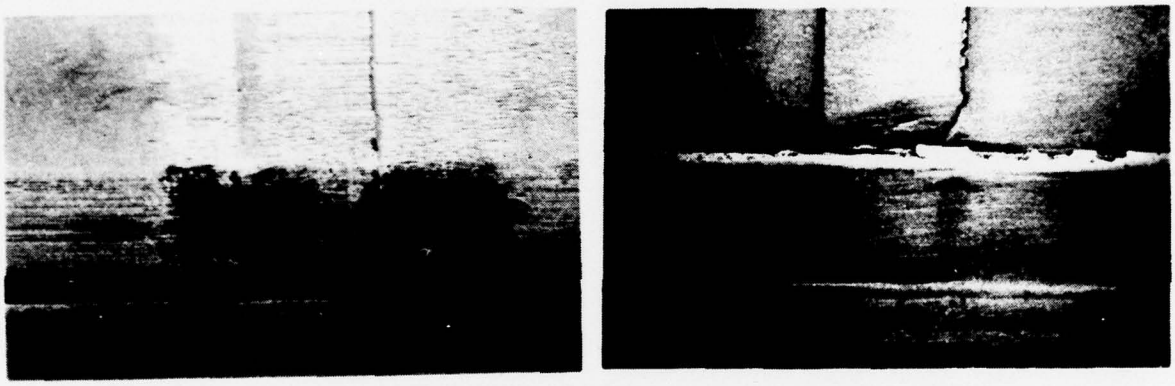

Inside Mag: 1X Outside

b) Lower circumferential bond joint at overlap with longitudinal cylinder joint.

Mag: 8X

c) Closeup view of weld patch at arrow in view (b).

FIGURE 45. VIEWS OF EXPLOSIVE BOND SURFACE APPEARANCE IN SELECTED AREAS FROM A-286 TANK NO. 5.

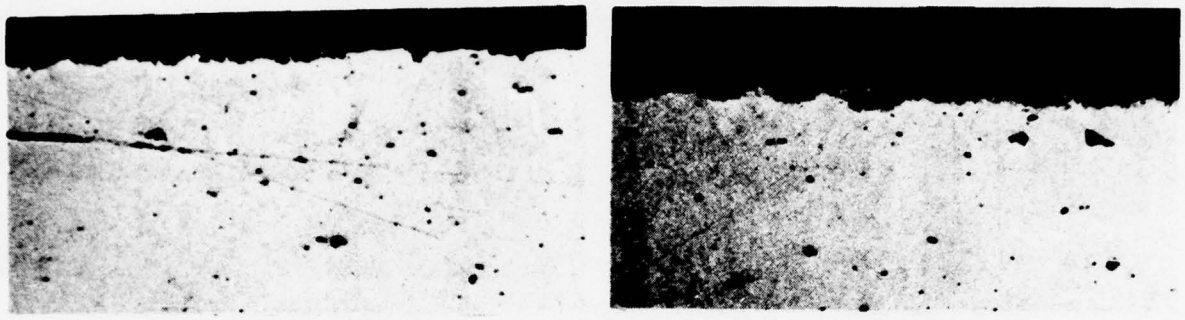

a) Near inner edge of bond overlap.

b) In central portion of bond overlap.

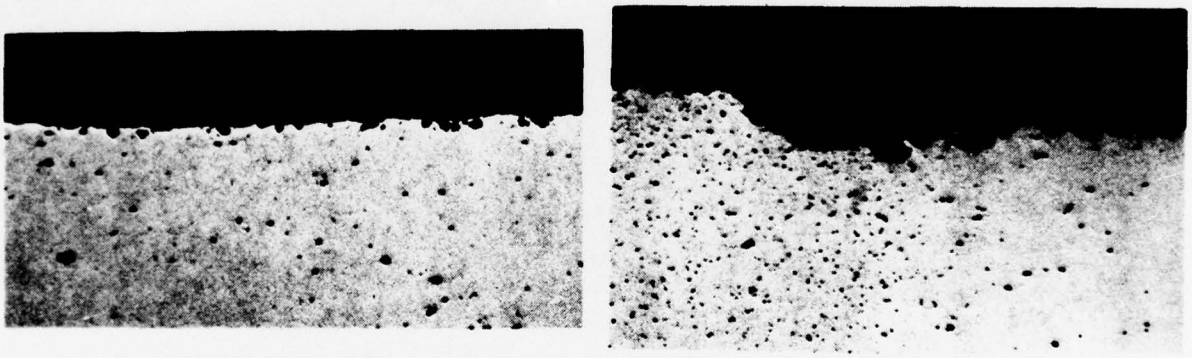

c) In base metal away from bond.

d) At edge of weld patch shown in Figure 45, view c.

All Views: Mag: 100X
Unetched

FIGURE 46. CROSS SECTIONS AT SURFACE ILLUSTRATING THE PRESENCE OF SHALLOW SURFACE ATTACK IN A-286 TANK NO. 5.

Mag: 2X

a) Stain along bond and on fitting surface.

Mag: 15X

b) Pits on surface of fitting at stain.

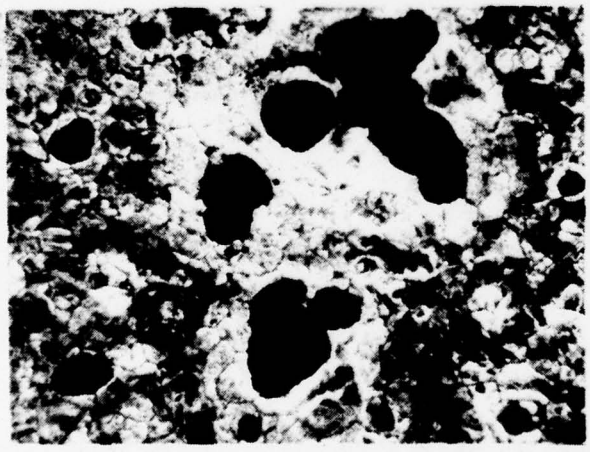

Matl: 321 SS

Mag: 100X

c) Detail view of surface pitting.

Mag: 100X

d) Cross section showing pits following intermetallic or inclusion stringers.

FIGURE 47. PITTING ON PROPELLANT SIDE OF OUTLET FITTING FROM TANK NO. 5 SHOWING IT TO BE THE RESULT OF END GRAIN ATTACK OF THE 321 STAINLESS STEEL BAR STOCK.

METALLURGICAL LABORATORY MET NO. 78-79011

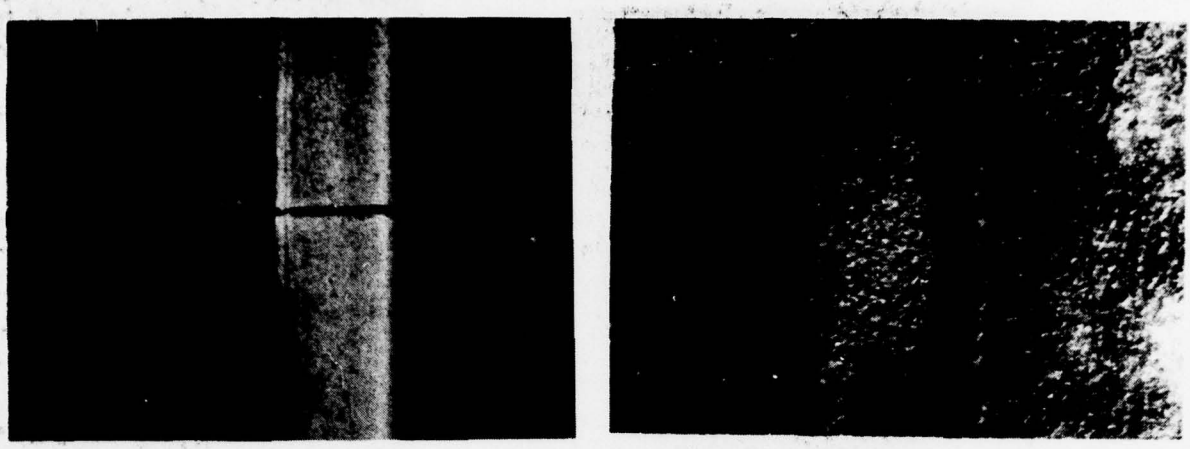

View (a) Mag: 1X View (b) Mag: 15X

Photomacrographs showing the distinct waterline, but also showing that on a magnified scale there was no difference in surface pitting in this region.

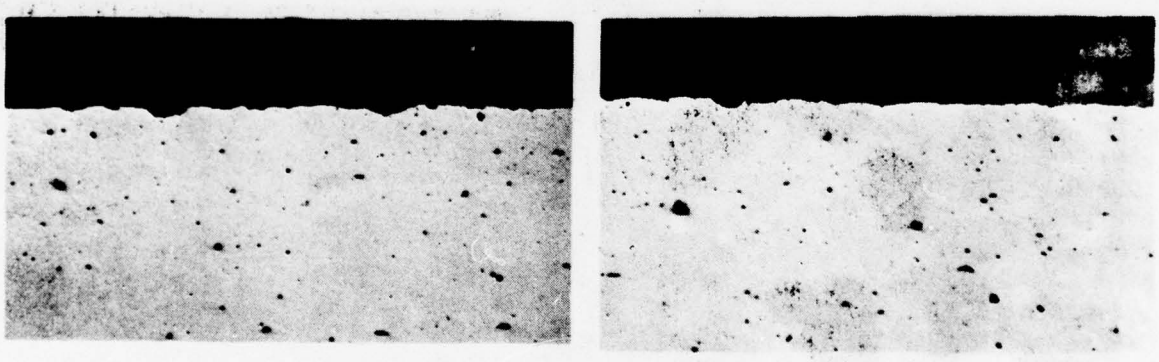

Mag: 100X Unetched

c) Cross section at surface on waterline showing some shallow pitting.

d) Cross section at surface approximately 1" from waterline showing similar pitting.

FIGURE 48. "WATERLINE" AT APPROXIMATE MIDPOINT OF TANK NO. 7 INTERIOR.

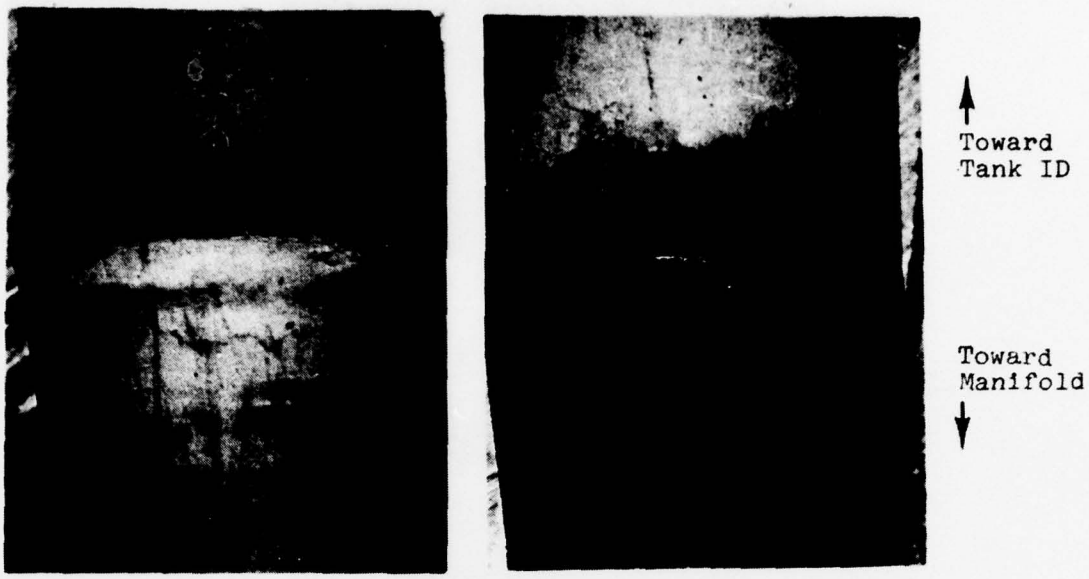

Mag: 4X

a) Tube at bond region where boss fitting is recessed, requiring tube to expand. Tear and corrosion/staining occurred at maximum expansion region.

Mag: 15X

b) Closeup view of staining around split at bond.

FIGURE 49. INTERNAL SURFACE OF UPPER TUBE FROM TANK NO. 5 AFTER SECTIONING OPEN TO EXPOSE SPLIT.

METALLURGICAL LABORATORY MET NO. 78-79011

Mag: 4X

a) Overall section view showing split to be just before maximum recess in fitting.

Unetched Mag: 100X

b) Detail view of split showing lack of any corrosion. Transverse fissures are at inclusions.

Mag: 100X

c) Etched view showing strain effects at arrows along inclusion streaks.

FIGURE 50. CROSS SECTION THROUGH TORN UPPER TUBE ILLUSTRATING THE 45° SHEAR, MECHANICAL FRACTURE APPEARANCE, TANK NO. 5.

Mag: 3X

a) Overall section view showing tube expanded into recess, but with a slight gap behind tube.

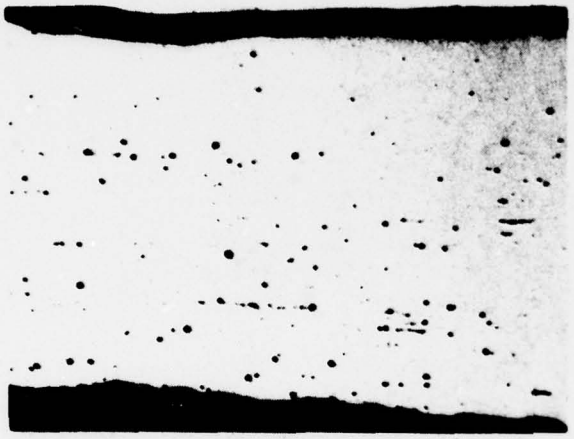

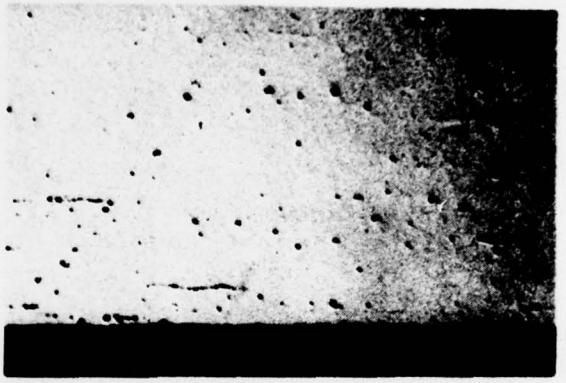

Tube at bond recess. Mag: 100X In tube away from bond.

b) Unetched views showing extensive amount of inclusions in AISI 321 stainless steel tubing.

Etched: Mixed Acids
Mag: 100X

c) Etched view showing strain effects along inclusions and start of 45° shear strain at arrow.

FIGURE 51. CROSS SECTION THROUGH TUBE BOND 180° FROM TEAR SHOWING STRAIN EFFECTS BUT NO SPLITTING OR TEARING, TANK NO. 5.

METALLURGICAL LABORATORY MET NO. 78-79011

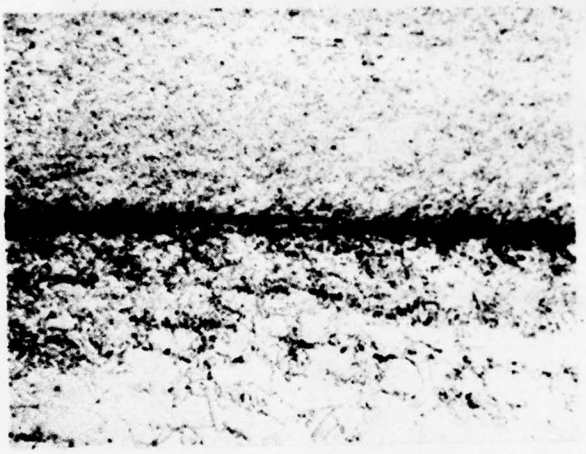

Etched: Mixed Acids Mag: 100X

a) Toward tank ID end. Note good, high strain and somewhat wavy bond, with no corrosion in crevice.

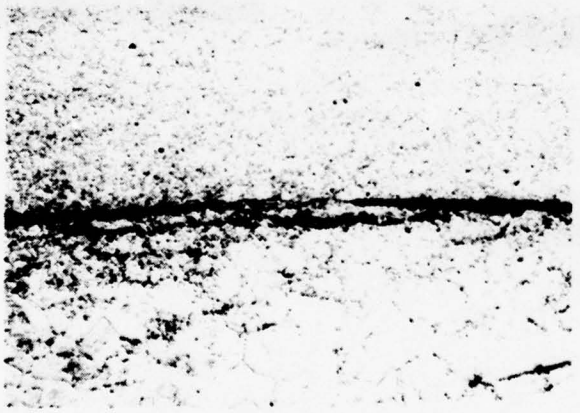

Mag: 100X

b) Toward tube end with poor bond starting but no abnormal corrosion.

FIGURE 52. ENDS OF TUBE TO FITTING CREVICE AT SPLIT TUBE SHOWING LACK OF ANY CORROSION EFFECTS, TANK NO. 5.

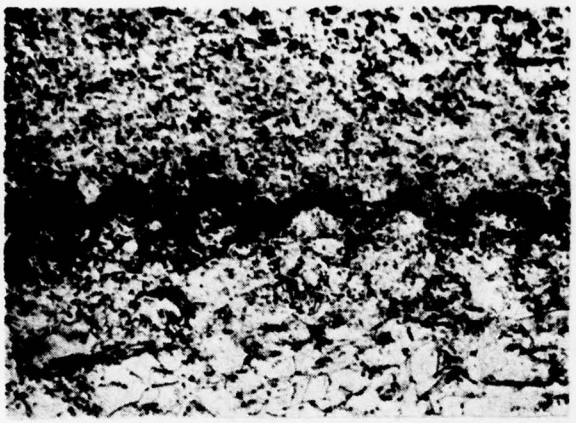

AISI 321 SS
Seamless Tubing

AISI 321 SS
Tank End Boss Fitting

Etched: Mixed Acids Mag: 100X

a) Bond in region between tank ID and bulge. Good bond with extensive strain and wave effects.

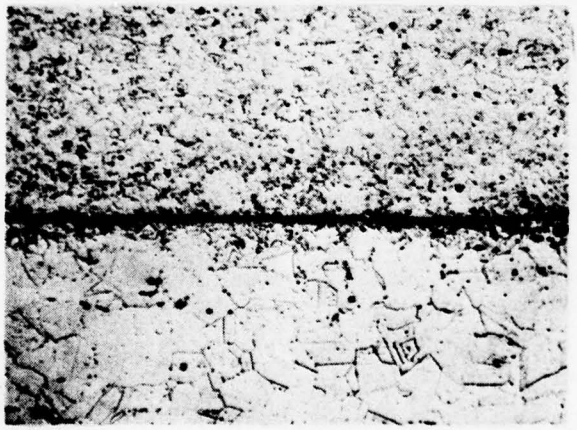

Etched: Mixed Acids
Mag: 100X

b) Bond in region beyond bulge from tank. Poor bond with no strain or wave effects.

FIGURE 53. EXPLOSIVE BOND STRUCTURE IN BONDED INLET/OUTLET TUBE REGION OF TANK NO. 5.

METALLURGICAL LABORATORY MET NO. 78-79011

Raised and pitted area shown in cross section below and in Figure 55 which follows.

Mag: 15X

a) Etched surface of shell near bond. See view (a) of Figure 47 for overall view of this area.

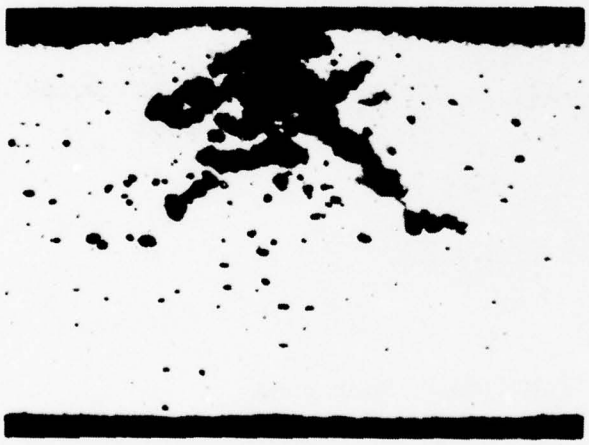

Unetched Mag: 50X

b) Cross section showing extensive pitting corrosion under raised area.

Unetched Mag: 200X

c) Detail view of corrosion.

FIGURE 54. CROSS SECTION OF PITTED AREA NEAR DOME TO OUTLET FITTING BOND OF TANK NO. 5 INTERIOR SURFACE.

METALLURGICAL LABORATORY MET NO. 78-79011

Mag: 50X

a) Overall view showing same general pattern of attack but with no surface outlet at this point.

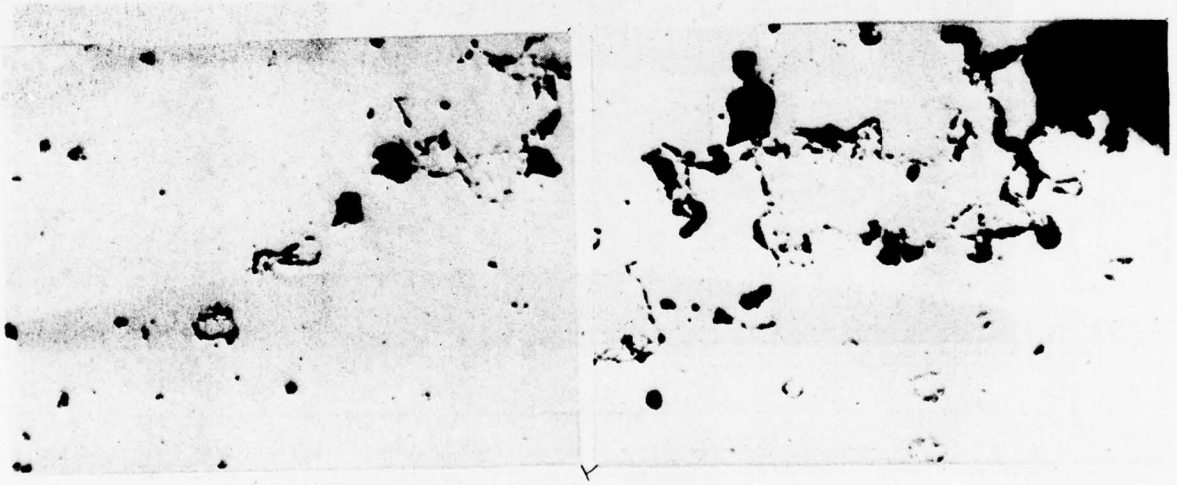

Mag: 200X Unetched

b) Detail views showing corrosive attack concentrated along intermetallic or inclusion particles.

FIGURE 55. CROSS SECTION OF PITTED AREA OF FIGURE 54 AFTER POLISHING 0.020 INCH FARTHER AWAY FROM BOND, TANK NO. 5.

METALLURGICAL LABORATORY MET NO. 78-79011

Mag: 25X

Tank No. 5

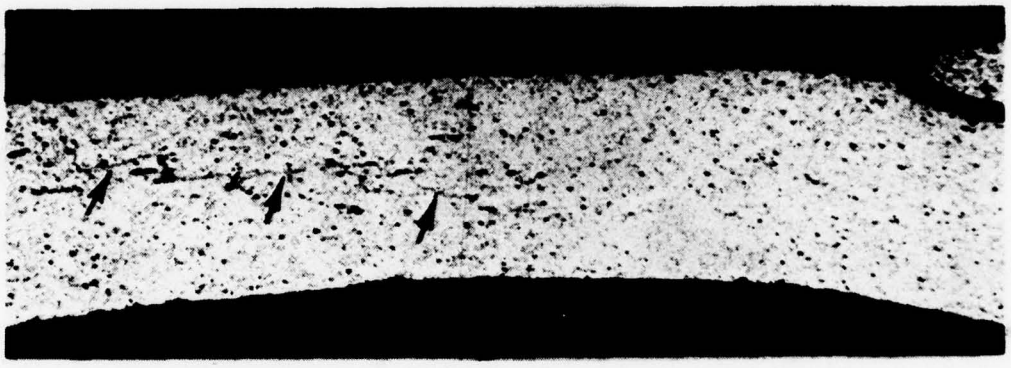

Mag: 25X

Tank No. 6

FIGURE 56. CROSS SECTIONS SHOWING INDICATION OF STRAIN AND/OR CORROSION EFFECTS APPROXIMATELY 0.1 INCH BEYOND EDGE OF BOND.

METALLURGICAL LABORATORY MET NO. 78-79011

Mag: 3X

a) Overall view of interior surface at bond.

Mag: 15X

b) Closeup of raised and pitted region at end of explosive progression.

Mag: 4X

c) Cross section showing relation of pitted area to bond.

FIGURE 57. VIEWS OF PITTED REGION NEAR DOME TO OUTLET FITTING BOND IN TANK NO. 7.

Mag: 25X

d) Detail view of pitting.

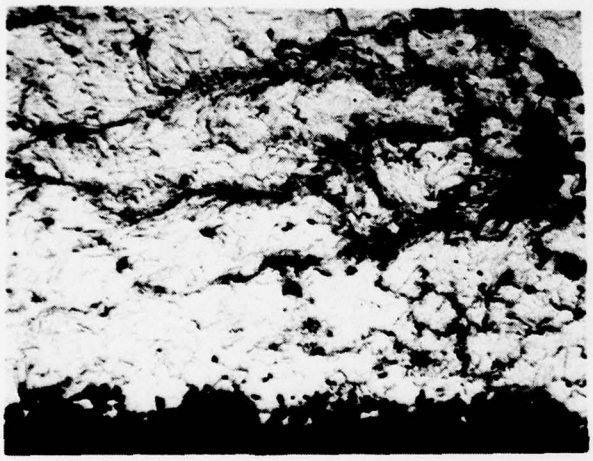

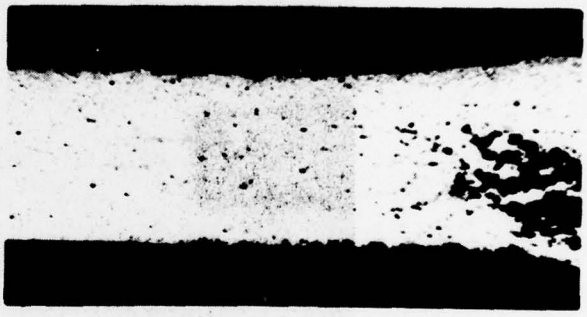

Mag: 25X

Mag: 100X

e) Strain effects in and near pitted area which promoted pitting.

FIGURE 57. VIEWS OF PITTED REGION NEAR DOME TO OUTLET FITTING (CONTINUED) BOND IN TANK NO. 7, INTERIOR SURFACE.

Mag: 4X

a) View of inside surface of bond overlap showing etched groove.

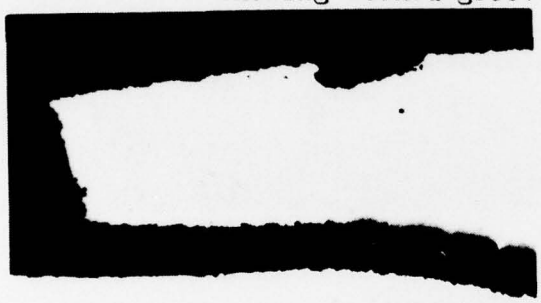

Mag: 32X

b) Cross section showing configuration of overlap plus crevice.

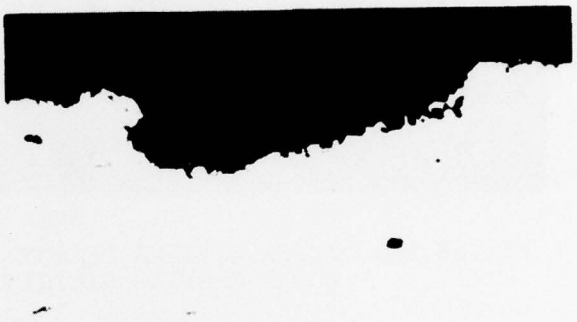

Mag: 100X

c) Detail view of attack in etched groove.

Unetched

Mag: 100X Etched - Mixed Acids

d) Cross section at start of crevice showing minor grain boundary attack.

FIGURE 58. LONGITUDINAL BOND IN CYLINDER SECTION OF A-286 EXPLOSIVE BONDED TANK NO. 5 SHOWING MINOR ETCHING OR CORROSION ATTACK.
METALLURGICAL LABORATORY MET NO. 78-79011

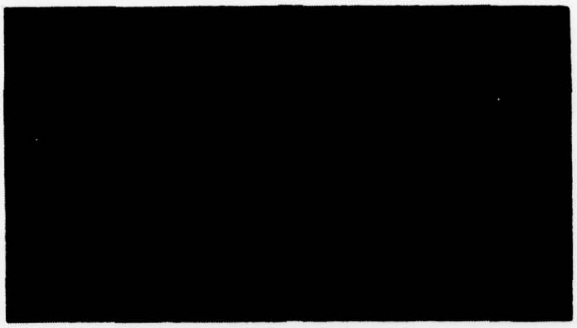

Mag: 1X

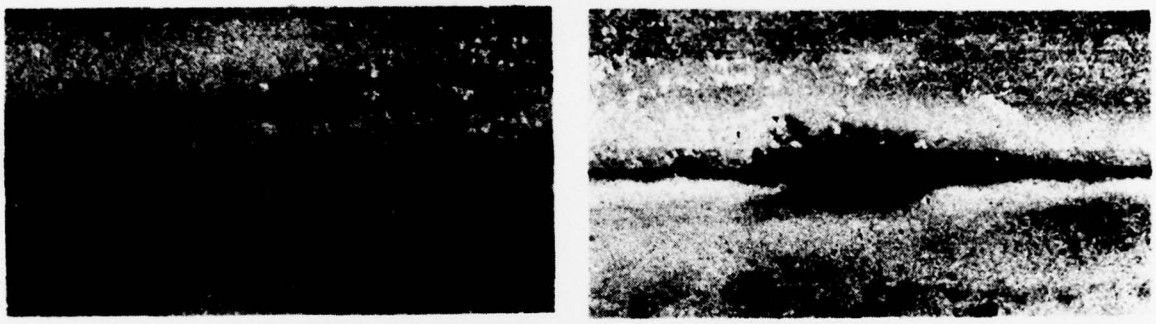

Mag: 4X

FIGURE 59. SURFACE VIEWS OF BOND OVERLAP REGION IN INTERIOR OF TANK NO. 6 SHOWING STAINING ALONG JOINT.

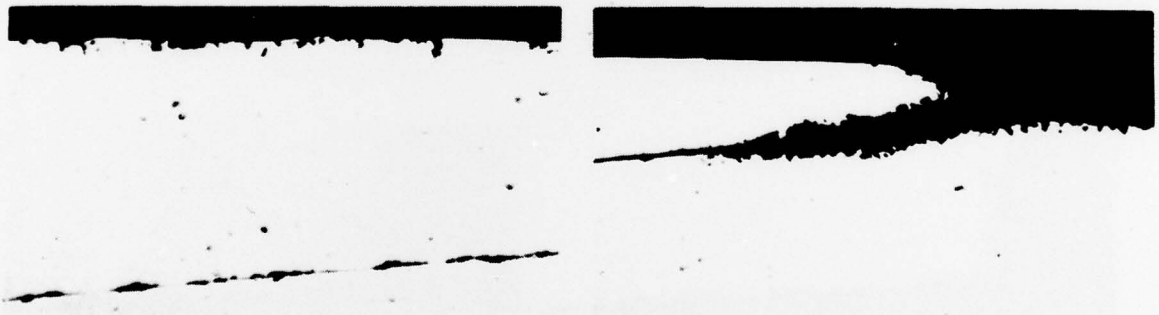

a) Over bond.

b) At interior bond edge.

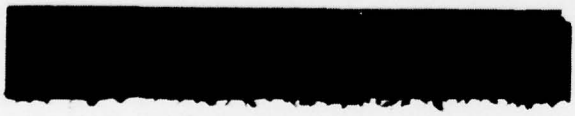

c) Over base metal.

FIGURE 60. CROSS SECTION VIEWS SHOWING MINOR ETCHING OR CORROSION ATTACK OF THE SURFACE LAYERS, TANK NO. 6.

Mag: 2X

a) Overall view of staining and deposits in outlet fitting

Mag: 15X

b) Detail view of stain and deposits along bond.

FIGURE 61. STAIN AND DEPOSITS ALONG THE OUTLET FITTING TO DOME BOND FROM A-286 TANK NO. 5.

Mag: 2X

a) Overall view of stained region.

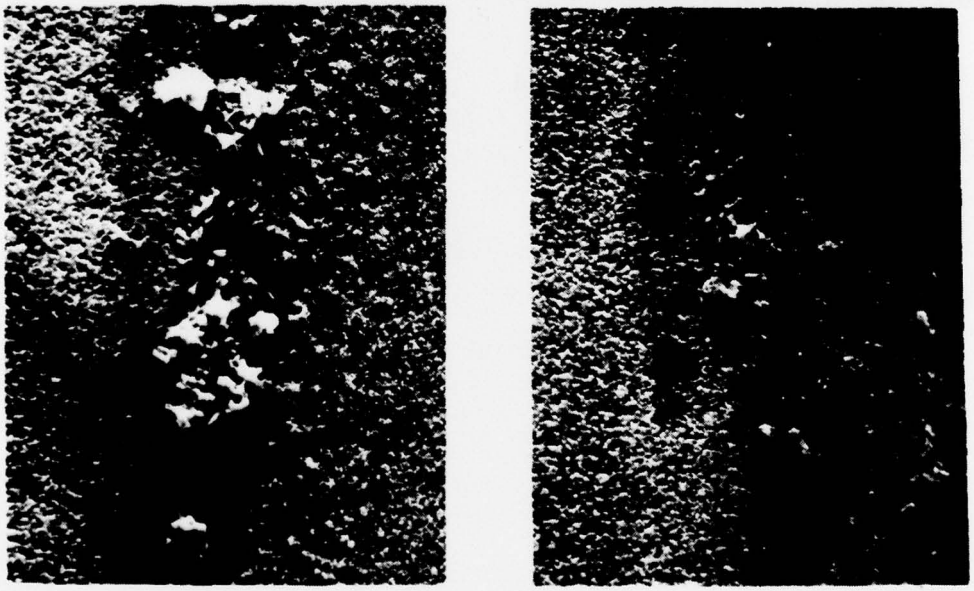

Mag: 15X

b) Closeup views of stain and deposits.

FIGURE 62. STAIN AND DEPOSITS ALONG BOND LINE OF OUTLET FITTING OF TANK NO. 6.

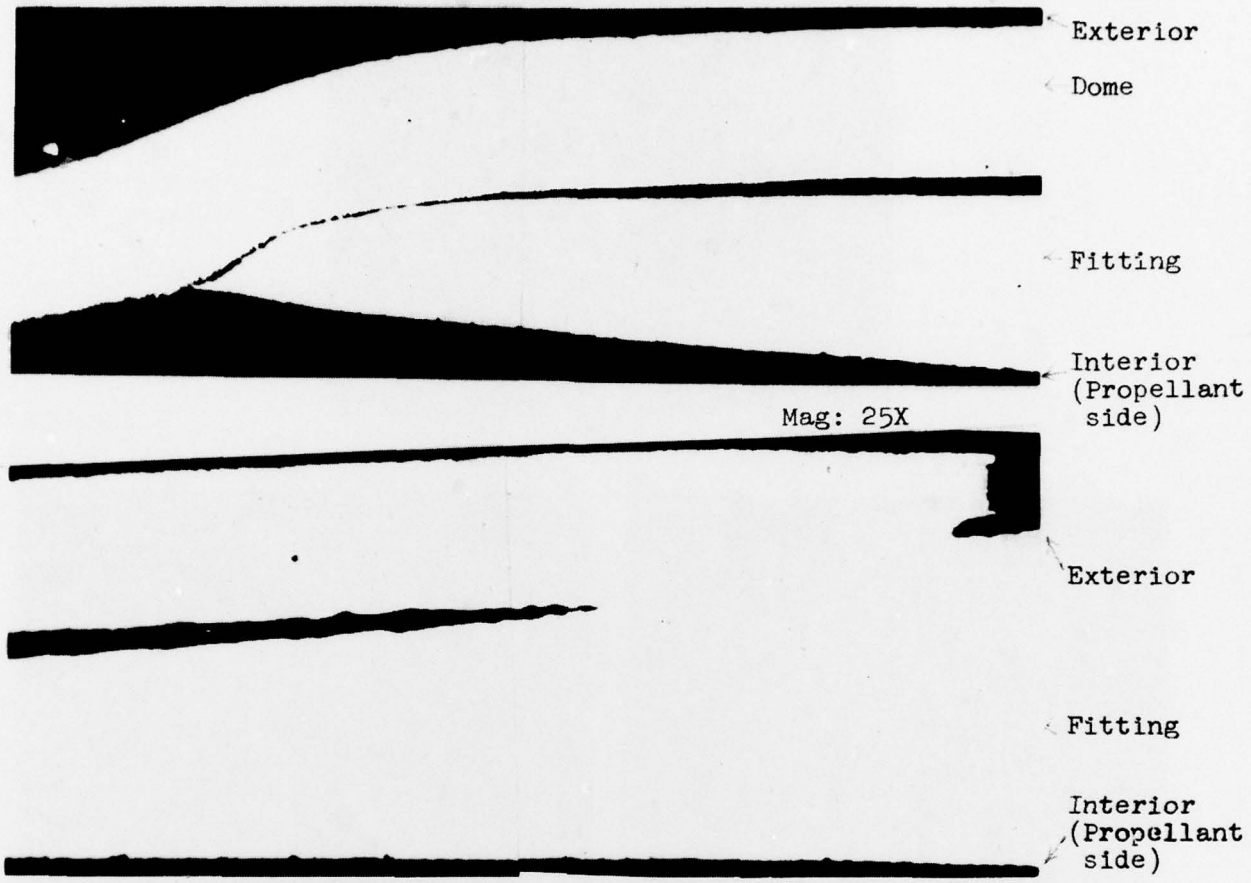

a) Section illustrating extensive cavity along bond, connected to interior, but sealed from exterior.

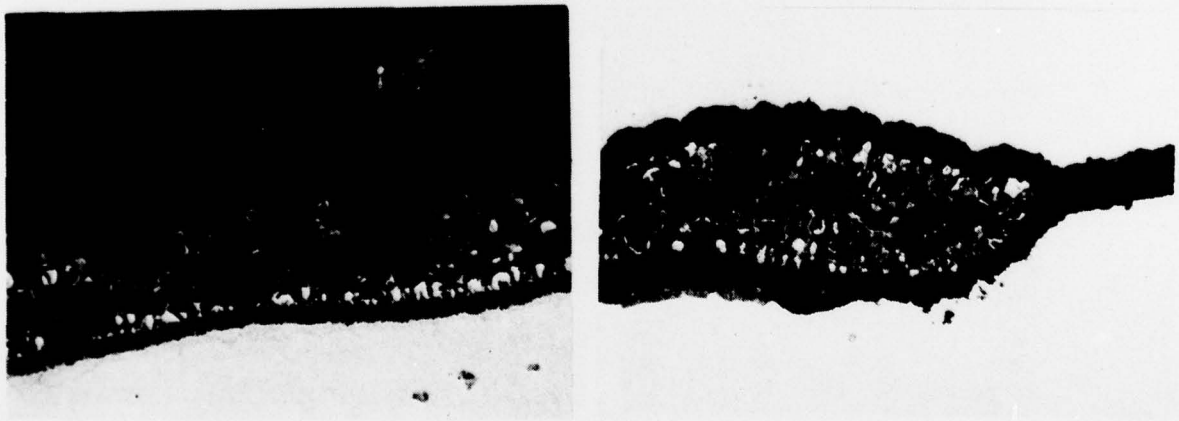

Mag: 500X

b) Detail views of crevice showing corrosion deposit indicative of oxygen starved corrosion of stainless steel.

FIGURE 63. SECTION THROUGH FITTING TO DOME BOND FROM TANK NO. 6 SHOWING CAVITY WHERE CORROSION PRODUCED STAINS AND DEPOSITS OBSERVED IN FIGURE 62.

a) Overall view of end of puddle.
Mag: 1X

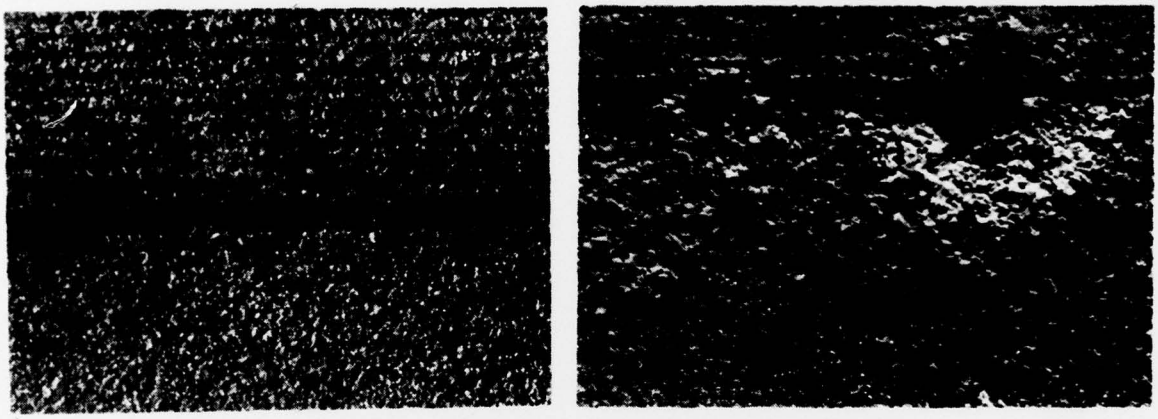

b) Detail views of surface attack and buildup of deposits.
Mag: 15X

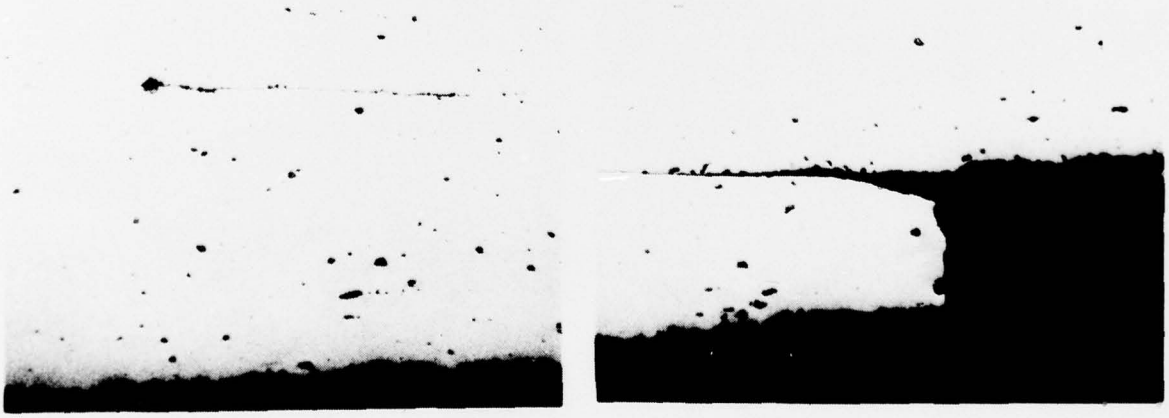

c) Section views showing slight attack in bond and along surface.
Mag: 100X

FIGURE 64. DETAIL VIEWS OF REGION AT DOME TO CYLINDER BOND IN TANK NO. 7 WHERE "PUDDLE" COLLECTED WHILE TANK WAS ON ITS SIDE, PROBABLY AFTER PROPELLANT DRAINING.

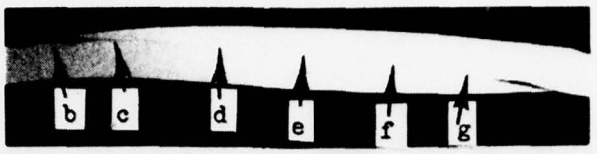

a) Overall view of cylinder bond showing location of views presented below. Letters in above section refer to view numbers below. Mag: 4X

b) Joint interface at exterior showing lack of bond and tight crevice.

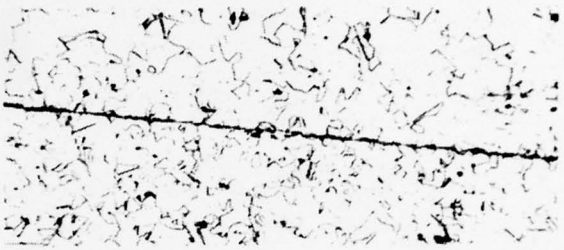

c) Interface region showing tight contact but no true bonding.

d) Bond area where there is intermittent melted material.

e) Area where melted material is almost continuous.

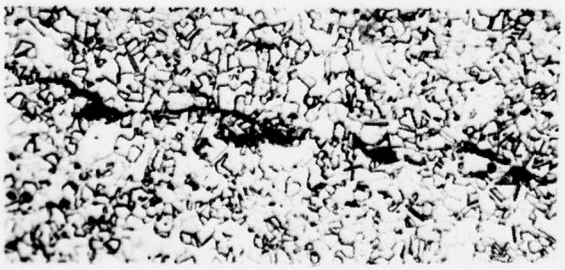

f) Area where wave action is pronounced.

g) Melted material contains pores.

All Views - Mag: 100X Etch: Mixed Acids Matl: A-286

FIGURE 65. DETAIL VIEWS OF EXPLOSIVE BOND STRUCTURE OF TANK NO. 5 IN THE LONGITUDINAL CYLINDER JOINT.

Overall view of joint is same as view (a) of Figure 65.

a) Interface region showing tight contact but no bond. Location indicated by "c" in Figure 65, view (a).

b) Area with intermittent good bond and then melted material. Location indicated by "d" in Figure 65, view (a).

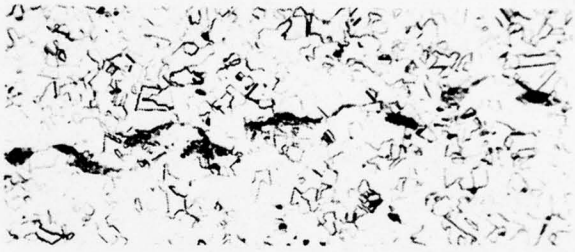

c) Wave action visible in melted material. Location indicated by "e" in Figure 65, view (a).

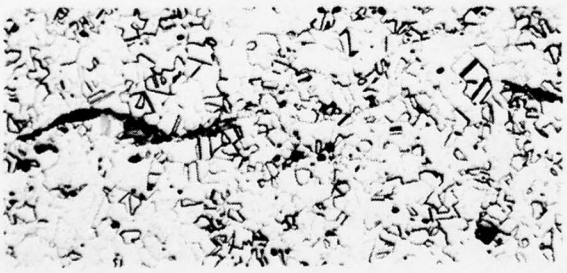

d) Between melted material good bonding is seen. Location indicated by "f" in Figure 65, view (a).

e) Extensive melted material with pores and cavities. Location indicated by "g" in Figure 65. view (a).

All Views - Mag: 100X; Etch: Mixed Acids; Matl: A-286 SS

FIGURE 66. DETAIL VIEWS OF EXPLOSIVE BOND STRUCTURE OF TANK NO. 6 IN THE LONGITUDINAL CYLINDER JOINT.

METALLURGICAL LABORATORY MET NO. 78-79011

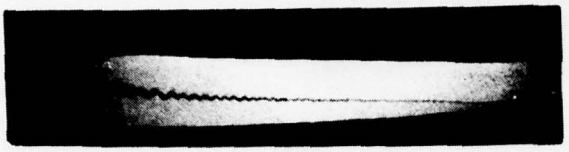

Mag: 4X

a) Overall view illustrating shape and overlap configuration of joint.

b) Bond near outer surface.

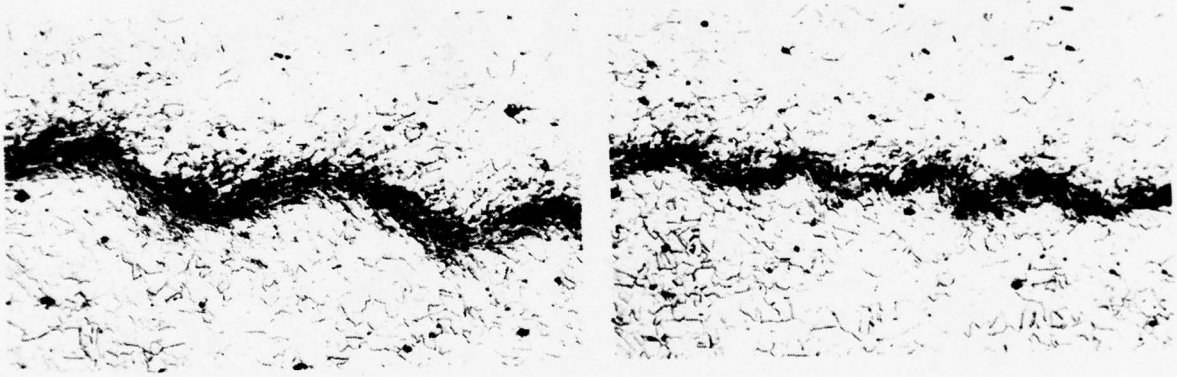

c) Bond in interior showing varying amounts of wave action.

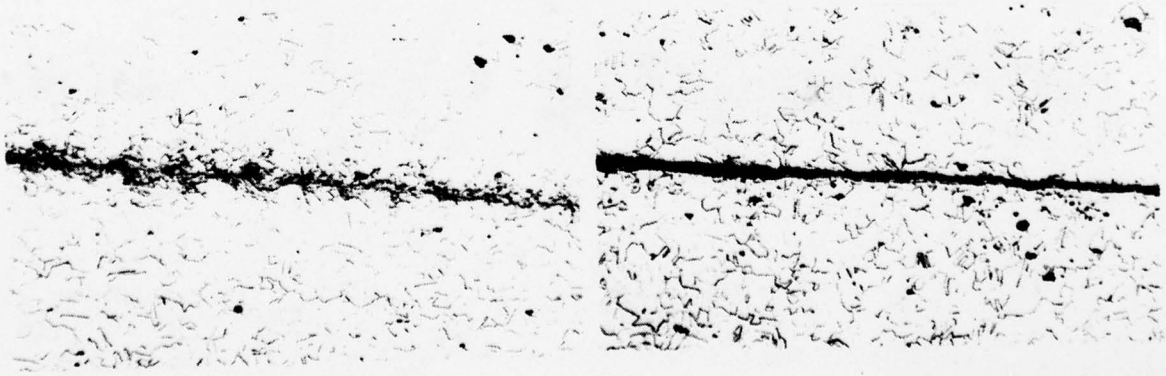

d) Bond when approaching ID showing tailoff of wave.

d) Bond near ID showing little bonding.

All Views - Mag: 100X

FIGURE 67. DETAIL VIEWS OF BOND STRUCTURE IN SOLID STATE EXPLOSIVE BOND TAKEN FROM CIRCUMFERENTIAL DOME TO CYLINDER BOND OF TANK NO. 5.

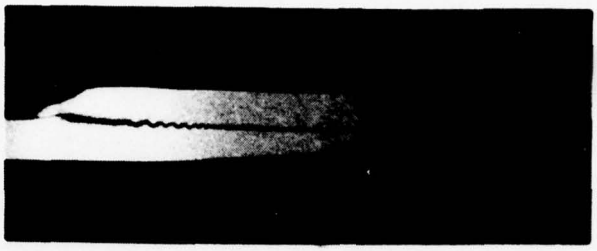

a) Overall view illustrating joint shape and showing location of detail views. Mag: 4X

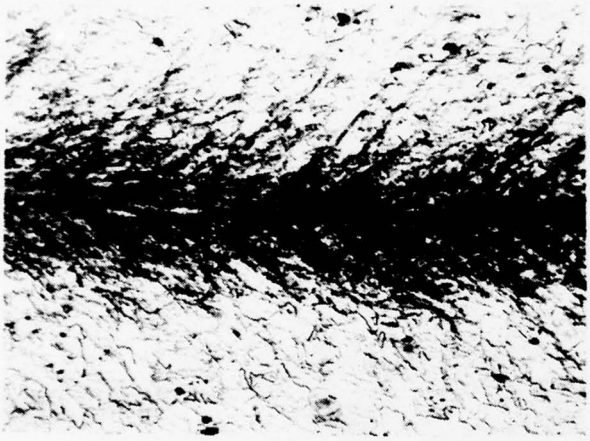

b) Bond near exterior the starting area with extensive strain but before wave action has started.

c) Wavy area with melted zones, gas pores and cracks.

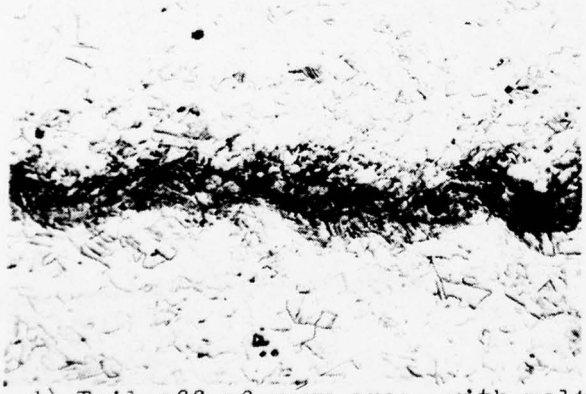

d) Tail-off of wavy area, with melted zones and pores still visible.

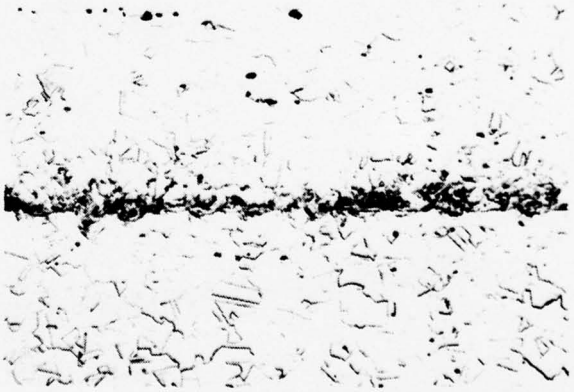

e) Interface near interior with only intermittent bonding.

All Views - Mag: 100X: Etch: Mixed Acids

FIGURE 68. DETAIL VIEWS OF EXPLOSIVE BOND STRUCTURE OF TANK NO. 7 IN THE CIRCUMFERENTIAL DOME TO CYLINDER JOINT.

METALLURGICAL LABORATORY MET NO. 78-79011

a) Overall view illustrating joint shape and showing location of detail views. Mag: 4X

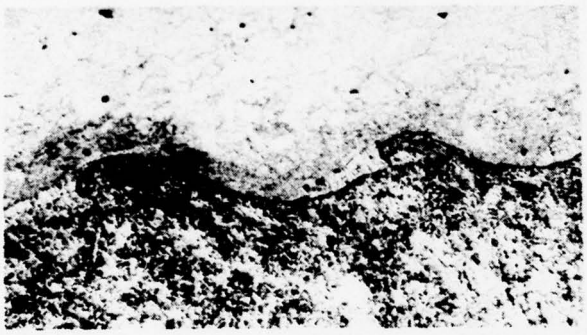

b) Wavy area near exterior. Very little strain indications and considerable melted material seen in interface.

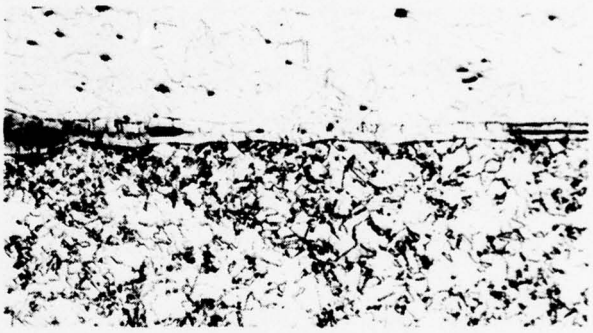

c) Central region of joint showing no wave or strain effects and occasional porosity.

Mag: 100X

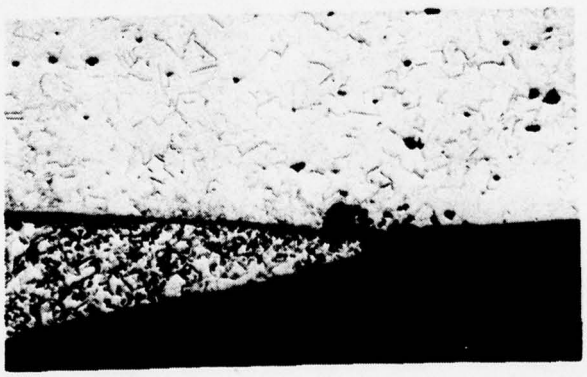

Mag: 100X

d) Interior edge of joint showing slight bonding with corrosion.

FIGURE 69. DETAIL VIEWS OF EXPLOSIVE BOND STRUCTURE OF TANK NO. 7 IN THE POLAR OUTLET FITTING TO DOME JOINT.

METALLURGICAL LABORATORY MET NO. 78-79011

Mag: 1X

a) Overall view of interior of bond.

Mag: 15X

b) Closeup view of tears at bond edge or slightly back from edge.

Dome Wall

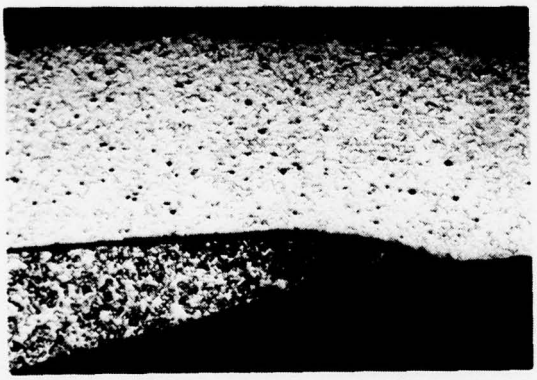

Mag: 32X

Outer edge of outlet fitting.

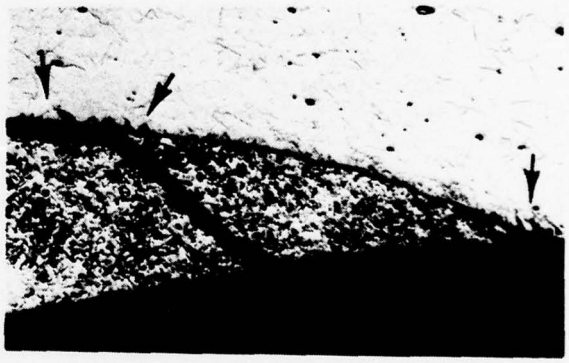

Mag: 100X

Etch: Mixed Acids

c) Section through tear showing outlet tip to be bonded but interior unbonded. Note the minor corrosion at junction between components as indicated by arrows.

FIGURE 70. OUTLET FITTING TO DOME BOND IN TANK NO. 7 SHOWING INTERMITTENT BONDING AND TEARING OF OUTERMOST LIP OF OUTLET COMPONENT.

METALLURGICAL LABORATORY MET NO. 78-79011

Mag: 4X

a) Overall view of cross section at bond.

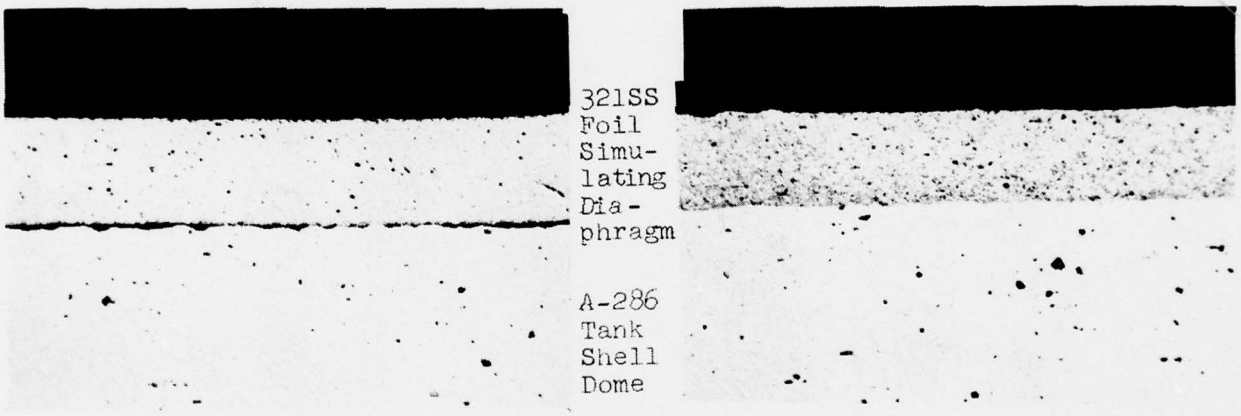

Mag: 100X

b) Section near foil end of explosive joint showing essentially no bonding.

c) Section near curled end of foil showing good bond to shell but none of the "waves" associated with normal bonds.

FIGURE 71. VIEWS OF BOND PRODUCED BETWEEN SIMULATED DIAPHRAGM STUB AND TANK SHELL IN A-286 TANK NO. 5.